MECHANISTIC STUDY OF ANTI-OBESITY EFFECT OF POLYMETHOXYFLAVONES THROUGH THEIR BIOAVAILABILITY, BIOTRANSFORMATION AND INTERACTION WITH GUT MICROBIOTA *IN VIVO*

By

MAN ZHANG

A dissertation submitted to the

School of Graduate Studies

Rutgers, The State University of New Jersey

In partial fulfillment of the requirements

For the degree of

Doctor of Philosophy

Graduate Program in Food Science

Written under the direction of

Dr. Qingrong Huang

And approved by

_____

_____

_____

_____

New Brunswick, New Jersey

October 2020

ABSTRACT OF THE DISSERTATION

MECHANISTIC STUDY OF ANTI-OBESITY EFFECT OF POLYMETHOXYFLAVONES THROUGH THEIR BIOAVAILABILITY, BIOTRANSFORMATION AND INTERACTION WITH GUT MICROBIOTA *IN VIVO*

By MAN ZHANG

Dissertation Director:

Dr. Qingrong Huang

Polymethoxyflavones (PMFs) are a unique class of flavonoids that have at least two methoxy groups on the flavone skeleton. About 80 PMFs have been identified from the citrus so far. Among them, tangeretin and nobiletin are the two most prevalent PMFs and widely studied for their biological activities. PMFs have demonstrated a broad spectrum of bioactivities, including neuroprotection, anti-inflammatory, anti-cancer, anti-obesity, anti-atherosclerosis activities. In particular, emerging studies find that PMFs have beneficial effect to maintain the metabolic homeostasis by regulating signals coordinating multiple organs, including the brain, pancreas, liver, adipose tissues, muscles and gastrointestinal (GI) track. However, the underlying mechanisms of their anti-obesity effect still remain unclear. This study aims to explore the anti-obesity activity and biological fate of PMFs in

in vivo by investigating their bioavailability, biotransformation and interaction with gut microbiota. Besides, we also have developed delivery systems with the aim of improving PMFs bioavailability. The delivery systems are found to play important roles on the biological fate of PMFs, and thus may influence their bioefficacy *in vivo*.

In the first part of this work, we have studied the interplay of PMFs and gut microbiota and its implication for obesity control. Using the high fat diet (HFD) induced obese mice, we investigate the modulation effect on gut microbiota by PMFs extracted from the aged citrus peels. PMFs are found to have prebiotic effect by reducing biomarkers of microbial dysbiosis caused by HFD and promoting beneficial bacteria, such as *Bifidobacteria* and *Lactobacillius*. PMFs treatment increases the fecal short chain fatty acids (SCFA) production. The metagenomic analysis of the feces shows that the xenobiotics metabolism of the gut microbiota is enhanced by PMFs treatment. Besides, we also study the biotransformation of nobiletin by gut microbiota and in the host organs (in the liver and brain) after 8-week feeding of nobiletin for the HFD-fed mice. The concentration ratio of demethylated metabolites in feces increases dramatically in the feces during the 8 weeks. Both the metagenomics and biotransformation analysis suggest that the long-term metabolic input of PMFs would enable gut microbiota with enhanced biotransformation activity for metabolizing PMFs.

PMFs have shown good anti-obesity activity from recent studies. However, the

biological fate of PMFs *in vivo* remains unclear. The second part of this study is to compare the bioavailability and biotransformation of a typical PMF--nobiletin in the lean- and obese rats. From the excretion study, gut microbiota demonstrates higher extent of demethylation activity than the host, since more di-demethylated nobiletin is found in the feces than the urine. The bioavailability of nobiletin in the lean- and obese- rats is similar, which is about 20%. Higher ratio of demethylated metabolites to nobiletin was found in the feces and plasma in the obese rats than the lean rats after oral administration of 100mg/kg nobiletin. The metabolites profile in the plasma after intravenous injection does not show significant difference for lean- and obese rats. Comparing the results for the oral and injected administration, it suggests that gut microbiota (the microbiome from the lean- and obese rats) plays important role on the biotransformation of PMFs *in vivo*.

Due to the multiple methoxy groups, PMFs have poor water solubility. We have developed two emulsion systems to enhance the bioavailability of PMFs: the conventional emulsion and organogel-based emulsion. The lecithin-based conventional emulsion with 1% nobiletin has an average droplet size of around 330 nm; has the viscoelastic and gel-like behavior; but could not completely prevent the crystallization of PMFs. According to the pharmacokinetic study using rat model, the conventional emulsion can increase the bioavailable nobiletin and its major metabolite in the blood by about 2 times, as compared to the oil suspension. To further optimize the emulsion formulation, we develop the organogel-based emulsion, which increases the solubility of PMFs by about 3.5 times in

the oil phase without crystallization in the room temperature. Furthermore, from the *in vitro* lipolysis results, the organogel-based emulsion shows better efficiency to improve the bioaccessibility of PMFs, compared to the conventional emulsion.

ACKNOWLEDGEMENT

I would like to thank my advisors Dr. Qingrong Huang and Dr. Chi-Tang Ho, who give me tremendous guidance and support during my Ph.D journey. Dr. Huang and Dr. Ho are excellent advisors with specific expertise in the food science field. They always inspire me to explore the “cutting edge” part of our field. Even though I have come crossed many difficulties and failures during the five years, their kindly support, patience and encouragement give me big confidence to solve problems and move on smoothly. It is my honor to work closely with my two advisors. I have learned a lot from them not only for the technical skills and academical appetite but also for their honorable personalities.

I also thank my committee members, Dr. Shiming Li and Dr. Qingli Wu. Dr. Shiming Li has provided useful comments for the synthesis and application of PMFs/their metabolites. Dr. Qingli Wu has provided insightful help and suggestions for the metabolite analysis using LC-MS/MS. With the support from my entire committee members, I am able to complete my project with high efficiency.

I want to express my gratitude to Dr. Xin Zhang, Dr. Denggao Zhao, Dr. Yanyan Ma, Dr. Guiying Huang, Dr. Yong Cao and Dr. Jie Xiao for their kind provision of research resources in China.

I greatly appreciate the guidance of the previous/senior students in our lab: Dr. Weiping Jin, Dr. Jieyu Zhu, and to-be-doctor Liang Wen. We have good discussions together and I have gained useful experimental skills and research insights from them. I also thank my friends Yijun Pan and Xudong Tang: we support each other and take the challenges for all the millstones in the Ph.D. study together. Special thanks to Yanping Xin for the synthesis of metabolites, Siyue Zhu, Qiaoru Dong and Baoer Yin for the support of some experiment. I am grateful to meet all the labmates, friends and visiting scholars in Rutgers University. We have a lot of enjoyable and memorable moments together during my Ph.D. study.

I greatly appreciate my husband, Hongliang Yu for his great support, my families and friends in China for their love.

TABLE OF CONTENTS

LIST OF TABLES

LIST OF FIGURES

CHAPTER I: INTRODUCTION

The epidemic of obesity has become a worldwide public health concern in recent years, especially in the developed countries. According to the World Health Organization (WHO), the overall prevalence of obesity among adults in the worldwide is about 13% in 2016 (*1*). In the united states, the obesity prevalence among adults has increased from 30.5% to 42.4% from 1999 to 2018 (*2*). The obesity is considered as a central features that increases risks for a cluster of metabolic disorders, such as dyslipidemia, insulin resistance, hypertension, type 2 diabetes, fatty liver diseases, atherosclerosis, etc (*3*). The excessive energy intake and insufficient physical activity are the two important environmental factors for the development of metabolic syndrome (MetS) (*4*). The low-grade or chronic inflammation, also called metaflammation (metabolically triggered inflammation), is found as a key feature of metabolic disorders (*3, 5*). The interface of metabolic regulation and immune response plays important role to maintain the metabolic homeostasis in our bodies. For example, in the condition of nutrient surplus, the immune cells in the metabolic tissues may sense and react the nutrient signals, and in turn influence the metabolic actions within neighboring cells by altering the glucose uptake or lipid metabolism (*5*). As these tissues and their produced mediators may cause systemic inflammatory response and metabolic dysfunction, the metabolic diseases often emerge as clusters of lipid- and

glucose- dysfunctions.

Flavonoids, an important group of phytochemicals, are abundant in our diets, especially in the beans, fruits and vegetables. Flavonoids are the secondary metabolites in plants with different metabolic functions, such as ultraviolet radiation protection, phytopathogen infection protection, auxin transport, male fertility, flower coloration, etc (*6*). Besides, accumulative studies have found that flavonoids-enriched diets have health benefits against metabolic disorders in animals and humans (*7, 8*). For the chemical structure, flavonoids are composed of a benzo-γ-prone skeleton (C6-C3-C6) with two benzene rings (ring A and B) joined by a linear 3-carbon chain (ring C) (*7*). According to the substitution patterns of the ring C, flavonoids can be divided into subgroups, such as flavones, isoflavones, flavonols, flavanones, flavanonols, flavan-3-ols and anthocyanins.

Polymethoxyflavones (PMFs) are a unique class of flavonoids that have at least two methoxy groups on the flavone skeleton. PMFs are identified in the citrus seeds, leaves, stems, juice, and abundantly in the citrus peels (*9*). About 80 PMFs have been identified from the citrus so far (*9*). Among them, tangeretin and nobiletin are the two most prevalent PMFs and widely studied for their biological activities. PMFs have demonstrated a broad spectrum of bioactivities, including neuroprotection, anti-inflammatory, anti-cancer, anti-obesity, anti-atherosclerosis activities (*9-11*). In particular, emerging studies find that PMFs have beneficial effect to maintain the metabolic homeostasis by regulating signals coordinating multiple organs, including the brain, pancreas, liver, adipose tissues, muscles

and gastrointestinal (GI) track. Moreover, PMFs shows very good bio-efficiency against dyslipidemia and obesity *in vitro* and *in vivo*, compared to some citrus flavanones (e.g. hesperidin and naringenin) (*12-14*). For example, nobiletin and tangeretin have higher efficiency to inhibit the secretion of cholesterol, triglyceride and apoB than hesperetin and naringenin in HepG2 cells (*13*). To achieve the similar anti-obesity effect *in vivo*, higher concentrations of naringenin is required to be supplemented in diets than nobiletin (*14*). The good bioefficacy of PMFs against metabolic disorders is supposed to associate with their particular chemical structures. However, it still remains unclear for the bioavailability-bioactivity relationships for PMFs. Therefore, it is important to understand the biological fate of PMFs *in vivo*, especially for their bioavailability and biotransformation.

As mentioned before, the metaflammation is associated with the development of metabolic disorders. The anti-inflammatory property is an important aspect of PMFs' bioactivities and would contribute to their regulation on the MetS. The anti-inflammatory activities of PMFs has been documented in several reviews (*9-11, 15, 16*). However, systemic review of PMFs on maintaining metabolic hemostasis is lacked. In particular, emerging studies find that PMFs can modulate circadian clock and gut microbiota in recent 5 years, besides of regulating lipid- and glucose- metabolism *in vivo*. This review aims to unveil recent discoveries for PMFs' role on metabolic disorders. We will start with a brief overview of metabolic homeostasis, followed by introduction of chemical structures of

PMFs. Then, PMFs in the GIT tract will be discussed, because GIT is an important organ system influencing the bioavailability and biotransformation of PMFs as well as their interplay with gut microbiota. Finally, the molecular mechanisms or possible pathways will be highlighted for several PMFs-mediated metabolic disorders.

1.1 Overview of metabolic homoeostasis

The long-term energy imbalance caused from poor physical activity and excessive calorie intake contributes to metabolic disturbance in our modern life (*17*). It is well recognized that the regulation of metabolic homeostasis is influenced by the crosstalk between the multiple peripheral organs and the central nervous systems (CNS) (*17*).

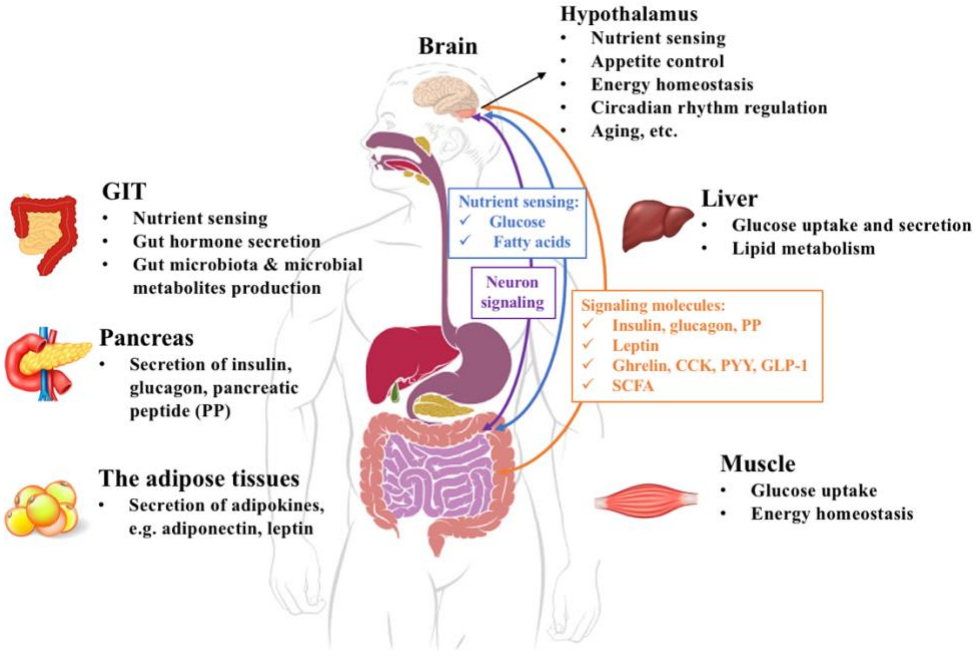

Figure 1: The regulation of metabolic homeostasis through the crosstalk of the central nervous system and peripheral organs.

Multiple peripheral organs are participated in maintaining the whole-body lipid- and glucose- and energy homeostasis, including the pancreas, gastrointestinal track (GIT), liver, adipose tissues and muscles (**Fig. 1**). After the meal, food is digested into nutrients in the GIT and then absorbed from the gut and enter the circulation system (*18*). The peripheral organs will sense the nutrient flux and respond by releasing signaling molecules. These molecules are identified to play an important role in the regulation of the whole-body metabolic homeostasis through interorgan communication axis. The pancreas secrets insulin, glucagon and pancreatic peptide (PP) by its β-, α- and F- cells, respectively. Insulin is an important hormone to reduce the circulating glucose and increase glucose uptake in the liver and muscles (*19*). Glucagon stimulates the glucose production and secretion by the liver and acted as the satiety signal (*20*). The PP has multiple functions, such as regulating pancreatic section, modulating energy expenditure, delaying gastric empty and exerting anorexigenic effect (*20-22*). The adipokines secreted by adipocytes, including adiponectin and leptin, have gained increasing respect for their role in energy homeostasis (*23*). Both adiponectin and leptin are reported to decrease hepatic lipogenesis and activate β-oxidation of fatty acids (*23*). Moreover, adiponectin could improve the insulin sensitivity(*23, 24*), and leptin could reduce appetite by interaction with the CNS (*22*). For the hormones produced by endocrine cells in the GIT, ghrelin is mainly released from the gastric mucosa; cholecystokinin(CCK) is released from small intestine; glucagon-like peptide 1 (GLP-1) and peptide tyrosine tyrosine (PYY) are mainly released from distal gut

(*21, 22, 25*). Except for ghrelin, the other gut hormones (CCK, GLP-1 and PYY) exert anorexigenic effect by triggering gut-brain axis (*22*). GLP-1 and PYY are reported to regulate gastric empty and insulin sensitivity (*21, 26*). Recent studies indicate that the secretion of the GLP-1 and PYY is associated with the gut microbiota (*27*). The microbiome is influenced by the diet components, and HFD-related microbiota is found to alter the host's energy harvest, inflammation, insulin resistance and fat accumulation by generating multiple microbial metabolites (*28*). For example, the short chain fatty acids (SCFA) produced by the gut microbiota are extensively studied for their beneficial effect on peripheral organs (e.g. the liver and adipose tissues) as well as the brain to maintain energy homeostasis for the host (*28, 29*). In terms of the gut-brain axis, SCFA modulate the central regulation of appetite and food intake by direct and in indirect mechanisms. The acetate, the main SCFA entering the circulation system, is found to suppress appetite directly by central hypothalamic mechanisms (*30*). Besides, SCFA may influence the appetite indirectly by promoting the secretion the anorexigenic gut hormones- GLP-1 and PYY (*27*) (*29*).

As the brain is exposed to various nutrients, it can detect the nutrient sensing and coordinate peripheral tissue-specific responses by hormone and neuron signaling (**Fig. 1**) (*17, 18*). The hypothalamus, located in the base of brain near the blood-brain barrier (BBB), is particularly vulnerable for the nutrient- and hormone sensing (*31*). The hypothalamus is an important regulator for many physiological processes, including nutrient sensing,

appetite, energy homeostasis, circadian clock, immune response and aging (*22, 31*). The arcuate nucleus (ARC) in the hypothalamus can receive the circulating nutrient/hormone signals directly, since the nucleus is partially located outside the BBB (*32*). In addition, the ARC nucleus contains both orexigenic and anorexigenic neurons, which are essential for appetite control. The orexigenic neurons can express the agouti-related protein (AgrP) and neuropeptide Y (NPY), while the anorexigenic neurons can express pro-opiomelanocortin (POMC) and cocaine and amphetamine-regulated transcripts (CART) (*22*). Both the AgrP/ NPY and POMC/ CART neurons contain the receptors of multiple signals for fat store (leptin, insulin and ghrelin), calorie information of the ongoing meals (CCK, PYY and GLP-1) and nutrients (glucose and fatty acids) (*33*). Therefore, the CNS receives the circulating chemical and neural input, integrates the information, generates food-reward signing and coordinates peripheral organs' response to maintain metabolic homeostasis (*34*). For example, the lipid sensing in the gut is found to activate the CCK-A receptor and trigger the gut-brain-liver axis to lower the hepatic glucose production (*18*).

Together, the metabolic homeostasis is regulated by interorgan communication axis through the sensing and reaction of nutrient flux and signaling molecules. In the following parts, we will introduce PMFs' chemical structure, elucidate PMFs' behaviors/roles in the specific cell/organ, and discuss PMFs-mediated metabolic disorders via this interorgan communication axis.

1.2 Chemistry of PMFs

Dietary flavonoids identified in fruits and vegetables have demonstrated disease chemopreventive effect in various biological systems (*35*). Citrus PMFs have at least two methoxy groups on the C6-C3-C6 flavone skeleton, as shown in **Fig. 2** (*9, 11*). With the technology development of separation and structure identification, about 80 PMFs have been identified in recent literature (*9*). Tangeretin (5,6,7,8,4′-pentamethoxyflavone) and nobiletin (5,6,7,8,3′,4′-hexamethoxyflavone) are the two prevalent PMFs abundantly existed in the citrus peels and widely studied for their profound bioactivities (*9*). Other less studied PMFs include: 5,6,7,4′-tetramethoxyflavone, sinensetin (5,6,7,3′,4′-pentamethoxyflavone), 3,5,6,7,3′,4′-pentamethoxyflavone, 3,5,6,7,8,3′,4′-heptamethoxyflavone, etc.(*10, 36*). Moreover, hydroxylated PMFs or demethylated PMFs, recognized by PMFs with hydroxyl groups substituting for methoxy ones, have received increasing attentions in recent years. The chemical structures of typical PMFs and demethylated PMFs are shown in **Fig. 2**. Demethylated PMFs have been identified in the citrus genus or as the metabolites of their PMFs counterparts (*15*). For example, 5-demethylnobiletin and 5-demethyltangeretin have been identified in the aged citrus peels (chenpi), and have an accumulative effect during the long-term aging process (*15*). The demethylation on the B-ring was found as the metabolic biotransformation pathway of PMFs *in vivo*. For example, 3′-demethylnobiletin, 4′-demethynobiletin and 3′,4′-didemethynobiletin have been identified in mouse urine after oral administration of nobiletin (*37, 38*). 4′-demethyltangeretin is identified as the major metabolite of tangeretin by liver microsomes or hepatocytes (*39*).

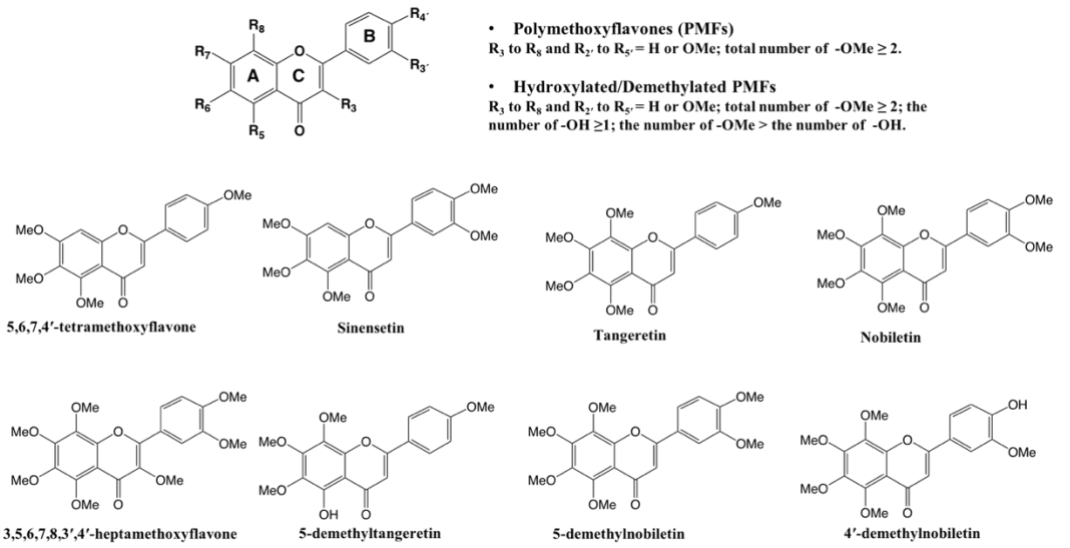

Figure 2: The chemical structures of PMFs and demethylated PMFs

Due to the multiple methoxy groups, the citrus PMFs have poor water solubility as well as limited oil solubility. PMFs have a higher solubility in the medium chain triglycerides (MCT) as compared to long chain triglycerides (*40*). The solubility in the MCT is about 4.4 mg/g for nobiletin (*41*), 4.3 mg/g for tangeretin (*42*) and 2.3 mg/g for 5-demethyltangeretin (*40*). The number of methoxy- and hydroxyl- groups plays an important role in the solubility and permeability of PMFs, as discussed in the previous review (*10*). In terms of the bioactivities, the hydroxyl groups of the flavonoids are associated with the antioxidant activity and cytotoxic effect, while the methoxy groups of the flavonoids refer to the interaction with cellular membranes, enzymes and other proteins (*15, 43-45*). Therefore, the structure-function relationship for citrus PMFs and demethylated PMFs needs further exploration.

1.3 PMFs in the gastrointestinal track

The GIT is an organ system extending from the mouth to the anus by the broadest definition (*46*). The GIT can be further divided into two parts—the upper tract and lower tract. The upper tract contains the mouth, stomach and small intestine (duodenum, jejunum and ileum). The upper track is responsible for food digestion, and the small intestine is regarded as the major site for the absorption of the nutraceuticals (*46, 47*). The lower tract refers to the large intestine containing cecum, colon, rectum and anus, where harbors a large population of microbes at this site (*46*). After the oral administration of food/nutrients, the GIT represents the largest interface among food environment, gut microbiota and our body. The intestinal epithelium contains several different cells with specific functions: enterocytes functioning as nutrient absorption; enteroendocrine cell functioning as hormone secretion; Paneth cells functioning as antimicrobial peptide secretion; goblet cells functioning as mucus production; tuft cells functioning as taste-chemosensory responses; and microfold cells functioning as antigen sampling (*48*). The GIT has great importance for the absorption, distribution, metabolism and excretion of dietary flavonoids (*49*). Therefore, the metabolic homeostasis effect of PMFs is closely associated with their interplay with the GIT. The orally administered PMFs can act on the GIT locally, such as interactions with lumenal contents, intestinal epithelial cells, gut microbiota, immune cells and endocrine cells. In addition, the GIT greatly impacts the systemic effect of PMFs by determining PMFs absorption and releasing microbiota-derived molecular signals in the circulation system.

1.3.1 Bioavailability

The oral bioavailability of nutraceuticals is defined as the fraction of the orally administered biocompound which is absorbed into systemic circulation the and becomes available to the site of action (*50*). The factors influencing the bioavailability of nutraceuticals can be divided into 3 categories: bioaccessibility, intestinal permeability and metabolism (*50, 51*). PMFs have limited bioaccessibility due to the poor water solubility, but high permeability due to the multiple methoxy groups (*10*). The absolute oral bioavailability of PMFs is the amount of PMFs entering into the systemic circulation via oral administration (po) relative to that via intravenous injection (iv), as expressed by the following equation (*52*):

$$F(\%) = (AUC_{po} * Dose_{iv})/(AUC_{po} * Dose_{po}) * 100$$

Where AUC stands for the area under the concentration-time curve; and Dose stands for the dosage of PMFs. In our unpublished data, the absolute bioavailability of nobiletin suspended in the carboxymethyl cellulose solution is about 20% via pharmacokinetic study using the Sprague-Dawley rats at the dosage of 100 mg/kg. For some common flavonoids with good regulation of metabolic syndromes, the absolute bioavailability of anthocyanins from berries and (-)-epigallocatechin-3-gallate (EGCG) from green tea is estimated less than 2% using the rat model (*53, 54*). Therefore, PMFs have a high bioavailability *in vivo*, as compared to the common flavonoids with multiple hydroxyl

groups. The bioavailability of PMFs is influenced by the number of methoxy- and hydroxyl groups on the flavone skeleton. Manthey, Cesar (*55*) found that the AUC of nobiletin was about 10-fold higher than tangeretin in the rat serum at the same dosage of 50 mg/kg. The absolute bioavailability of tangeretin is about 27%, when tangeretin is fully dissolved in the saline consisting of 10% Tween 80 and 20% DMSO (*52*). These *in vivo* studies indicate that the high bioavailability of PMFs may result from their good intestinal permeability, and the bioaccessibility is the limiting factor for their bioavailability enhancement.

Our *in vivo* study has shown that the viscoelastic emulsion can increase the bioavailability of nobiletin from 20% to 46%, as compared to the oil suspension (data not published). Therefore, tailoring delivery systems with the aim of bioaccessibility enhancement is a promising way to improve the bioavailability of PMFs. In recent years, multiple delivery systems have been developed to improve the bioaccessibility of PMFs, including nanoparticles (*56, 57*), emulsion systems (nanoemulsions, viscoelastic emulsions and Pickering emulsions) (*40, 58-61*), self-emulsifying systems (*62, 63*) and amorphous solid dispersions (*64, 65*). Limited studies have addressed the bioavailability-bioactivity relationships for PMFs *in vivo*. Ting, Chiou (*66*) found that the regulation on tumorigenesis was more effective by tangeretin emulsion than the unformulated suspension in the mice with azoxymethane (AOM)/dextran sodium sulphate (DSS) induced colitis related colon tumorigenesis. In a rat model with acute liver injury, the

treatment of amorphous solid dispersion of nobiletin had better attenuation effect on hepatic damage than the crystalline nobiletin (*64*). 5-demethyltangeretin loaded in self-microemulsifying system, compared to its suspended form, was more effective to inhibit the tumor growth in the colon cancer xenograft mice (*63*). These studies suggest that the higher bioefficacy of PMFs *in vivo* is associated with the increased bioavailability by delivery systems. However, the bioavailability-bioactivity relationship remains elusive for PMFs' regulation of metabolic syndromes.

1.3.2 Interplay with gut microbiota

Given the limited bioavailability, the major part of PMFs after oral administration will enter the colon and interact with gut microbiota harboring in this site. It is estimated that the gut microbiota weighs about 1-2 kg in our human bodies and the microbial genes exceed 100 times of the human genome (*28*). Therefore, there have been growing recognition of humans as the superorganism consisting of human and microbial cells (*67, 68*). Recent studies have demonstrated that the compositional change of gut microbiota is associated with the host's energy hemostasis, insulin sensitivity, lipid metabolism, and inflammation status (*69*).

The interaction of PMFs and gut microbiota is bidirectional: 1) the PMFs presented in the colon impact on the colonic microbial composition; 2) the gut microbiota will metabolize the PMFs and generate metabolites with higher bioactivity (further discussed in 1.3.3). Both the changed gut microbiota and altered PMFs contribute to the health benefits of PMFs. An *in vitro* study indicated that tangeretin and nobiletin showed anti-

microbial effect on *Pseudomonas fluorescens* and *Pseudomonas aeruginosa* by destroying the cell membrane permeability and inhibiting protein synthesis (*70*). Another *in vitro* study found that PMFs contributed the most anti-microbial activity against *Staphylococcus aureus* for the flavonoid fraction of the tangelos juice (*71*). In addition to the antimicrobial activity against pathogens, PMFs could selectively increase or decrease the relative abundance of specific bacteria in the colonic microbial community *in vivo* (*72-74*). For example, Tung, Chang (*72*) found that PMFs modulated gut microbiota via increasing *Prevotella* and decreasing *rc4-4* bacteria in the high fat diet (HFD) induced obese mice. Besides, PMFs shows prebiotics effect by improving probiotic bacteria in the colon digesta of mice, such as *Lactobacillus* (*72, 73*) and *Bifidobacteria* (*73*). The modulation of gut microbiota by PMFs is linked to the host's health benefit, which will be further discussed in section 1.4.

1.3.3 Biotransformation

In terms of the biological fate, the biotransformation of orally administered PMFs occurs in the colon by gut microbiota or in the host after absorption. For the microbial conversion, the common metabolic pathways of flavonoids include deconjugation, C-ring cleavage, decarboxylation, reduction, dehydroxylation and demethylation (*75, 76*). Once absorbed from the GIT, the flavonoids will undergo phase I and phase II metabolism in the gut-intestinal cells and subsequently in the liver via circulation system. The biotransformation enzymes involving in the phase I/II include cytochrome P-450, UDP-glucuronosyltransferases, glutathione *S*-transferases, sulfotransferases, etc. (*77*).

The common metabolic pathway of PMFs is demethylation. The bioconversion of

PMFs has received increasing attentions, since it generates demethylated metabolites with increased biological activity (*15*). For example, the urinary metabolites of nobiletin in mouse, 3′-demethylnobiletin, 4′-demthylnobiletin and 3′,4′-didemethylnobiletin demonstrate better anti-inflammation activity than nobiletin in RAW264.7 macrophage (*38*). 5-demethylnobiletin, identified as a minor demethylated metabolite of nobiletin in mouse urine (*78*), is more effective to inhibit colon cancer than nobiletin *in vitro* and *in vivo* (*79*).

Recent reports for the colonic biotransformation of PMFs are still very limited. The human intestinal bacterium, *Blautia* sp. MRG-PMF1 is reported to demethylate PMFs isolated from *Kaempferia parviflora* using the *in vitro* anerobic fermentation (*76, 80*). Several other bacteria are associated with the demethylation on polyphenols/flavonoids, such as *Eubacterium limosum, Eubacterium callanderi, Lactobacillus, Streptococcus* and *Clostridium (75).* In our recent excretion study, we collect and measure the metabolites profile of feces from rats every 12 hours within 48 hours after orally administered nobiletin. It is found that the demethylation extent (expressed by the concentration ratio of metabolites/nobiletin) increased with the colonic fermentation time. Moreover, the demethylation extent depends on the composition of microbiome: the microbiome of the obese rats yields higher extent of demethylated metabolites than the microbiome of normal rats. Long term administration of nobiletin and 5-demethylnobiletin inhibited the colitis driven colon carcinogenesis in mice (*81, 82*). In the colon mucosa of mice administered nobiletin and 5-demethylnobiletin, the three demethylated metabolites on the B-ring (3′-, 4′, and 3′,4′-positions) were about 20-fold and 1.56-fold higher than their parent compounds, respectively (*81, 82*). 4′, 5-didemethyltangertin (xanthomicrol) was identified

as the major metabolite of 5-demethyltangeretin with the demethylation on the 4′-position (*83*). The concentration of xanthomicrol in the mouse colon was about 3.1-fold higher than the 5-demethyltangeretin after 4-week feeding of 5-demethyltangeretin (*83*). These metabolites in the colon mucosa are suspected to be generated from the gut microbiota or intestinal cells of the mice. Given the high concentration of metabolites in the colon and their good bioefficacy on colon cells, it indicates that the chemopreventive effect of PMFs on the colitis is associated with their demethylated metabolites (*81, 82*).

1.3.4 The anti-inflammation effect on GIT

The metabolic syndromes are characterized as a systemic chronic inflammation (*8*). PMFs have shown good anti-inflammatory activities *in vitro* and in *vivo* studies, and their molecular mechanisms have been summarized in previous reviews (*9-11, 16*). The beneficial action of PMFs on inflammatory bowel disease (IBD) is a good example of their anti-inflammatory effect on GIT. IBDs are disorders characterized by chronic inflammation of the GIT, including Crohn's disease and ulcerative colitis (*84*). PMFs, , such as nobiletin (*81, 85, 86*), tangeretin(*87*), sinesetin (*88*), 5-demethylnobietin (*82*), etc. have been reported to attenuate colitis using the animal models. For these animal models, DSS and 2,4,6-trinitrobenzene sulfonic acid (TNBS) are often used to induce the colitis. The protective effect of PMFs might result from two aspects: the anti-inflammatory effect in the mucosa and interaction with gut microbiota.

The transcriptional factor nuclear factor-kappa B (NF-κB) is the important inflammatory and immunological manipulator that connect inflammation and metabolic response (*8*). The activation of NF-κB promotes the gene-coding of proinflammatory

cytokines/enzymes, such as interleukin-1β (IL-1β), interleukin-6 (IL-6), tumor necrosis factor-α (TNF-α), inducible nitric oxide synthase (iNOS) and cyclooxygenase-2 (COX-2).(*16*) The overproduction of prostaglandins E_2 and NO stimulated by iNOS and COX-2 is related to inflammation, DNA damage and tumorigenesis (*16*). In the colitis-associated colon carcionogensis mouse model, the oral intake of nobiletin and 5-demethylnobiletin can significantly decrease the levels of IL-6, IL-1β, TNF-α in the colon mucosa as compared to the control group (*81, 82*). Similarly, another research group find that nobiletin and sinensetin can decrease inflammatory cytokines level (e.g. IL-6 and IL-1β) and enzyme expression (e.g. MPO, iNOS and COX-2) in the colon using the TNBS-induced colitis rat model (*85, 88*). Both nobiletin and tangeretin demonstrate anti-inflammatory effect on the lipopolysaccharides (LPS)- and IgE-mediated stimulation in human intestinal mast cells (*89*). Moreover, this anti-inflammatory effect of nobiletin is observed in the IL-$10^{-/-}$ mice, since nobiletin treatment reduces the tissue damage, cellular infiltration, mast cell number and degranulation and fibrotic changes in the colon (*90*). Given higher concentration of demethylated metabolites were found in the colon mucosa (*81, 82*), the anti-inflammatory effect of PMFs *in vivo* is an overall outcome of PMFs and their metabolites.

The bacteria-derived LPS is identified as a triggering factor for the progression of inflammation and metabolic diseases (*91*). HFD feeding increases the proportion of LPS-producing microbiota and circulating concentration of plasma LPS (*69, 91*). For example, several LPS-produced bacteria are promoted by HFD, such as *Escherichia*, *Desulfovibrionaceae* and *Enterobacter* (*69*). Host recognition of the gut microbiota by Toll-like receptors (TLRs) controls the inflammatory response to LPS (*92*). Given the high

concentration of PMFs in the GIT, their modulation on gut microbiota is supposed to become the onset of their anti-inflammatory effect. A recent study finds that the microbial LPS synthesis pathway was suppressed by nobiletin via metagenomic analysis of the feces from HFD-fed mice (*93*). However, this linkage between PMFs and gut microbiota is poorly investigated for IBD. A relative study shows that PMFs have beneficial effect on gut microbiota modulation using the benzo[α]pyrene-DSS induced colorectal carcinogenesis mice (*94*). In particular, PMFs are supposed to increase the prevalence of butylate-producing probiotics (e.g. *Oscillospira* and *Ruminococcaceae*) and decrease the abundance of colorectal cancer (CRC)-related bacteria (e.g. *Porphyromonadaceae* and *Lactobacillus ruminis*) (*94*).

1.3.5 Intestinal barrier function

The intestinal mucosal barrier is regarded as the first line for the host to protect against commensal bacterial or invading pathogens (*48*). This physical barrier is composed of epithelium cells connected by tight junctions (TJ), which are multi-protein complexes span the intestinal membrane and provide tight, ion- and water-impermeable seals between cells (*48*). The interaction of TJ proteins (e.g. occluding, claudin family, and zonula occludens-1 (ZO-1) with actin cytoskeleton is linked to the cell polarity and permeability function (*95*). In addition, the epithelium is protected by the overlying intestinal mucus layer produced by goblet cells of the host. The disruption of the barrier function leads to the increased intestinal membrane permeability, which is associated with chronic diseases, such as IBD, obesity, etc. (*95*).

The internal barrier properties of PMFs are investigated by both *in vitro* cells study

and *in vivo* animal models. The trans epithelial electric resistance (TEER) was used to evaluate the barrier function in the cell lines (Caco-2 and RAW264.7 cells) (*85, 88, 96*). The LPS and TNF-α induced cells has a defective barrier function and a lower TEER values than the untreated cells. Nobiletin and sinensetin are reported to alleviate the decrease of TEER in the barrier dysfunction cell models (*85, 88*). Moreover, PMFs shows protective effect on the intestinal barrier function in the DSS-induced and TNBS-induced colitis mouse/rat model (*85, 86, 88, 96*). The protective mechanisms of PMFs are found to associate with the inhibition of Akt-NF-κB-myosin light chain kinase (MLAK) pathway (*85*) and the activation of 5'-adenosine monophosphate-activated protein kinase (AMPK)-UNC-51 like autophagy activating kinase 1(ULK1) pathway (*88*). In addition, the beneficial role of PMFs may results from their regulation on the TJ. For example, nobiletin is found to upregulate the expression of TJ proteins, including ZO-1 (*96*), occluding (*96*), claudin-2 (*96*), claudin-5 (*97*) and claudin-7 (*86*).

The gut microbiota receives increasing research attentions due to its role on intestinal barrier function. The long-term HFD feeding leads to intestinal barrier dysfunction, characterized by reduced expression of TJ proteins, mucus layer thickness and anti-microbial peptide production (*95, 98, 99*). *Akkermansia muciniphila*, a mucin-degrading bacterium and residing in the mucus layer, is reported to increase the levels of intestinal acylglycerols and improve the barrier function (*99*). In our recent study, PMFs-supplemented diet could reverse the reduction of *Akkermansia* spp. caused by HFD in the mouse model (*73*). Moreover, the fecal short chain fatty acids (SCFA) was increased by PMFs in a dose dependent manner (*73*). The microbiota-derived SCFA not only provide energy source for the colonocyte, but also enhance the barrier function and maintain

intestinal homeostasis (*34, 100, 101*).

1.4 PMFs-mediated metabolic syndromes

PMFs have shown multiple health benefits against the MetS. This part will focus on the molecular mechanisms and possible pathways of the beneficial effect of PMFs on: 1) the regulation of circadian clock; 2) the regulation of lipid metabolism and dyslipidemia; 3) the regulation of glucose metabolism and insulin sensitivity; 4) anti-obesity activity; 5) the protection against cardiovascular diseases.

1.4.1 Regulation of Circadian clock

The circadian clock is the biological process with intrinsic and entrainable oscillations in response to daily environmental changes, especially the light-dark cycles. Almost all organisms ranging from microorganisms to humans on the earth develop the timing system of circadian clock (*102*). The clock circadian in mammals is hierarchically organized to affect various physiological processes: the suprachiasmatic nuclei (SCN) in the hypothalamus is the central pacemaker that coordinates the circadian rhythms in peripheral tissues (*103*). Several factors may lead to the circadian misalignment for animals and humans, such as unregular light shift, meal timing and nutritional challenge (e.g. HFD) (*104*). The circadian misalignment is associated with increased risks of metabolic disorders, including obesity and diabetes (*105*). Very recently, PMFs, especially nobiletin, are found to improve metabolic homeostasis by enhancing circadian functions (*93, 106, 107*).

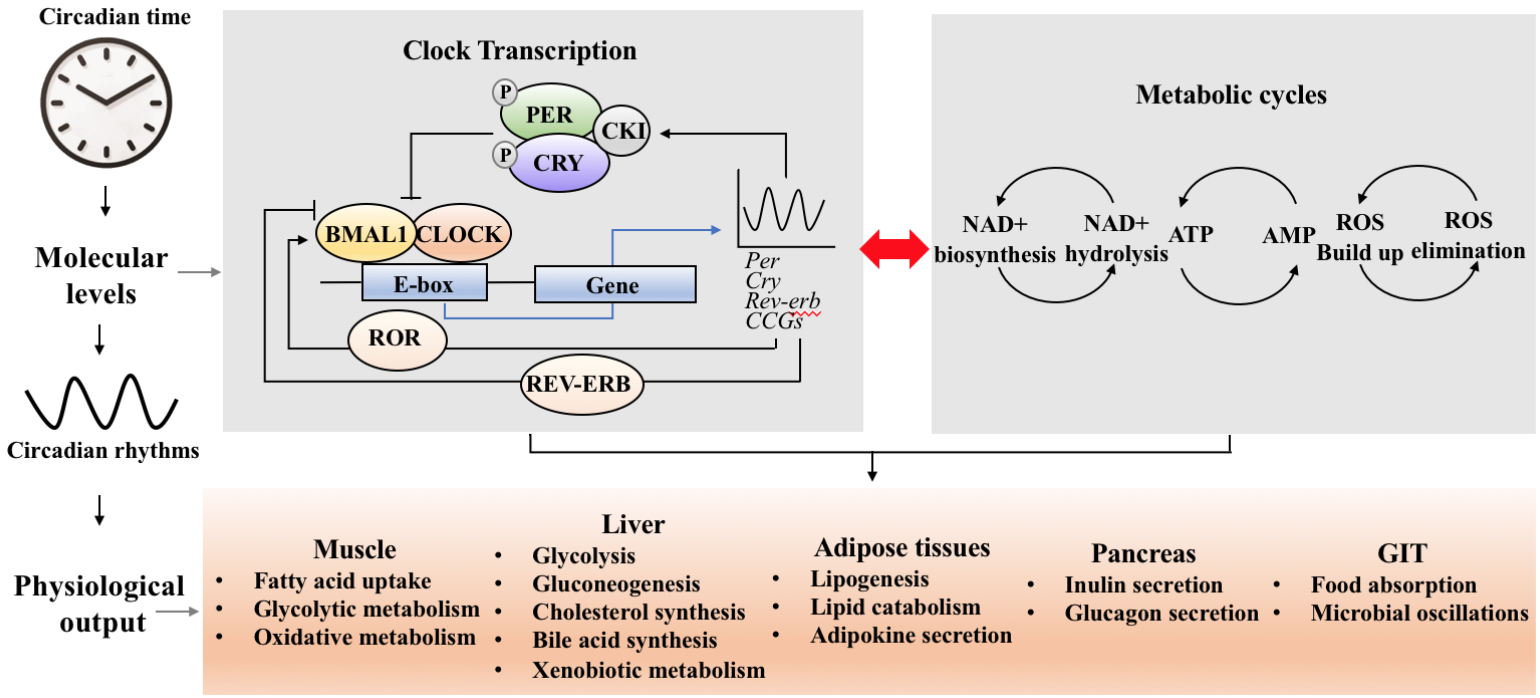

Figure 3: The molecular mechanisms of circadian clock and physiological output

1.4.1.1 The interplay of circadian clock and metabolic signals at the molecular level

The circadian clock is coordinated by the transcriptional-translation feedback loops involving the transcriptional activators CLOCK and BMAL1 as well as period proteins (PERs) and cryptochromes (CRYs) (*108*), as shown in **Fig. 3**. The dimerization of CLOCK and BMAL1 activates the transcription of multiple targeted genes through E-box promoter elements, such as *Per*, *Cry*, nuclear hormone receptor (*Rev-erb*) and clock controlled genes (CCGs). The translated PERs and CRYs are accumulated rhythmically and form heterodimer which in turn represses the CLOCK-BMALl. This core loop is post-transcriptionally regulated by casein kinases (CK1) targeting PERs degradation and adenosine monophosphate (AMP) kinase targeting CRYs degradation (*103*). In addition to the core feedback loop, the REV-ERBs and retinoid acid receptor-related orphan receptors (RORs) in the stabilization loop completely bind to shared consensus elements and promote the robust oscillatory of *Bmal1* expression (*102*).

There is reciprocal control between clock and metabolic signaling (**Fig. 3**). On the one hand, the clock transcription factors have direct and indirect influence on the regulation of metabolic genes. The genetic and genomic analysis demonstrates that many genes embedded in metabolic pathways are under circadian regulation, especially for the glycogenesis, cholesterol synthesis and xenobiotic metabolism in the liver (*109*). Many studies have found that mice with clock gene deletion have impaired glucose-, lipid-, and energy homeostasis (*105*). The cycling of circadian transcriptional activators and repressors regulates the oxidative phosphorylation, gluconeogenesis, vesicle trafficking, RNA processing and protein translation by influencing the metabolic cycles in various

peripheral tissues, such as nicotinamide adenine dinucleotide (NAD^+) biosynthesis cycle, kinase cycle and peroxiredoxin cycle (**Fig 3**) (*108, 110*). For example, CLOCK-BMAL1 controls the gene expression of nicotinamide phosphoribosyltransferase (*Nampt*), and thus influencing the cycling of NAD^+ and the related enzymes. The NAD-dependent deacetylases-SIRT1 and SIRT6 are regulated by circadian clock; and in the meanwhile they participate in many metabolic processes (*104*). SIRT1 is found to involve in inflammation, cellular metabolism and aging (*111*), while SIRT6 involves in lipid and carbohydrate metabolism(*104, 112*).

On the other hand, the clock also receives the input of metabolic flux and nutrient signaling (*108, 110*). For example, *Bmal1* transcription is modulated by peroxisome proliferator-activated receptor α (PPARα) and proliferators-activated receptor gamma coactivator 1-α (PGC1α) (*113*). AMPK, a widely investigated energy regulator, provides metabolic information to circadian clock by mediating the phosphorylation and degradation of CRYs (*114*). NAD-dependent deacetylases (e.g. SIRT1 and SIRT6) influenced by clock circadian can in turn feedback to interact with CLOCK-BMAL1 complex (*110, 112*).

1.4.1.2 The physiological output of circadian clock and metabolic signals

The physiological output of this reciprocal interaction between clock circadian and metabolic cycling is tissue-specific (*108*). The metabolic processes under circadian control in peripheral tissues are shown in **Fig 3**. For example, the liver clock promotes the synthesis of glycogen cholesterol and bile acid in the wake/feeding period, while it promotes glycogenolysis and gluconeogenesis in the sleep/fast period. In the GIT, both intestinal

epithelium cells and gut microbiota have the circadian rhythms, as various intestinal activities (e.g. food digestion, gastrointestinal motility, gastric empty and nutrition absorption) occur in a circadian pattern (*104, 115*). In particular, accumulating studies have found that gut microbiota play a critical role on the clock-metabolism interplay in the host (*104, 116, 117*). The food components and feeding rhythms influence the diurnal oscillations of gut microbiota, leading to the profile change of microbial composition, metabolites (e.g. SCFA) and function over the course of a day (*116, 117*). The microbial dysbiosis is linked to the metabolic status of the host. A good example is that the microbial dysbiosis induced by jet-lag promotes obesity in mice; and the obesity is transferable in the germ-free mice receiving fecal transplantation of the jet-lag microbiome (*117*). Besides of the liver and GIT, important physiological processes responsible for metabolic homeostasis in the muscle, adipose tissues and pancreas are found to have circadian rhythms.

1.4.1.3 Advances of PMFs regulation on circadian clock

Even though PMFs are studied for their health benefit of metabolic homeostasis for years, the investigations of PMFs' role on circadian clock are still in their infancy. A recent state-of-the-art study finds that nobiletin, as well as tangeretin, enhances the *PER2::Luc* rhythm using fibroblasts after chemically screening a large group of small molecules (*106*). Similarly, another cell study shows that nobiletin increases the amplitude, lengthens the period and delays the phase of *PER2::Luc* rhythm in fibrolasts (*118*). Besides, nobiletin demonstrates good anti-obesity effect in the wild type C57BL/6J mice fed with HFD, while this anti-obesity effect is not significant in the HFD-fed clock-disrupted $Clock^{\Delta 19/\Delta 19}$ mice (*106*). It indicates that the bioefficacy of nobiletin against MetS may rely on its modulation

on clock circadian to some extent. Moreover, nobiletin improves the clock transcript oscillations in the livers of HFD-fed mice (*106*). This benefit of nobiletin is associated with its activation on RORs, which plays important roles on circadian rhythms in the stabilization loop of molecular oscillators (*102, 106*). The interplay of clock and glucose/lipid metabolism was further investigated in hepatocytes (*107*). Using the palmitate-treated HepG2 and primary hepatocyte cells, nobiletin is found to restore the circadian rhythms, improve glucose uptake via stimulating insulin receptor substrate 1 (IRS-1)/Akt pathway, modulate lipid metabolism via AMPK/SIRT1 pathways and reduce the overproduction of ROS (*107*). After the silence of Bmal1 in the hepatocytes using small interfering RNA (siRNA), the modulation effect of key enzymes by nobiletin was dampened, including the p-IRS-1, p-AKT, p-AMPK, and p-ACC (*107*). It suggests that nobiletin regulates cellular glucolipid homoeostasis in a Bmal1-dependent manner. Besides of the liver, the pancreas is found as another peripheral organ targeted by nobiletin (*119*). The secretion of inulin and glucagon by pancreatic islet β- and α- cells is under the clock control (*120*). The islets from T2D patients have dampened amplitudes of clock rhythms, as compared to the healthy controls (*119*). The treatment of nobiletin on these T2D islet cells can boost the circadian amplitude and insulin secretion (*119*). Similar to nobiletin, PMFs from *Kaempferia parviflora* are reported to enhance the amplitude, extend the period and delay the phase in NIH3T3 cells (*121*). Moreover, the extracts of *Kaempferia parviflora* supplemented diet help mice more quickly to adapt to the jet lag (6-hour phase advance) by monitoring the locomotor activity rhythm (*121*).

Aging is associated with increasing risks of chronic diseases and declined metabolic functions (*102*). Multiple age-related physiological processes have shown impaired clock

rhythms, such as SCN firing rate, body temperature and hormone (e.g. cortisol and melatonin) secretion (*102*). As the clock modifier, nobiletin improves the metabolic fitness (e.g. locomotor activity, sleep consolidation, body temperature and median lifespan) in aged mice fed with regular diets (*122*). Moreover, nobiletin is found to modulate cholesterol metabolism and mitochondrial respiration in the metabolic challenged (HFD-fed) aged mice (*93, 122*). Previous studies have indicated that the nuclear receptors-- RORs and REV-ERB in the circadian stabilization loop (shown in **Fig. 3**) also function in the lipid homeostasis, cholesterol metabolism and bile acid (BA) synthesis (*123-125*). Nobiletin, as the target of RORs, decreases the serum LDL/VLDL and LDL/HDL level, prevents serum BA leakage, improves the hepatic genes for BA synthesis and remodels BA-related gut microbiota in aged mice fed with HFD (*93*). In addition, the RORs-nobiletin axis fortifies the mitochondrial respiration in the skeletal muscles of HFD-fed aged mice, which leads to increased ATP production and decreased ROS generation (*122*).

1.4.2 Regulation of lipid metabolism and dyslipidemia

The dyslipidemia is characterized as the abnormal high level of lipids (e.g. cholesterol and triglycerides (TG) in the blood, which is regarded as an important contributor for the enhanced lipid deposition in tissues (*126*). Accumulating studies have found that PMFs attenuate the dyslipidemia *in vivo*. 1% PMFs-supplemented diet effectively reduces the total cholesterol (TC), LDL and VLDL in the serum of hamsters with diet-induced hypercholesterolemia (*12*). In addition, daily intake of 62.5mg/kg and 125 mg/kg PMFs for 4 weeks significantly decrease the serum TC and TG level in the hamsters with fructose-induced insulin resistance (*127*). The modulation on serum lipid

profile in HFD-fed mice/rats, especially the lowering effect of LDL/vLDL, has been observed for nobiletin (*128, 129*), tangeretin (*130*), heptamethoxyflavone (*131*), sudachitin (*132*) respectively. The adipose tissues and liver are important organs for the lipid metabolism. Thus, 3T3-L1 and HepG2 cells models are usually used to investigate the regulatory mechanisms of PMFs on lipid metabolism at the molecular level.

Evidenced by 3T3-L1 cell studies, PMFs involve in the cellular lipid metabolism by inhibiting adipogenesis/lipogenesis, promoting fatty acid oxidation and modulating the secretion of adipocytokines. Nobiletin is found to significantly reduce the lipid accumulation in 3T3-L1 cells by activating AMPK pathway and blocking the expressions of adipogenesis transcription factors, such as PPARγ and CCAAT/enhancer binding proteins(C/EBPα) (*133*). The regulation of PPARγ and C/ EBPα is important for growth arrest of the preadipocytes in their early stage of differentiation (*134*). Similar inhibitory effect on adipogenesis was also observed for other PMFs, e.g. heptamethoxyflavone (*135, 136*). Lipogenesis occurs in the late stage of adipocyte differentiation and is characterized as the extensively increased synthesis of fatty acids and triacylglycerols (*134*). SREBP-1 is a lipogenesis-related transcriptional factor, which increases the expression of lipogenic enzymes, such as acetyl-Co A carboxylase(ACC) and fatty acid synthase (FAS) (*134*). PMFs and hydroxyl PMFs are reported to inhibit lipogenesis in adipocytes by decreasing the expression of SREBP-1, ACC and FAS (*136, 137*). The breakdown of triacylglycerol in cells includes two steps: 1) hydrolyzing triacylglycerol by lipases (e.g. hormone-sensitive lipase(HSL)) and releasing fatty acids; 2) degrading fatty acids in the mitochondria via β-oxidation (*134*). A recent study finds that nobiletin induces 3T3-L1 cell to the brown adipocyte-like phenotype (*138*). The brown adipocytes, compared to white

adipocytes, are characterized as higher thermogenic ability and mitochondrial content as well as much extensive expression of brown fat-related genes, such as uncoupling protein 1 (UCP1), PR domain-containing 16/encoding gene (PRDM16), peroxisome proliferator-activated receptor gamma co-activator 1-alpha (PGC-1α) (*134, 138*). The binding of PGC1-α and PPARα stimulates the mitochondria biogenesis and fatty acid oxidation (*126*). The activation of browning in white adipocytes by nobiletin lead to enhanced expression of lipases (e.g. HSL), PGC1-α and PPARα (*138*). Therefore, the augmentation of lipid catabolism might be another reason for the reduced lipid accumulation by PMFs in 3T3-L1 studies. Besides of lowering lipid accumulation, nobiletin and tangeretin regulate adipocytokine secretion in 3T3-L1 cell via stimulating the insulin-sensitizing factor-adiponectin and inhibiting the insulin-resistance factor-monocyte chemoattractant protein(MCP)-1 (*24, 139*).

Liver is the critical organ regulating the glucose, lipid/lipoprotein and cholesterol metabolism (*140*). Although primary hepatocytes are ideal to investigate the hepatic metabolism, HepG2 cells are more widely used due to their easy access. HepG2 cells are commonly used as the *in vitro* models for the hepatic production of apolipoprotein B (apoB), which comprises apolipoproteins with LDL and vLDL (*141*). Kurowska, Manthey (*141*) find that the exposure of HepG2 with 72.8 μM tangeretin significantly inhibits the net secretion of apoB as well as the intracellular synthesis of triacylglycerol, free cholesterol and cholesteryl esters. Similarly, nobiletin is found to reduce apoB secretion in HepG2 by activating the mitogen-activated protein kinase (MAPK)-extracellular signal-related kinase (ERK) signaling pathways (*128*). In terms of the structure-function

relationship, nobiletin and tangeretin have stronger inhibitory effect on the apoB secretion, cholesterol synthesis and TG synthesis in HepG2 cells, as compared to sinensetin and other citrus flavanones (e.g. naringenin and hesperetin) (*13*). The underlying mechanisms of the lipid lowering effect of PMFs are explored in HepG2 and primary hepatocytes via : 1) activating AMPK pathways and inhibiting lipogenesis-related genes' expression (e.g. FAS and stearoyl-CoA desaturase) (*107*) (*142*); 2) activating pathways involving in fatty acid oxidation (e.g.PGC-1α) (*107, 128*); 3) increasing the gene expression of LDL receptor (LDLR) and stimulating LDL uptake (*128, 143*); 4) activating MAPK-ERK pathways and inhibiting the expressions of microsomal triglyceride transfer protein (MTP) and diacylglycerol acyltransferase (DGAT) (*128, 141*).

1.4.3 Regulation of glucose metabolism and insulin resistance (IR)

The chronic hyperglycemia and defective insulin sensitivity increase the risks for the development of diabetes and cardiovascular disease (*144*). In particular, hyperglycemia and insulin resistance are associated with excessive oxidative stress, increased inflammatory state, mitochondrial dysfunction, etc. (*144, 145*). Moreover, there is a crosstalk between the adipocyte and liver/muscle in terms of the systemic lipid- and glucose- homeostasis, since the dysfunctions of adipokines (e.g. adiponectin and MCP-1) would contribute to insulin resistance (*23, 146*).

PMFs have shown to maintain glucose homeostasis through *in vitro* and *in vivo* studies. Glucose transporters (GLUT) are group of membrane proteins that promote the transport of glucose across the cell membrane. For example, GLUT4 plays important roles on glucose homeostasis and the dysfunction of GLUT4 is associated with insulin resistance

and diabetes (*147*). Qi, Guo (*107*) find that nobiletin increases the glucose uptake in the HepG2 cells treated with palmitate. Specifically, nobiletin is reported to modulate the phosphorylation of insulin receptor substrate 1 (IRS-1), increase the expression of GLUT2, and promote the phosphorylation of glycogen synthase kinase-3 (GSK) (*107*). Tangeretin is found to increase the glucose uptake and promote GLUT4 translocation from the cytosol to plasma membrane in C2C12 myotubes via AMPK signaling pathways (*148*). Sudachitin (5,7,4′-trihydroxy-6,8,3′-trimethoxyflavone) enhances the expressions of GLUT1 and GLUT3 in the skeleton muscle myocytes *in vitro* (*132*). The *in-vitro* inhibitory effect on α-glucosidase activity by 5-demethylnobiletin (12.86 ± 7.13%) and 5-demethylsinensetin (17.18 ± 8.33%) is not very significant at the concentration of 0.75 mM, but these two PMFs show moderate anti-hyperglycemic effect using the rat model (*149*). This suggests that some other mechanisms may contribute to the regulation of PMFs on glucose metabolism.

The commonly used methods to evaluate glucose homeostasis and insulin sensitivity *in vivo* are glucose tolerance test (GTT) and insulin tolerance test (ITT). PMFs have shown to improve glucose homeostasis in different animal models. Using the high fructose diet induced IR hamsters, the treatment of PMFs (62.5- and 125 mg/kg) for 4 weeks can decrease the serum insulin level and improve the impaired insulin sensitivity (measured by GTT), as compared to the control group (*127*). Similar effect is also observed in C57BL/6J mice fed with PMFs-supplemented HFD for 15 weeks: PMFs extracted from the aged peels effectively prevent the hyperglycemia/hyperinsulinemia and improve insulin sensitivity according the results of GTT and ITT (*150*). In particular, nobiletin is reported to attenuate hyperglycemia and insulin resistance in the HFD-induced obese mice, obese diabetic *ob/ob*

mice and HFD-fed LDLR-deficient ($Ldlr^{-/-}$) mice (*128, 146, 151*). Lee, Cha (*146*) suggest that the modulation effect of nobiletin on glucose homeostasis *in vivo* may result from its regulation of adipokines production in WAT and gene expressions of GLUT1, GLUT4 in WAT and muscle. In terms of the tissue-specific effect of insulin, nobiletin enhances the skeleton muscle insulin sensitivity evidenced by reduced TG in muscles and normalized peripheral glucose disposal (*128*). Besides, nobiletin increases the hepatic insulin sensitivity evidenced by hyperinsulinemic-euglycemic clamps studies and pyruvate tolerance test (*128*). The oral administration of tangeretin (100 mg/kg) for 30 days significantly decreases the plasma glucose, restores the carbohydrate metabolic enzyme activities in the liver, restores the GLUT4 expression in the heart of streptozotocin-induced diabetic rats (*152, 153*). Similarly, sudachitin is also reported to increase GLUT4 expression in the liver and muscle in the DIO mice (*132*).

A randomized, placebo-controlled and double-blind human study finds that the PMFs supplementation is helpful to reduce the glucose tolerance, TC and LDL in participants (n=19) with mild hyperglycemia (100-150 mg/dL fast glucose) (*154*). The treated groups receives 2*525 mg/day Diabetinol^{TM}, which contains more than 62% PMFs extracted from orange peels with the concentration ratio 4:1 for nobiletin and tangeretin (*154, 155*). After 84-day treatment, Diabetinol^{TM} shows significant reduction ($P<0.01$) in plasma glucose at 30, 60 and 120 minutes after GTT as compared to the initial level at the 0-day treatment, while the placebo has similar effect on GTT during the experiment (*154*).

1.4.4 Anti-Obesity

The obesity epidemic is recognized as the worldwide public health concern. Due to

the imbalance of energy intake and expenditure, obesity is developed with the main phenotypes of excessive fat accumulation, insulin resistance, low-grade systemic inflammatory state, etc. (*67*). Recent studies demonstrate that PMFs process good anti-obesity activities, especially in the HFD-induced obese animal models (*9, 15*).

Several studies have found that the PMFs extract from different sources of citrus peels can effectively prevent the body weight gain, hepatic lipid accumulation and the mass of adipose tissues in the HFD-induced obese mice (*72, 74, 150, 156, 157*). Besides, PMFs extract also improve the insulin sensitivity and plasma lipid profiles (e.g. lowering TC, apoB100, or TG) in those diet induced obese (DIO) mice (*74, 150, 156*). Moreover, the PMFs extract/mixture with higher concentration of hydroxyl PMFs have better anti-obesity effect (*72, 137*). Besides of investigating the overall effect of PMFs extract, several PMFs are studied individually for their anti-obesity effect, including nobiletin (*128, 151, 158*), tangeretin (*130*), 3,5,6,7,8,3′,4′-heptamethoxyflavone (*131*), sudachitin (*132*), etc. Inspired by the concept of prodrugs, our previous study obtains 5-acetyloxy-6,7,8,3′,4′-pentamethoxyflavone (5-Ac-Nob) through chemical modification of 5-demethynobiletin in order to enhance its bioavailability (*159*). 5-Ac-Nob is more effective to reduce the TG accumulation than 5-demthylnobieltin in 3T3-L1 studies, and effectively attenuates lipid accumulation by triggering AMPK pathways in DIO mice (*159*). Since excessive fat and insulin resistance are typical phenotypes of obesity, many studies explore the molecular mechanisms of PMFs on obesity prevention in the views of regulating lipid- and glucose homeostasis (discussed in parts 1.4.2 and 1.4.3). Several pathways might contribute to the anti-obesity activity of PMFs using the animal models: 1) activating AMPK pathways and inhibiting lipogenesis in the liver and adipose tissues (*137, 150, 159*); 2) promoting the

expressions of enzymes involving in lipolysis and fatty acid oxidation in the liver and adipose tissues (*128, 129, 131, 156*); 3) promoting the expression of thermogenesis/browning genes (e.g. UCP1 and PRDM16) in brown- and white adipose tissues (*157*); 4) modulating the expressions of adipokines in the adipose tissue (*129, 151*); 5) inducing mitochondrial respiration and energy expenditure (*14, 122*); 6) improving hyperglycemia and insulin sensitivity (*128, 132, 150*), 7) decreasing the secretion of pro-inflammatory cytokines in the liver and plasma (*129*).

The interplay with gut microbiota is received increasing research interest for PMFs' role on obesity prevention. The variation of gut microbiota is regarded as a critical factor for the pathogenesis of obesity (*34, 67*). Given its numerous genes and cells, gut microbiota harbors a lot of functions, which can be selectively influenced by diets and closely associated with the host's metabolic diseases (*160*). The critical impact of gut microbiota on obesity can be observed from the germ-free mice, which is resistant to the HFD-induced obesity. Studies have found that germ free mice receiving fecal microbiota transplantation (FMT) from obese- or jet-lag donors have more significant weight gain and fat accumulation than those receiving FMT from normal donors (*67, 117*). Many dietary polyphenols, as an important component in human diets, are found to modulate gut microbiota and attenuate the HFD-induced obesity (*69*). The altered composition of gut microbiota has local effect in the GIT: it influences the microbial energy harvest from the diets; colonic metabolism for nutrients and polyphenols; GIT gene reprograming; intestinal permeability control, etc. (*34*). Besides, the microbial metabolites can be absorbed into circulation system, and thus having the systemic effect for obesity development/prevention. The colonic metabolites of polyphenols might enhance the bioactivity of the parent

compounds (*75, 77*). Other microbial metabolites or signals released by GIT might interact with remote organs and regulate the metabolic homeostasis in the host, such as SCFA, LPS, bile acids (BA), brain chain amino acids (BCAA), gut hormones (GLP-1, CCK, PYY), etc. (*34, 69*).

The studies of PMFs and gut microbiota remain very limited. The compositional change of gut microbiota by PMFs seems not quite consistent in the studies using the DIO mice (*72-74, 93*). Several factors might contribute to this difference: initial microbiome, environment, compositions and dosage of PMFs, treatment time, and diets compositions. The reduced ratio of Firmicutes to Bacteroidetes has been observed by PMFs treatment, which indicates that PMFs might lower the microbial efficacy of energy harvest (*73, 74*). Two studies have found that PMFs enhance the relative abundance of *Allobaculum* and *Lactobacillus* in feces as compared to the HFD control group (*72, 73*). Moreover, Zhang, Zhu (*73*) find that the dynamics between *Allobaculum* and *Akkermansia* in the colonic digesta was influenced by PMFs treatment in a dose- and time- dependent manner. Zeng, Li (*74*) find that PMFs significantly enrich *Bacteroides ovatus*, and daily gavage of *Bacteroides ovatus* for 8 weeks can effectively attenuate obesity in HFD-fed mice. Several commensal bacterial involving BA metabolism are altered by PMFs treatment (*73, 93*), such as *Acetatifactor* and *Bilophila*. Besides of the microbial compositional change, recent advanced techniques (e.g. LC-MS, GC-MS, NMR, metagenome sequencing) allow us further investigated the colonic metabolites as well as the altered gene pathways. Our recent rat excretion and pharmacokinetics study of nobiletin indicates that gut microbiota has greater demethylation activity than the host and might yield more diversified demethylated nobiletin or even ring-fission metabolites (unpublished data). PMFs

treatment increases the fecal SCFA (*73*), which have multiple beneficial roles on obesity control, such as gut barrier maintenance, inhibition of pathogenic microbes, AMPK pathways activation in liver and adipose tissues, appetite control, etc. (*34*). Different from SCFA, higher circulating levels of bacterial-derived BCAA and LPS are related to higher risks for obesity (*69*). Through the metabolic profiling analysis, PMFs are found to regulate the BCAA in the feces and host serum (*74*). In particular, the circulating levels was significantly reduced by PMFs for valine, leucine, isoleucine and phenylalanine ($P< 0.05$) (*74*). Nohara, Nemkov (*93*) find that nobiletin reduces the microbial pathways of LPS biosynthesis through analyzing the functional target profiles of nobiletin treatment as compared to the HFD control group. Together, recent studies suggest that gut microbiota is an important pathway for the anti-obesity effect of PMFs.

1.4.5 Regulation of Cardiovascular Disease (CVD)

CVD is the number one cause of deaths in developed countries; and the diet is considered as a main contributor for the development of CVD (*161*). Many *in vitro* and *in vivo* studies have shown that PMFs demonstrate protective roles against the CVD, especially for atherosclerosis (*9, 144, 162*). In recent findings, gut microbiota, as the "metabolic filter" of our diet, is linked to CVD (*100, 161*). Dietary polyphenols, such as tea polyphenols and apple polyphenols, are reported to involve in CVD prevention by modulating gut microbiota (*163*). However, the linkage between PMFs and gut microbiota and its role on CVD prevention remains unclear and needs further investigations.

Atherosclerosis is the leading cause for CVD. The atherosclerotic lesions are formed by by the accumulation of lipoproteins and monocyte-derived macrophages within the wall

of arterial blood vessels (*164*).The protective effect of PMFs on atherosclerosis may come from two aspects: 1) reducing the circulating levels of apoB, LDL, VLDL (detailed discussions refer to 1.4.2); 2) preventing macrophage-derived foam cell formation and lesion development in the vessel wall. Several scavenger receptors (SRs) in the macrophage are found to recognize and uptake modified LDL, such as CD36, class A scavenger receptor (SR-A) and lecithin-like oxidized LDL receptor-1 (LOX-1). The over-expressions of SRs lead to foam-cell formation, and have pro-atherogenic effect *in vivo* (*165*). Nobiletin (100μM) effectively inhibits (50-72%) the SR-A mediated metabolism of acetylated LDL (acLDL) in J774A.1 macrophages (*164*). Besides, nobiletin remarkably reduces the expressions of SRs and adhesion molecules induced by 12-O-tetradecanoylphorbol-13-acetate (TPA) in THP-1 human monocyte-like cells (*166*). Moreover, the *in vivo* metabolites of nobiletin (3′-demethylnobiletin, 4′-demethylnobiletin and 3′,4′-didemethylnobiletin) show comparable or even higher inhibitory activity on SRs than nobiletin (*166*). 5-demthylnobiletin, a bioactive accumulating in the aged citrus peels, also exhibits higher potential to prevent the monocyte-to-macrophage differentiation and foam-cell formation than nobiletin in THP-1-derived macrophage (*165*). Similar structure-relationship has been observed for heptamethoxyflavone and 5-demethylheptamethoxyflavone (*167*). Both heptamethoxyflavone and 5-demethylheptamethoxyflavone effectively inhibit the uptake of oxidized LDL in THP-1 cells with the later having higher inhibitory effect (*167*).

Some other factors may contribute to the cardioprotective effects by PMFs directly or indirectly: 1) preventing the proliferation and migration of vascular smooth muscle cells (VSMC); 2) lowering oxidative stress and systemic inflammation; 3) preventing the

development of atherosclerotic plaques; 4) modulating platelet function, etc. (*144, 162*). Tangeretin was found to prevent the proliferation and migrations of rat aortic smooth muscle cells by inhibiting the PI3K/AKT signaling pathways (*168*), and effectively reduce the blood pressure in the hypertensive rats (*169*). Besides, tangeretin reserves the cardiac mineral metabolism and membrane-bound ATPase activity by lowering the cellular oxidative stress and proinflammatory cytokines in the streptozotocin-induced diabetic rats (*152*). Nobiletin supplementation (0.3% in diets) reduces the plaque area by 83% in $Ldlr^{-/-}$ mice after 26-week HFD feeding, as compared to the HFD control group (*128*). Moreover, nobiletin also demonstrates beneficial effect in the intervention model using $Ldlr^{-/-}$ mice with diet-induced obesity (*14*). The treatment of nobiletin (0.3% in diets) for 12 weeks does not alter the atherosclerotic lesion size, but effectively reduces the aortic cholesterol accumulation and plaque macrophage content (*14*). Platelet dysfunction is involved in the pathogenesis of thrombosis and CVD (*144*). Both tangeretin and nobiletin are found to modulate plate signaling and function using *in vitro* and *in vivo* models (*170, 171*). In detail, tangeretin and nobiletin suppress the thrombus formation by inhibiting platelet aggregation, granule secretion, integrin αIIbβ3 inside-out and outside-in signaling, calcium mobilization and platelet adhesion (*170, 171*).

The microbial modulation of CVD receives increasing attentions in recent years (*100, 161, 163*). The diet is the important factor shaping the microbial community, and gut microbiota can convert nutrient into microbial metabolites. Several microbial metabolites affect the CVD pathogenesis, such as trimethylamine N-oxide (TMAO), BA, SCFA, LPS, etc. (*100, 163*). For example, the bile acid metabolism is altered in patients with chronic heart failure: their serums contain higher level of primary BA and lower level of gut

microbiota-derived secondary BA, compared to the healthy controls (*172*). Even though PMFs have shown cardioprotective effect, very limited studies have unraveled the microbiota-host interaction. Two recent studies have found that PMFs can attenuate the harmful effect caused by TMAO *in vivo* (*173, 174*). The precursors of TMAO are trimethylamine (TMA) containing compounds, which are abundant in animal diets or high-fat foods, such as choline, L-carnitine, phosphatidylcholine, betaine, etc. (*100*). Gut microbiota can cleavage these precursors and release TMA through serval identified microbial enzyme complexes (e.g. CutC/D, CntA/B and YeaW/X) (*100*). TMA then enters the circulation system and is bio-transformed into TMAO by flavin monooxygenases (FMO) in the liver (*161*). The high level of TAMO is associated with high risks for CVD in both animal- and clinical studies (*175, 176*). PMFs show protective effect against TMAO in animals treated with choline chloride and L-carnitine (*173, 174*). Nobiletin is found to reduce cardiovascular inflammation by lowering the systemic oxidative stress and pro-inflammatory cytokines in choline chloride treated rats (*174*). Chen, Li (*173*) find that PMFs remarkedly reduce the plasma TMAO, hepatic FMO3 mRNA levels and vascular inflammatory marker-vascular cell adhesion molecule-1 (VCAM-1) in mice treated with L-carnitine. Moreover, PMFs increase the relative abundance of *Bacteroides* and *Akkermansia* in the cecum, compared to L-carnitine-treated control group (*173*).

1.5 Conclusions

Given the increasing obesity prevalence among adults, the MetS is becoming a common health concern in our modern life. The metabolic homeostasis *in vivo* is regulated by the crosstalk of CNS and peripheral organs, such as the adipose tissues, pancreas, liver,

muscle and GIT. PMFs have local effect on gastrointestinal tract (GIT) by interacting with gut microbiota and intestinal membrane; and also have systemic effect after entering or releasing signal molecules into the circulation system. The molecular mechanisms or possible pathways have been discussed for PMFs' modulation on metabolic disorders, including improving clock dysfunction, dyslipidemia, insulin resistance, obesity and cardiovascular disease. This review would strength the mechanistic understanding of PMFs' health benefits and provide scientific support for functional food development for PMFs.

CHAPTER II: I AGED CITRUS PEEL (CHENPI) EXTRACT CAUSES DYNAMIC ALTERATION OF COLONIC MICROBIOTA IN HIGH-FAT DIET INDUCED OBESE MICE

2.1 Introduction

Obesity is becoming a worldwide public concern in recent years. Considering the negative health impact and huge economic burden on individuals, effective dietary interventions/strategies are urgently needed for obesity prevention. In the food research area, identification of natural bioactive compounds with anti-obesity activity has received increasing attentions due to their excellent bio-efficacy and long-term safety (*177*). Some dietary phytochemicals including polyphenols, terpenoids, phytosterols and organosulfur compounds have demonstrated high potential to counteract obesity (*178, 179*). Flavonoids are an important group of polyphenolic compounds and exist abundantly in human diet, such as fruits, vegetables, tea and cereals.[*180*] Polymethoxyflavones (PMFs), bearing more than 2 methoxy groups on the flavonoid skeleton and existing abundantly in citrus peels, have been proven to prevent metabolic syndromes including obesity and diabetes (*11*).

The aged citrus peels, namely *chenpi* in Chinese, have been used as traditional medicine for digestive disorders and dietary supplement in China (*181*). To produce *chenpi*, fresh peels of *Citrus reticulata* are dried in the sunlight, and then stored in a moisture-controlled condition for years. During the natural aging process, 5-hydroxylated (5-OH) PMFs are accumulated in *chenpi* by auto or biotransforming from PMFs (*15*). 5-OH PMFs

are found to deliver higher efficacy for anti-cancer and anti-inflammatory activities, compared with their counterpart (*15, 182*). Our previous studies have shown that PMFs extracted from *chenpi* could attenuate obesity dose-dependently by influencing energy/lipid metabolisms through *in vitro* and *in vivo* experiments (*136, 150*). Moreover, 5-OH PMFs demonstrated better anti-obesity activity than PMFs (*136*), which indicated the potential of application *chenpi* for ameliorating obesity due to its particular PMFs profile.

The anti-obesity mechanisms of PMFs have been explored in the present studies (*9, 24, 133*). Several possible pathways, including suppressing adipogenesis and differentiation in preadipocytes and adipocytes, inducing brown adipocyte-like phenotype, inhibiting digestive enzymes, modulating adipocytokine secretion, and regulating hepatic glucose-, lipid- and energy metabolism are involved in their anti-obesity effect (*9, 11, 138*). Notably, increasing studies have shown that the gut microbiota is of great importance for hosts' health status, such as energy regulation, colorectal cancer prevention, pathogen inhibition and immune function maintenance (*183*). Due to the poor water solubility and limited bioavailability (*52*), most PMFs will enter the colon and interact with the gut microbiota after oral administration. Therefore, the gut microbiota might play an important role for the anti-obesity activity of PMFs, but relative works are still very limited.

The composition of gut microbiota is found to correlate with body weight status (*184*). For example, increased Firmicutes and decreased Bacteroidetes have been observed in obese mice or people, compared with their lean counterparts (*185, 186*). Better understanding the crosstalk between the host and the gut bacterium has raised increasing attentions in recent years. For example, the abundance of *Akkermansia* and *Allobaculum* at

the genus level is reported to enrich in weight-reduced mice, and negatively associate with leptin concentration in systemic circulation (*187*). Some phytochemicals with preventive effect on obesity development, such as berberine (*188, 189*) and grape polyphenols, could selectively increase the growth of these two colonic bacteria (*190, 191*). Therefore, the anti-obesity mechanisms of PMFs, especially the colonic microbial pathways, need further exploration. To the best of our knowledge, there is only one recent study investigating the relationship of the citrus peel extract (CPE) and gut microbiota using high-fat diet (HFD) mouse model (*72*). It was found that one type of CPE could influence the colonic community of symbiotic and pathogenic microorganisms, evidenced by increasing *Prevotella* and decreasing *rc4-4* bacteria (*72*). However, possible mechanisms including short chain fatty acid (SCFA) production, dose-dependent manner, and dynamic microbial change are not well discussed. Therefore, the anti-obesity mechanisms of PMFs, especially the colonic microbial pathways, need further exploration.

This study aims to explore the modulation effect of PMFs on the gut microbiota and understand its implication for obesity prevention. Inspired by the usage of *chenpi* as dietary supplement for gastrointestinal health maintenance in China, 5-OH PMFs enriched *chenpi* extract was exploited in this work. The influence of PMFs on the gut microbiota was accessed through fecal SCFA analysis and microbial compositional change in a dose- and time-dependent manner. Moreover, this paper is the first work to investigate the changed microbial functionality by PMFs through metagenomic analysis. The results will provide scientific support to develop *chenpi*-based functional food and strengthen our understanding of the mutualisms of specific colonic bacteria, phytochemicals and host in terms of obesity control.

2.2 Materials and Methods

2.2.1 The Extraction and Quantification of PMFs in chenpi

The *chenpi* extract was obtained through our previous method with minor modification (*150*). Briefly, grounded *chenpi* was extracted by *n*-butane via the continuous phase transition extraction method. The remaining extract after removing *n*-butane was further purified by hexane and ethyl acetate assisted with silica gel column chromatography. The concentration of PMFs in *chenpi* extract was determined by HPLC using our method previously published (*59*). The PMFs profile of *chenpi* in this study was shown in **Fig.4**. The percentages of nobiletin, tangeretin, and 5-OH nobiletin in *chenpi* extract were about 40.0, 29.4 and 11.7%, respectively. Nobiletin content has been used as a biomarker to access the anti-inflammation and memory improvement bioactivities of CPE from different origins (*192, 193*). *Chenpi* extract in this study belonged to the category with high bioactivity based on previous definition (*192, 193*). Moreover, the high percentage of 5-OH nobiletin indicated that about 20% of nobiletin originally existed in fresh citrus peels transformed to 5-OH nobiletin during the aging process.

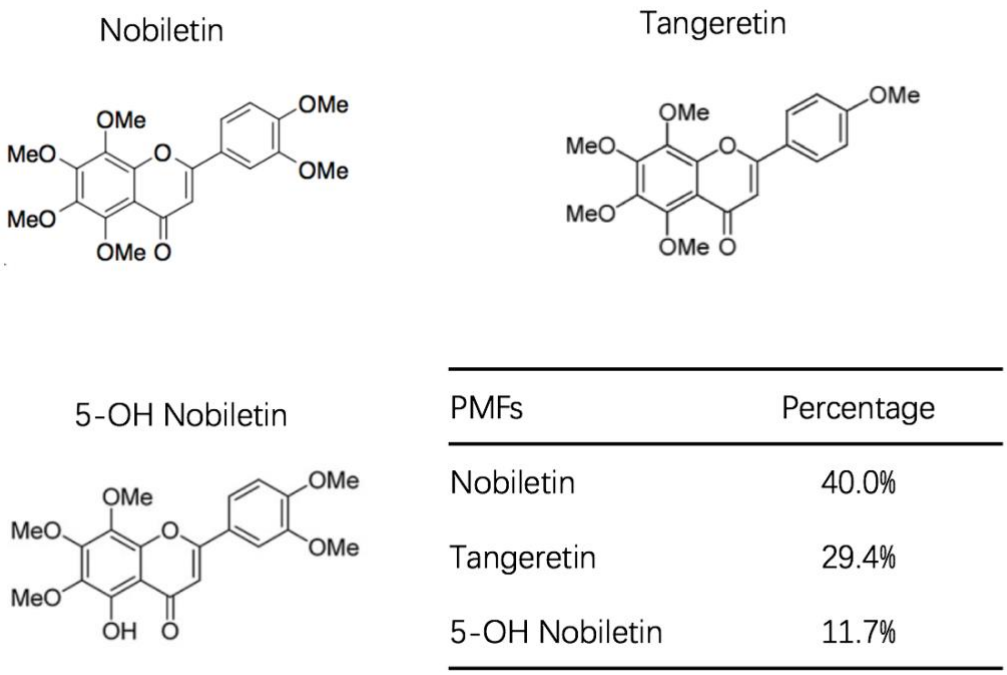

PMFs	Percentage
Nobiletin	40.0%
Tangeretin	29.4%
5-OH Nobiletin	11.7%

Figure 4: The chemical structures and compositions of key polymethoxyflavones (PMFs) in *chenpi* extract.

2.2.2 Animals and Materials

Before the experiment, six-week-old male C57BL/6J mice were treated with antibiotics (200 mg/kg/day neomycin sulfate and 200 mg/kg/day streptomycin) for 3 days (*194, 195*), and then orally administrated 200 μL/time human fecal suspension for ten days (once daily in first 3 days, and every other day in the rest) (*196*). To produce the fecal suspension, the fresh stools from 3 healthy volunteers aged from 20-25 were diluted by 10-fold PBS buffer (pH≈7.0) containing 10% glycerol. After well mixing and centrifugation, the fecal supernatant was divided into several cryotubes and transferred to -80 °C freezer immediately for storage (*196*). After receiving human fecal flora, the mice were randomly divided into four groups (n=8 per group). They were provided with HFD (60% fat calorie),

HFD with 0.25% *chenpi* extract (LP), HFD with 0.5% *chenpi* extract (HP), and normal diet (ND, 10% fat calorie), respectively. The protocol and experimental procedures for this study were approved by the Ethical Committee of Experimental Animal Care in Ningbo University (Approval No: SYXK 2013-0191). All the mice diets (TP23300 for HFD and TP23302 for ND) were purchased/processed from Trophic Animal Feed High-Tech Co. Ltd (Jiangsu, China). The mice were housed in cages in specific pathogen-free environment, controlled light condition (12 h light-dark cycle), controlled temperature/humidity condition, and allowed to get access to water/food freely throughout the experiment. Food intake was recorded daily, and mice weight was recorded weekly. Mice feces were collected 3 times a week. After 11-week regimen, mice were sacrificed by cervical dislocation after 6 hours food deprivation. The liver, heart, spleen, kidney, perirenal and epididymal adipose tissues, brain and lung were collected, immediately weighted and frozen in liquid nitrogen, and then stored in -80 $^{\circ}$C freezer.

2.2.3 Histopathological Examinations

Perigonadal adipose tissue and liver were fixed in 4% paraformaldehyde solution, dehydrated by ethanol solutions, and embedded in paraffin. After preparing the tissue sections, the adipose tissue was stained with hematoxylin and eosin (H&E) and liver was stained with oil red. Images were obtained by Nikon microscope under 200x magnification.

2.2.4 Short Chain Fatty Acid (SCFA) Analysis

SCFA profiles were measured by gas chromatography-mass spectroscopy (GCMS-QP2010, Shimadzu, Kyoto, Japan) equipped with a DB-WAX column (30 m*0.25

mm*0.25 μm). 100 mg feces sample was soaked with 0.5 mL saturated NaCl solution and homogenized by bead homogenizer (Servicebio, Wuhan, China). The suspension was added 125 μL sulfuric acid and 50 μL internal standard (2-methylhexanoic acid) solution, and then extracted by 1 mL diethyl ether. The concentrations of SCFA including acetic acid, propionic acid, butyric acid, isobutyric acid, valeric acid and isovaleric acid were calculated according to internal standard.

2.2.5 Bacterial Composition Analysis

The method for sequencing and data analysis was described previously (*197*). Briefly, DNA from mice feces was extracted by E.Z.N.A. Stool DNA Kit (D4015, Omega, Inc., Norcross, GA, USA) based on the manufacturer's instruction. The total DNA in elution buffer was stored at -80 ℃ until PCR amplification and sequencing measurement by LC-Bio Tech Co., Ltd (Zhejiang, China) on the Illumina MiSeq platform. After merging paired-end reads (FLASH) and quality control (fqtrim, V0.94), sequence with more than 97% similarity were assigned to the same operational taxonomic units (OTUs) via Vsearch (v2.3.4). The OTUs were classified by Ribosomal Database Project, and OTU abundance were normalized according to a standard of sequence number.

2.2.6 Metagenomic Analysis

The extracted DNA was fragmented by dsDNA Fragmentase, and DNA library was constructed using TruSeq Nano DNA LT Library Preparation Kit (FC-121-4001). After quality filtration, the sequencing reads were assembled to construct the metagenome of the gut microbiota. All coding regions sequences (CDS) of metagenomic contigs were

predicted by MetaGeneMark v3.26, and unigenes were obtained by clustering CDS via CD-HIT v4.6.1. The functional annotation of unigenes were obtained by aligning them against database via DIAMOND v 0.7.12.

2.2.7 Statistical Analysis

Experimental data were presented as mean ± standard deviation. The significant difference among groups was tested using student test or one-way ANOVA followed by Bonferroni test using StataSE v15 and reported as different letters if p-value<0.05. The statistical difference of microbial structure among groups was test using linear discriminant analysis effect size (LEfSe) (*198*).

2.3 Results

2.3.1 *Chenpi* Extract Reduced Body Weight Gain and Food efficiency

The anti-obesity effect of *chenpi* in this study (as shown in **Table.1**) was consistent with our previous report (*150*). Diets supplemented with LP and HP significantly attenuated mice body weight gain than HFD after 11-week feeding. In terms of the dose-dependent manner, HP led to very significant reduction on the food efficiency (expressed by body weight gain/food intake), as compared to LP and HFD. The intake of PMFs did not significantly affect the weight of liver, spleen and lung, but could alleviate the weight gain of kidney caused by HFD.

Table 1: Body weights, food behaviors and organ weights of mice under different chronic oral treatments: high-fat diet (HFD), HFD plus 0.25% *chenpi* extract (LP),

HFD plus 0.5% *chenpi* extract (HP) and normal diet (ND).

	HFD	LP	HP	ND
Initial weight	20.667±1.510[a]	20.571±1.253[a]	20.575±0.809[a]	20.5±1.281[a]
Final weight	31.661±2.662[a]	26.36±1.164[b]	25.464±1.478[b]	25.6±2.267[b]
Food intake	1.995±0.157[b]	1.749±0.192[a]	2.050±0.514[bc]	2.183±0.417[c]
Food efficiency	0.069±0.012[a]	0.042±0.008[b]	0.029±0.006[c]	0.033±0.007[bc]
Fat	2.168±0.644[a]	1.189±0.304[b]	0.992±0.284[b]	1.095±0.336[b]
Liver	1.086±0.125[a]	1.063±0.050[a]	1.075±0.125[a]	0.976±0.113[a]
Lung	0.163±0.019[a]	0.175±0.020[a]	0.186±0.029[a]	0.173±0.036[a]
Spleen	0.107±0.0202[a]	0.087±0.021[a]	0.102±0.022[a]	0.1155±0.043[a]
Kidney	0.377±0.061[a]	0.320±0.013[ab]	0.336±0.055[ab]	0.306±0.035[b]

2.3.2 *Chenpi* Extract Reduced the Mass of Adipose Tissues, Adipocyte Size and Hepatic Lipid Accumulation

Chenpi extract showed strong inhibitory effect on the mass accumulation of white adipose tissue (WAT, Table.1), adipocyte enlargement (**Fig. 5A**), and lipid accumulation in the liver (**Fig. 5B**) in mice fed with HFD. Moreover, higher dosage of *chenpi* in diets might be more effective to prevent adipocyte enlargement and hepatic lipid deposition.

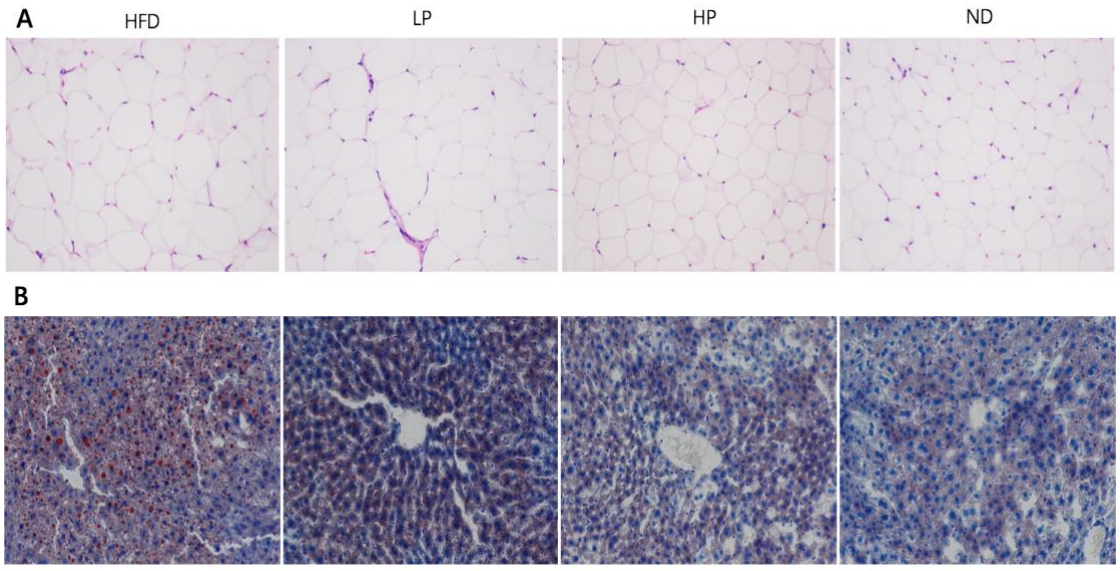

Figure 5: The influence of chenpi extract on the adipose tissues (A) and livers (B) of mice under different chronic oral treatments: high-fat diet (HFD), HFD plus 0.25% chenpi extract (LP), HFD plus 0.5% chenpi extract (HP) and normal diet (ND).

2.3.3 *Chenpi* Extract Promoted SCFA Production by Gut Microbiota

As shown in **Fig. 6**, *chenpi* extract exhibited prebiotic effect by promoting the colonic bacteria's SCFA production in mice fed with HFD for 11 weeks of the regimen. The total SCFA levels were the summed molars of acetic acid, propionic acid, butyric acid, isobutyric acid, valeric acid and isovaleric acid. The concentration of total SCFAs in feces of mice fed with HFD, HFD with 0.25% *chenpi*, HFD with 0.5% *chenpi*, and ND was 19.461±1.344 μM/g, 25.756±1.607 μM/g, 28.027±1.169 μM/g, and 36.612±3.614 μM/g, respectively. In detail, the change of acetic acid and propionic acid stimulated by *chenpi* treatment were the most significant among SCFAs: the increase of acetic acid contributed to the dominant component of total SCFAs change, while propionic acid had the highest ratio of increase (nearly two times). *Chenpi* slightly increased the production of butyric acid, isobutyric acid

and isovaleric acid, but had no significant influence on valeric acid (see Table.2).

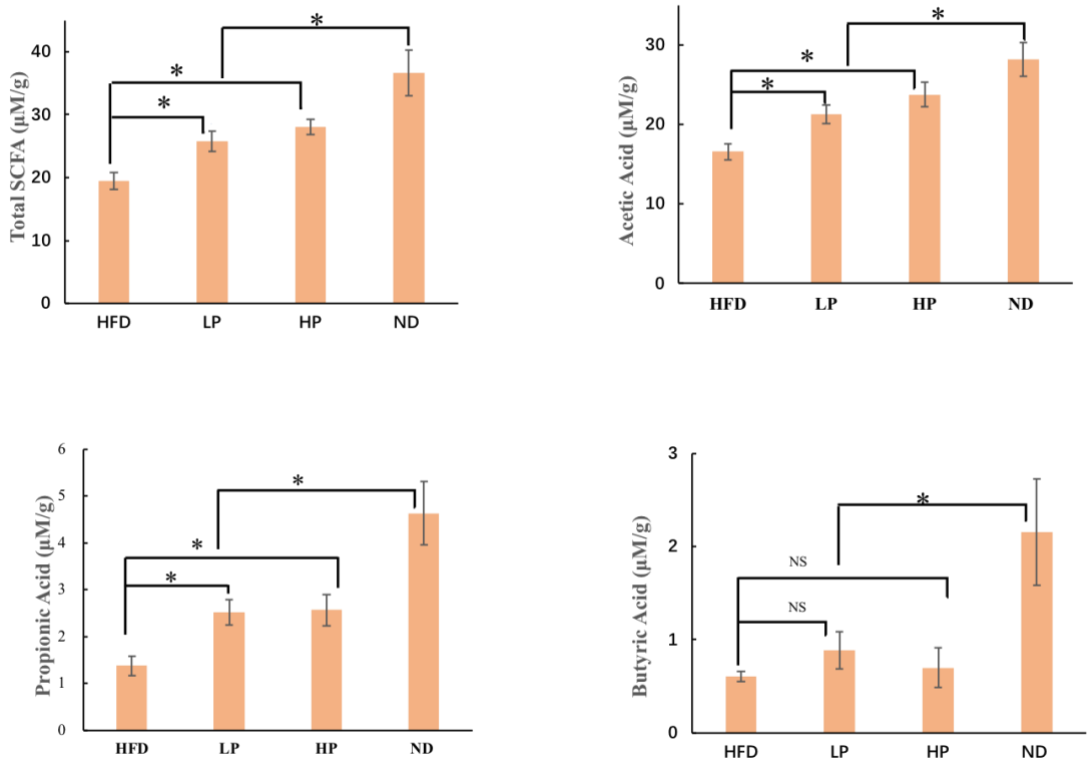

Figure 6: Chenpi extract treatment altered the fecal short-chain fatty acids (SCFA) profiles in mice fed with high-fat diet (HFD). Statistical differences compared to relative abundance in the HFD group were presented as * if $p < 0.05$.

Table 2: The concentrations of isobutyric acid, isovaleric acid and valeric acid in feces of mice under different chronic oral treatments: HFD, LP, HP and ND.

μM/g	HFD	LP	HP	ND
Isobutyric acid	0.203 ± 0.013^{a}	0.326 ± 0.055^{a}	0.300 ± 0.054^{a}	0.408 ± 0.067^{b}
Isovaleric acid	0.351 ± 0.029^{a}	0.421 ± 0.038^{ab}	0.416 ± 0.066^{ab}	0.578 ± 0.102^{b}
Valeric acid	0.336 ± 0.068^{a}	0.351 ± 0.051^{a}	0.282 ± 0.049^{a}	0.625 ± 0.120^{b}

Different letters (i.e., a, b) in superscript indicated the statistical significance level $p<0.05$.

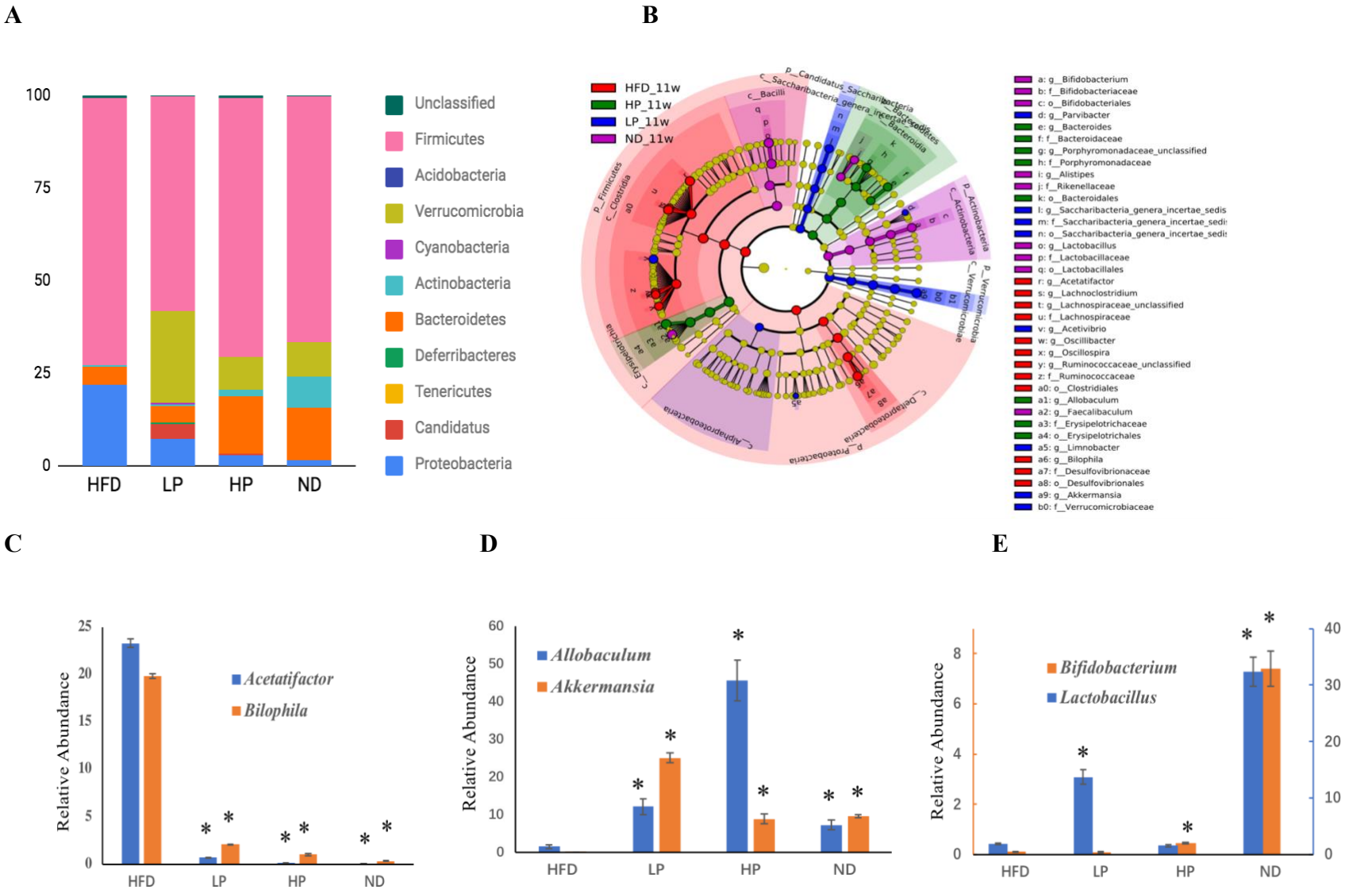

Figure 7: *Chenpi* extract treatment altered the fecal microbial components in mice fed with HFD after 11 weeks: (A) compositional change at the phylum level; (B) microbial structural change under different treatments by LEfSe analysis (the threshold on the logarithmic linear discriminant analysis (LDA) score was 4.0); (C) (D) (E) typical microbial change at the genus level. Statistical differences compared to relative abundance in the HFD group were presented as * if $p < 0.05$.

2.3.4 *Chenpi* Extract Modulated the Structural Composition of Gut Microbiota

At the phylum level (**Fig. 7A**), Firmicutes, Bacteroidetes, Proteobacteria, Verrucomicrobia and Actinobacteria accounted for more than 95% relative abundance of the overall fecal microbiota of mice in the four groups. Two indexes at the phylum level (**Fig. 7A**) demonstrated significant difference among groups- The ratio of Firmicutes/Bacteroidetes (F/B, $P<0.001$) and relative abundance of Proteobacteria ($P<0.001$). F/B for HFD, LP, HP, and ND was 15.32±0.25, 13.19±0.81, 4.62±0.88, 4.82±0.67, respectively. Obviously, the F/B ratio was dose-dependently decreased by *chenpi* in mice fed with HFD, and HP could even lower F/B ratio to the similar level of ND. Besides, the relative abundance of Proteobacteria was decreased significantly with the rank order for different treatments: HFD > LP > HP > ND. Compared with HFD, LP, HP and ND led to a higher percentage of Verrucomicrobia. In addition, HP increased the relative abundance of Actinobacteria to nearly 200% compared with HFD, while LP did not show significant influence on Actinobacteria.

Fig. 7B illustrated the enriched bacteria for each group at the levels of class, order, family and genus after 11 weeks of the regimen. At the class level, long-term ingestion of HFD instead of ND would increase the proportion of *Clostridia* and *Deltaproteobacteria,* but decreased the proportion of *Bacilli* and *Actinobacteria* in the colonic digesta. However, *chenpi* supplementation attenuated this microbial change caused by HFD. Besides, LP led to the enrichment of *Verrucomicrobiae* and *Saccharibacteria*, and HP led to the enrichment of *Bacteroidia* and *Erysipelotrichia*. The change at the order level was similar with class-

level change. At the family level, *Ruminococcaceae, Lachnospiraceae*, and *Desulfovibrionaceae* were more prevalent in the gut microbiota of HFD-fed mice, while *Lactobacillaceae* and *Bifidobacteriaceae* were more dominant in the gut microbiota of ND-fed mice. PMFs in *chenpi* could reduce the relative abundance of *Ruminococcaceae, Lachnospiraceae*, and *Desulfovibrionaceae* dose-dependently. Moreover, *Verrucomicrobiaceae* and Saccharibacteria were enriched in the colonic digesta by the lower dosage (LP) of *chenpi*; while *Porphyromonadaceae, Bacteroidaceae*, and *Erysipelotrichaceae* were enriched by the higher dosage (HP) of *chenpi*.

The change of typical bacteria at the genus level represented more biological information by *chenpi* treatment. Two dominated colonic bacteria (each relative abundance≈20%) in HFD-fed mice, *Acetatifactor* and *Bilophila*, underwent the most dramatic decrease by *chenpi* treatment (**Fig. 7C**). *Chenpi* could also inhibit the relative abundance of *Oscillibacter*, unclassified *Lachnospiraceae*, unclassified *Ruminococcaceae*, *Lachnoclostridium*, *Oscillospira*. In addition, PMFs in *chenpi* exhibited promotional effect on certain bacteria. The most significantly promoted bacteria at the genus level by *chenpi* treatment were *Allobaculum a*nd *Akkermansia*. PMFs supplemented in HFD could even increase the relative abundance of *Allobaculum a*nd *Akkermansia* to a similar/higher level of ND group (**Fig. 7D**). In terms of the promoting effect on probiotics in mice fed with HFD, LP was more effective in enriching *Lactobcillus*, while HP was more effective in enriching *Bifidobacterium* (**Fig. 7E**).

2.3.5 *Chenpi* Extract Affected the Dynamics of *Akkermansia* spp. and *Allobaculum* spp.

Given the dramatic bloom of *Allobaculum a*nd *Akkermansia*, the dynamics of these

two bacteria were investigated. The dose-effect of *chenpi* treatment was demonstrated in **Fig. 8A**, represented by the summed relative abundance of *Allobaculum a*nd *Akkermansia* (SAA). It seemed that higher SAA was associated with lower weight status. Long term treatment of HFD significantly inhibited SAA as compared to ND, while PMFs could enhance SAA significantly and dose-dependently. The trade-off effect of HFD and PMFs could be observed through the dynamic change of SAA under the HP treatment along with the feeding time (**Fig. 8B**). In the first 8 weeks, the SAA decreased slightly, meaning that the inhibitory effect by HFD was the dominant factor. At the 11th week, SAA was higher than the original level in the first week, indicating that the promotional effect by PMFs was dominant in the long-term feeding.

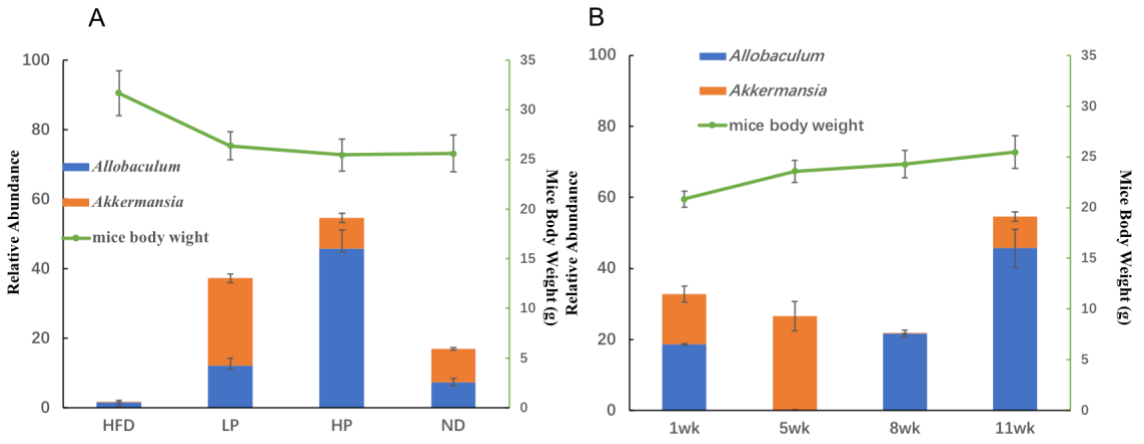

Figure 8: The changes of the summed relative abundance of Allobaculum and Akkermansia (SAA) under different treatment (A) and over time in the HP group (B).

2.3.6 *Chenpi* Extract dynamically changed the functional pathways of gut microbiota

Kyoto Encyclopedia of Genes and Genomes (KEGG) was used to investigate the functional pathways of microbiome. **Fig. 9** and **Fig. 10** showed the differentiated functions caused by 0.5% *chenpi* extract for 5- and 11- week treatment, respectively.

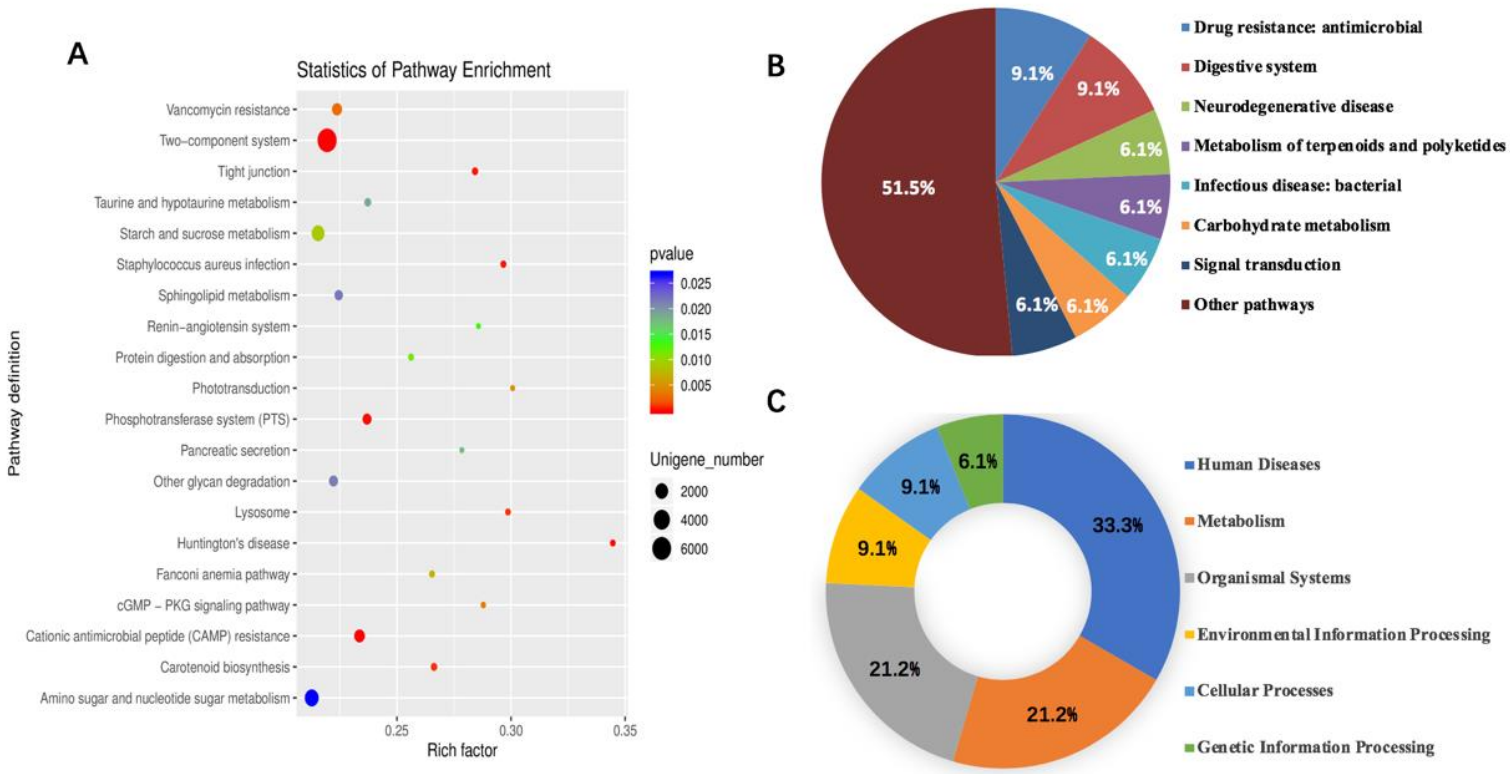

Figure 9: The functions according to the 33 differentiated expressed unigenes between HFD and HP for 5-week treatment: the scatter plot of the most 20 enriched pathways from the 33 unigenes (A), functional classification of 33 differentiated expressed unigenes (B), further classification of functions from 9B (C).

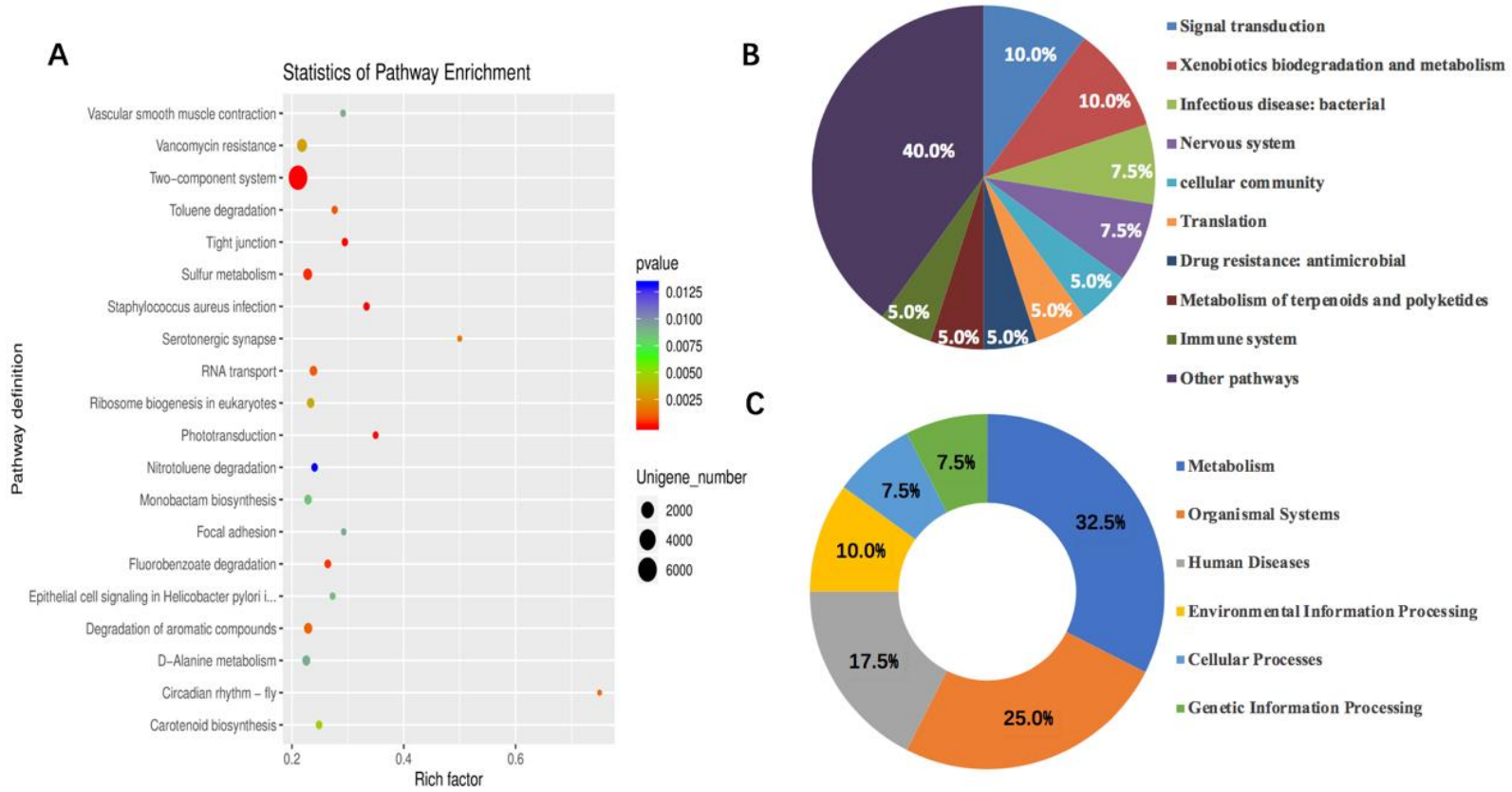

Figure 10: The functions according to 40 differentiated expressed unigenes between HFD and HP for 11-week treatment: the scatter plot of 20 most enriched pathways from 40 unigenes (A), functional classification of 40 differentiated expressed unigenes (B), further classification of functions from 10B (C).

The scatter plots (**Fig. 9A** and **Fig. 10A**) demonstrated the top 20 significantly enriched KEGG pathways according to the P values of the differentially expressed unigenes between HFD and HP in the 5^{th}- and 11^{th}-week. The two-component system pathway contained the most unigenes in terms of their numbers at both time intervals. Six pathways--vancomycin resistance, two component systems, tight junction, staphylococcus aureus infection, phototransduction and carotenoid biosynthesis were differentially expressed in both 5^{th} week and 11^{th} week. The rich factors of these 6 pathways increased along the treatment time with the exception of carotenoid biosynthesis. The Huntington's disease pathway had the highest rich factor (≈0.34) among the differential pathways in the 5^{th} week, while circadian rhythm pathway had the highest rich factor (≈0.78) in the 11^{th} week.

Fig 9B showed the most enriched functions through the classification of 33 significantly differentiated pathways ($P \leq 0.05$) identified after 5-week treatment of HFD and HP. Drug resistance, digestive systems were the top two types of function signaling in the gut microbiota altered by *chenpi*, followed by neurodegenerative disease, metabolism of terpenoids and polyketides, infectious disease (bacterial), carbohydrate metabolism and signal transduction. These enriched functions derived from 33 differentiated pathways (**Fig. 9B**) were further classified into five types of biological processes as shown in **Fig. 9C**, including human disease, metabolism, organismal systems, environmental information processing (EIP), cellar processes, and genetic information processing (GIP). The percent of altered functions by 5-week *chenpi* treatment was 33.3% for human disease, 21.2% for metabolism, 21.2% for organismal systems, 9.1% for EIP, 9.1% for cellular process and

6.1% for EIP, respectively.

Fig. 10B showed the most enriched functions through the classification of 40 significantly differentiated pathways (P≤0.05) identified after 11-week treatment of HFD and HP. Signal transduction, xenobiotics biodegradation and metabolism were the top two functional signaling, followed by infectious disease (bacterial), nervous system, cellular community, translation, drug resistance (antimicrobial), metabolism of terpenoids and polyketides, immune system (**Fig. 10B**). **Fig. 10C** demonstrated the further classification of enriched functions from **Fig. 10B**. Most of enriched functions (32.5%) after 11-week *chenpi* treatment were involved in the process of metabolism, 25% in organismal systems, 17.5% in human disease, 10% in EIP, 7.5% in cellular process and 7.5% in GIP.

2.4 Discussion

Obesity is associated with increasing risks of many metabolic syndromes, including heart disease, hypertension, dyslipidemia, and diabetes (*199*). Growing evidences have shown the anti-obesity effect of dietary flavonoids, but the knowledge of their undying mechanisms is still limited (*180*). This study observed that *chenpi* effectively slowed down the body weight gain using diet-induced obese (DIO) mouse model. Besides, energy metabolism was enhanced by *chenpi* dose-dependently as the evidence of food efficiency, adipocyte enlargement, and lipid accumulation in liver. Different from emphasizing the hosts' energy metabolism in our previous work (*136, 150*), this study demonstrated that the modulation effect on the gut microbiota was another important pathway for the anti-obesity mechanisms of 5-OH PMFs-enriched *chenpi* extract.

SCFA produced by the gut microbiota was one of the pathways for *chenpi* extract to deliver their anti-obesity activity. SCFA played an important role in human health, such as

feeding colonocyte, maintaining gut barrier and inhibiting pathogenic microbe proliferation by acidic pH condition (*100*). The SCFA could be absorbed rapidly from the gut rumen, but each SCFA had different subsequent distribution, fate and metabolism in host. For example, only acetate had relatively high concentration in peripheral blood; propionate was mostly metabolized in the liver; butyrate was preferentially used as the energy source by gut epithelial cells so that its concentration in systemic circulation was low (*92*). SCFAs also acted as the signal chemicals of the gut microbiota to participate in regulating energy metabolism and appetite by contacting with distant organs including adipose tissues, liver and brain (*34*). For example, SCFAs were found to increase lipid oxidation and decease fatty acid synthesis in liver by activation of AMPK pathway (*200*). This study showed that fecal total SCFAs were increased by *chenpi* treatment dose-dependently; acetic acid and propionic acid had the most amplification among SCFAs. As these two SCFAs were easy to enter systemic circulation and then interacting with remote organs, they were supposed to partially contribute to the enhanced level of AMPK reported in our previous study (*150*).

Chenpi extract was able to affect energy harvesting by shaping the gut microbial structure from the microbial analysis. Previous study found that the obese microbiome in both mice and human had higher capability to harvest energy, and was characterized by increased Firmicutes and decreased Bacteroidetes (*185*). The reduction of F/B by *chenpi* extract in dose-dependent manner was identified in this study, suggesting that the changed microbial component might lead to lower efficacy for energy harvest. Besides, another decreased phylum--Proteobacteria in the LP and HP group suggested that *chenpi* could alleviate the microbial disorder caused by HFD, since the outgrowth of Proteobacteria was

regarded as a marker for microbial dysbiosis in obese microbiome (*201*). Moreover, the promotional effect on Verrucomicrobia and Actinobacteria implied that *chenpi* led to the stimulation of functional bacteria in the colon.

The modulation effect of *chenpi* extract on the gut microbiota at the genus level was represented by the inhibition of bile acid (BA)-metabolizing bacteria, as well as the promotion of probiotics and functional bacteria.

Chenpi extract could alleviate the outgrowth of *Acetatifactor* and *Bilophila* caused by HFD in a dose-dependent manner. Previous studies found that the increased abundance of *Bilophila* was linked to high fat diet, bile acid metabolism, and a high risk for inflammatory bowel disease (IBD) (*202*). Some strains of *Acetatifactor* were also reported to positively associated with concentrations of secondary BA (*203, 204*). In the host body, the BA pool was efficiently recycled through the enterohepatic circulation, and about 5% was excreted through feces daily (*204*). As the receptors of BA in the liver and intestine were also involved in glucose homeostasis, lipid metabolism and energy expenditure, the disturbance of BA pool caused by microbial dysbiosis might lead to metabolic disorders such as obesity and insulin resistance (*204*). For example, HFD composed of saturated fat could lead to increased amounts of secondary BA and the expansion of bile-tolerant microbe--*Bilophila wadsworthia*, compared with normal diet (*205*). The decreased intestinal BA-related microbes were also observed by drinking Pu-erh tea, and associated with reduced hepatic cholesterol and lipogenesis (*206*). Thus, the dramatical inhibitory effect of PMFs on these BA-related bacteria indicated that the improved fat-bile-gut connect might be a pathway for the anti-obesity effect of PMFs.

Chenpi extract demonstrated prebiotic effect evidenced by the promoted

Lactobacillus and *Bifidobacterium*. The dosage of PMFs played an important role on the beneficial microbial component. As compared to HFD, LP increased the relative abundance of *Lactobacillus* by 615%, and HP increased the relative abundance of *Bifidobacterium* by 320%. *Lactobacillus* and *Bifidobacterium* have been found to be associated with obesity prevention (*207*). The promotional effect on *Lactobacillus* was also observed in another study using citrus peels (*72*). *Bifidobacterium,* another well-known beneficial bacterium responsible for oligosaccharide metabolism, had illustrated protective effects against IBD (*208*). Therefore, the bloomed *Lactobacillus* and *Bifidobacterium* by *chenpi* treatment might contribute to the prevention of microbial dysbiosis caused by HFD.

Allobaculum and *Akkermansia* were the bacteria experiencing the most significant elevation by *chenpi* treatment at the genus level. *Allobaculum* relative abundance was reported to correlate with hormone secretion, SCFA production, plasma HDL concentration and gut barrier integrity (*187, 188, 191*). Moreover, the elevation of *Allobaculum* has been identified to counteract obesity by the treatment of PMFs, berberine and grape polyphenols (*72, 188, 209*). In this study, the relative abundance of *Allobaculum* in HP group was even higher than in ND group. Similar phenomenon was observed for *Akkermansia* abundance. *Akkermansia muciniphila* had been identified as a mucin-degradation bacterium and could reverse the metabolic disorders caused by HFD, including fat-mass gain, adipose tissue inflammation and insulin resistance (*99*). Dietary intervention, such as fiber or polyphenol treatment, had shown the capability to increase the *Akkermansia* spp. prevalence (*99, 190, 210*). Both *Allobaculum* and *Akkermansia* had shown similar effect on circulating leptin concentration, and inhibitory effect on inflammation markers (*187*).

One of the interesting findings in this study was the dynamics of *Allobaculum* and

Akkermansia in the dose- and time-dependent manner, which made it distinguishable from the previous work (*72*). **Fig. 8A** demonstrated the dose-effect: *Akkermansia* was dominated in the LP group; and *Allobaculum* was dominated in the HP group after 11-week regimen. Moreover, SAA increased with the dosage of *chenpi* treatment (HP>LP>HFD). The dynamic change of SAA overtime (**Fig. 8B**) in the HP group showed similar trend with the dose manner: *Akkermansia* was dominant in the short-term feeding (5-week), and then *Allobaculum* outperformed after 8-week feeding. Possible explanation for the dynamics of *Allobaculum* and *Akkermansia* might be linked to the accumulation effect of PMFs in the colon. 11-week feeding for LP and 5-week feeding for HP might correlate with a relative low level of PMFs in the colon, and thus both of them lead to the domination of *Akkermansia.* When PMFs in the colon increased either by the accumulation for longer treatment time or higher dosage from oral administration, *Allobaculum* would outperform *Akkermansia*. When the content of PMFs in the colon was high enough, these two bacteria could coexist and grow well to adopt the prebiotic environment. In our future study, the interaction of PMFs and selective strains of *Akkermansia* and *Allobaculum* will be studied via *in-vitro* fermentation.

The metagenomic analysis provided the functional insight for the altered the gut microbiota by PMFs at the different treatment time. In general, some pathways were enhanced dynamically in terms of the increased rich factor, such as two-component system, tight junction, staphylococcus aureus infection, etc. Besides, the enriched functions of microbiome at both time intervals were both corresponded to pathogen prevention (e.g. staphylococcus aureus infection) and specific metabolism (e.g. terpenoids and polyketides). However, the phenotypes of enriched functions seemed different for different treatment

time. Drug resistance and digestive systems were the top two categories of enriched functions in the 5th week, while signal transduction and xenobiotics biodegradation and metabolism were the top two categories in the 11th week (**Fig. 9B** vs. **Fig. 10B**). Moreover, more differentially expressed pathways were involved in metabolism in the 11th week (32.5%, **Fig. 10C**) as compared to 5th week (21.2%, **Fig. 9C**). For example, fluorobenzoate degradation and toluene degradation (**Fig. 10A**) were enriched in 11th week, as well as nitrotoluene degradation and benzoate degradation (not listed in **Fig. 10A**). As these pathways involved in benzoate derivates and belonged to xenobiotics degradation, it might indicate that the metabolism of PMFs by the gut microbiota were enhanced along with the treatment time. Another interesting information provided by **Fig. 10A** was that the altered unigenes by PMFs might also participate in the regulation of circadian dysbiosis after 11-week HFD feeding. Circadian dysbiosis was thought as a metabolic disease and could be caused by diet-induced obesity (*116*). A recent study demonstrated that nobiletin could enhance circadian rhymes in a *Clock* gene-dependent manner in the liver of the DIO mice (*106*). Besides, the gut microbiota was found to reflect host's circadian rhyme by exhibiting diurnal oscillations in composition and metabolites production, and these microbial oscillations could be influenced by diet compositions (*116*). The finding in this study indicated that the gut microbiota might be a potential target for PMFs to modulate the circadian dysfunction caused by HFD-induced obesity. In our ongoing study, the metabolism of PMFs by the gut microbiota as well as the relationship between the PMFs-altered gut microbiota and circadian rhymes will be further explored.

2.5 Conclusion

In summary, *chenpi* extract has strong prebiotic effect as indicated by the elevated

production of SCFA and the bloom of *Lactobacillus* and *Bifidobacterium* in the HFD-induced obese mice model. Moreover, the inhibition of *chenpi* on *Acetatifactor* and *Bilophila* suggested that the fat-bile-gut interaction might contribute to the anti-obesity of PMFs. *Chenpi* treatment significantly enriched two functional bacteria (i.e., *Akkermansia* and *Allobaculum*) at the genus level. The prevalence of *Akkermansia* and *Allobaculum* was dose- and time-dependent by *chenpi* treatment. The metagenomics analysis of the gut microbiota showed that several pathways were enhanced by PMFs significantly and dynamically, such as the two-component system, tight junction, etc. The improved biological process of metabolism especially on benzoate-derivatives might be associated with the increased microbial biotransformation of PMFs in the colon. Overall, this study suggested that the modulation on the gut microbiota importantly contributed to the anti-obesity mechanisms of PMFs *in vivo*.

CHAPTER III: BIDIRECTIONAL INTERACTION OF NOBILETIN AND GUT MICROBIOTA IN MICE FED WITH HIGH FAT DIET

3.1 Introduction

Nobiletin, one of the most prevalent polymethoxyflavones (PMFs), exists exclusively in citrus plants, especially in their peels (*11*). There are six methoxy groups on its flavone skeleton distributing at the 5, 6, 7, 8-positions on the A-ring and 3′, 4′-posintions on the B-ring (Fig.1). Studies have shown that nobiletin demonstrates beneficial effect on obesity control, inflammation and cancer prevention, brain function improvement, etc. (*9, 11, 133, 211*). In terms of its anti-obesity activity, both cell- and animal studies have been conducted to investigate the underlying mechanisms. Evidenced by the 3T3-L1 cell study, nobiletin could effectively inhibit adipogenesis, increase AMP-activated protein kinase, and induce brown adipocyte-like phenotype (*133, 138*). Several mouse studies have shown that nobiletin could regulate adipo- and proinflammatory cytokine (*24, 129*), and improve hyperglycemia, dyslipidemia and insulin resistance (*146, 151*).

The pathogenesis of obesity is complicated. Recent studies indicate that gut microbiota plays a pivotal role on host obesity (*67, 185*). Given its numerous cell and gene pool, the colonic microbiota is regarded as an important organ inside the host, and performs many functions to maintain the host's health status (*67*). It is estimated that about 90% of the orally administered dietary phytochemicals would reach the colon and undergo biotransformation by gut microbiota (*92*). Some colonic metabolites even exhibit better

biologic activity than their precursor (*77*). On the other side, phytochemicals have been reported to shape the composition of gut microbiota (*188, 190, 212*). Besides, accumulative researches find that the anti-obesity effect of some phytochemicals is associated with their modulation on gut microbiota (*188, 190, 212*). Therefore, the bidirectional interaction of phytochemicals and gut microbiota has important implication for the host' health.

Nobiletin has been found to undergo biotransformation *in vivo*, but seldom studies investigate its bioconversion by gut microbiota (*11, 15*). The most common metabolic pathway of PMFs is the demethylation on the methoxy groups. The typical metabolites of nobiletin identified in the mouse urine, colonic mucosa, and liver microsome include: 3'-demethylnobiletin (3'-DMN), 4'-demethylnobiletin (4'-DMN) and 3',4'-dimethylnobiletin (3',4'-DDMN) (*37, 81, 213*). The metabolites demonstrated more potent anti-inflammatory and anti-atherogenic activity than nobiletin (*77*). Moreover, a long-term study showed that the concentration of the demethylated metabolites was about 20-fold higher than nobiletin in mouse colonic mucosa (*81*). Thus the protective effect of orally administered nobiletin on colon carcinogenesis might strongly correlate with its metabolites (*81*). Together, these studies indicate that the metabolites are an important pathway contributing to the overall bioactivity of nobiletin.

To the best of our knowledge, there is no recent study that reveals the bidirectional interaction of nobiletin and gut microbiota, and its role on obesity control. This study aims to explore nobiletin metabolism by colonic microbiota in mice fed with high fat diet (HFD), as well as its metabolism in mouse liver and brain. Besides, the modulation effect of nobiletin on the gut microbiota composition and the microbial metabolites-short chain fatty acids (SCFA) will be investigated. This study will substantiate our understanding of the

anti-obesity mechanisms of nobiletin and provide scientific evidence to develop nobiletin-based functional food.

3.2 Materials and Methods

3.2.1 Animals and Materials

After adapting to the cage environment, six-week-old male C57BL/6J mice were fed antibiotics (200 mg/kg/day streptomycin and 200 mg/kg/day neomycin sulfate) for 3 days (*195*), and then treated with 200 μL/time human fecal suspension by oral gavage for ten days (once daily in first 3 days, and every other day in the rest) (*196*). The fecal suspension was made from diluted fresh stools from 3 healthy volunteers aged from 20-25 with 10-fold PBS buffer (pH≈7.0) containing 10% glycerol. After well mixing and centrifugation, the fecal supernatant was divided into several cryotubes and stored in -80 ℃ freezer until further usage. After receiving human fecal flora, the mice were divided into 2 groups (n=8 per group) randomly and supplied with HFD (60% fat calorie) for 8 weeks. Mice in the experimental group (NOB) were given 100 mg/kg nobiletin daily, while mice in the control group (HFD) were given blank vehicle. The mouse diets (TP23300) were purchased from Trophic Animal Feed High-Tech Co. Ltd (Jiangsu, China). Nobiletin was suspended in 0.3% carboxyl methylcellulose and administered daily by gavage. The experimental protocol was approved by the Ethical Committee of Experimental Animal Care in Ningbo University (Approval No.: SYXK 2013-0191). Mice were housed in cages in specific pathogen-free environment, controlled light condition (12 h light-dark cycle), and allowed to get access to food and water freely throughout the experiment. Food intake and mice

weight was recorded daily and weekly, respectively. Mice feces were collected 3 times a week for the measurement of SCFA, nobiletin metabolism and microbial component. All feces were collected at same time- just before the daily gavage of nobiletin (around 10:00 am). After 8 weeks of experimental regimen, mice were sacrificed after 6 hours food deprivation. Mice tissues were collected, weighted, immediately frozen in liquid nitrogen, and then stored in -80 ℃ freezer.

3.2.2 Histopathological Examinations

Mice livers were cut and fixed in 4% paraformaldehyde solution, dehydrated by a series of ethanol solutions, and then embedded in paraffin. Tissue sections were cut and stained with oil red. Images were captured by Nikon microscope under 200x magnification.

3.2.3 The synthesis of Nobiletin metabolites

The demethylated metabolites of nobiletin were synthesized according to our previous methods (*214*). Briefly, the B-ring metabolites of nobiletin, 3'-DMN, 4'-DMN, 3',4'-DDMN, were synthesized through 5-step reactions(*214*). Each of the B-ring metabolites was identified using NMR after the final reaction and purification (see supplementary information).

3.2.4 Biotransformation of Nobiletin

The biotransformation study contained two parts. The first part was to investigate the excreted nobiletin from feces within 48 hours after a single gavage of 100 mg/kg nobiletin. The feces were collected at the following intervals after oral administration: 0-6th hour, 6th-

12^{th} hour, 12^{th}-24^{th} hour, 24^{th}-36^{th} hour, and 36^{th}-48^{th} hour. Feces collected at different time intervals were lyophilized and weighed before further analysis. The second part of biotransformation study was to detect the concentration change of nobiletin and its metabolites in the feces after 1-, 2-, 4-, 8-week of feeding nobiletin. Besides, the mice liver and brain were chosen as the representative tissues and collected after the 8-week study for analyzing nobiletin biotransformation in the mice body.

100 mg feces samples were mixed with 800 μL 80% methanol with 0.2% acetic acid. Samples were homogenized for 2 minutes by bead homogenizer (Servicebio, Wuhan, China), vortexed for 20 min and then centrifuged at 10000 rpm for 10 min. The extraction process for feces was repeated twice and the supernatant was combined for analysis. Liver and brain samples were washed by PBS to remove blood and wiped dry. The tissue samples were homogenized in PBS by bead homogenizer, and then treated with 2U sulfatase (Sigma, St. Louis, MO, USA) and 500U β-glucuronidase (Sigma, St. Louis, MO, USA). After well mixing, the homogenate was incubated at 37 ℃ for 45 min. Equal volume of ethyl acetate with PBS was used to extract nobiletin and its metabolites for twice. After mixing and centrifugation, the combined ethyl acetated was removed by blowing nitrogen, and the remaining samples were dissolved by 80% methanol with 0.2% acetic acid for LC-MS analysis. Hesperitin was used as the internal standard for all measurement. Identification and quantification of nobiletin and its metabolites was used by UPLC (UltiMate 3000, Dionex, Sunnyvale, CA, USA) with mass spectroscopy (Q-Exactive, Thermo Scientific, Waltham, MA, USA) equipped with a C18 Hypersil Gold column (100 mm*2.1 mm, 1.9 μm, Thermo Scientific, USA).

3.2.5 Short Chain Fatty Acids Analysis

SCFA profiles were detected by gas chromatography-mass spectroscopy (GCMS-QP2010, Shimadzu, Kyoto, Japan) equipped with a DB-WAX column (30 m*0.25 mm*0.25 μm). 100 mg feces were mixed with 0.5 mL saturated NaCl solution, followed by homogenization via bead homogenizer (Servicebio, Wuhan, China). The suspension was added 125 μL 50% sulfuric acid (v/v) and 50 μL internal standard solution (2-methylhexanoic acid), and then extracted by 1 mL diethyl ether. The concentrations of SCFA were calculated based on internal standard, including acetic acid, propionic acid, butyric acid, isobutyric acid, valeric acid and isovaleric acid.

3.2.6 16S rRNA Gene Sequencing for Microbial Component Analysis

The method for 16S rRNA sequencing and data analysis was described previously (*197*). Briefly, DNA from mice feces was extracted by E.Z.N.A. Stool DNA Kit (D4015, Omega, Inc., Norcross, GA, USA) based on the manufacturer's instruction. The total DNA in elution buffer was stored at -80 ℃, until PCR amplification and sequencing measurement by LC-Bio Tech Co., Ltd (Zhejiang, China) on the Illumina MiSeq platform. After merging paired-end reads (FLASH) and quality control (fqtrim, V0.94), sequence with more than 97% similarity were assigned to the same operational taxonomic units (OTUs) via Vsearch (v2.3.4). The OTUs were classified by Ribosomal Database Project, and OUT abundance were normalized according to a standard of sequence number.

3.2.7 Statistical Analysis

All data were presented as mean ± standard deviation. All biological samples were

measured at least three times. Student's t test was used for comparison between two groups, and statistical significance level was reported if p value<0.05. Linear discriminant analysis Effect Size (LEfSe) was conducted to analyze the microbial structural change among different groups.

3.3 Results

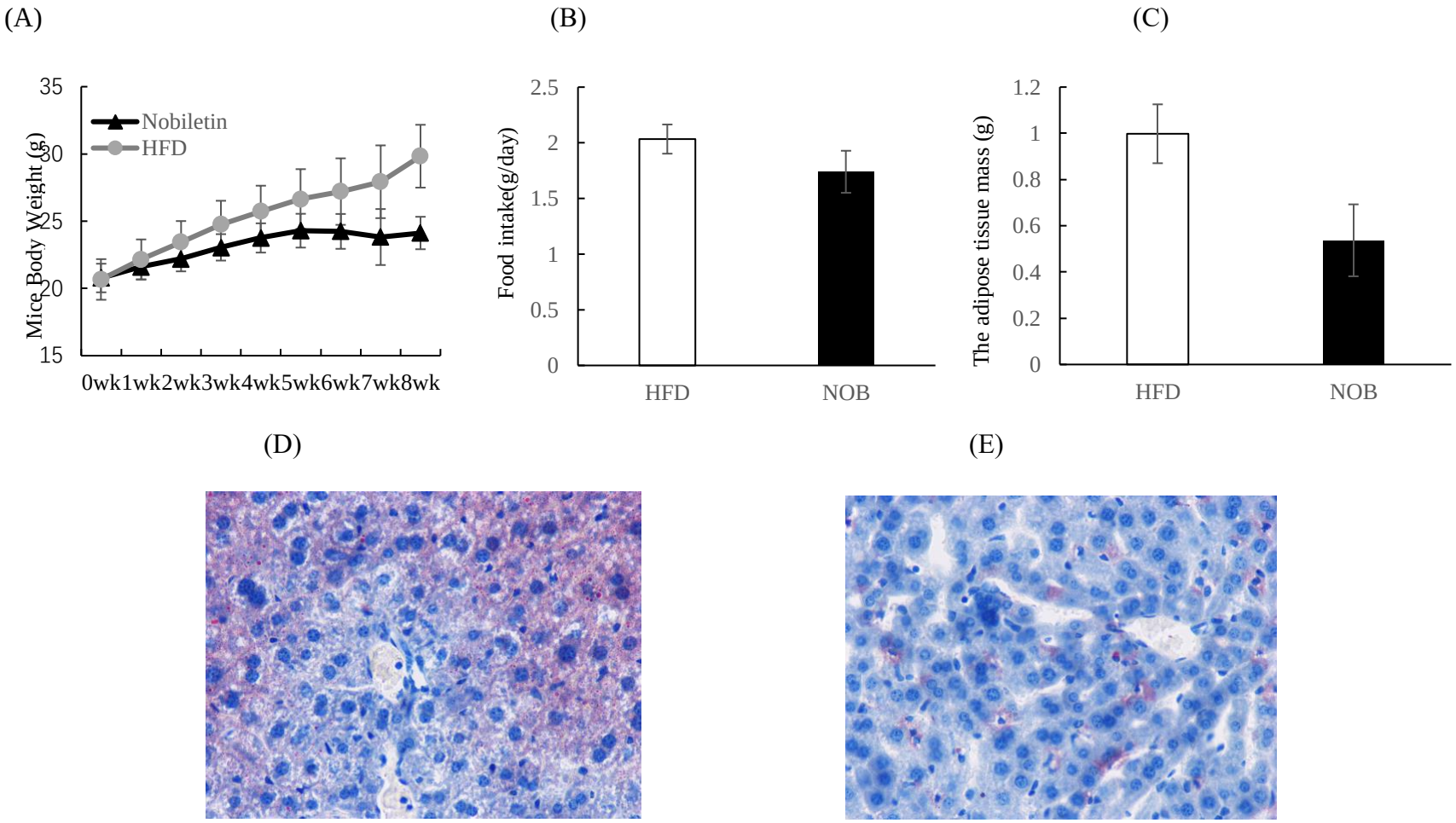

Figure 11: The influence of nobiletin in mice feeding with high fat diet: (A) the body weight, (B) food intake, (C) the mass of adipose tissues, (D)representative pictures for hepatic lipid accumulation in control group and (E) in experimental group.

3.3.1 The influence of nobiletin on mice body weight, food intake, the mass of adipose tissue and hepatic lipid accumulation

As illustrated in **Fig. 11A**, the orally administered nobiletin could significantly reduce the mice body weight gain. The mice body weight in the two groups started to have statistical difference in the third week at the significance level of $P<0.05$. Even though the averaged food intake in NOB group was about 14% less than the HFD group (**Fig. 11B**), the reduced food intake could not account for the reduction of body weight (≈19%). Moreover, the averaged mass of the adipose tissues in mice fed with nobiletin was about 53% of that in mice fed with HFD (**Fig. 11C**). Besides, the hepatic lipid accumulation was dramatically suppressed by nobiletin as shown in (**Fig. 11D**). Similar with previous reports (*146, 151*), this study showed that nobiletin exhibited good anti-obesity effect in mice fed with HFD.

3.3.2 Nobiletin metabolism in the feces excreted in 48 hours

The amount of nobiletin and its metabolites excreted from the feces was shown in **Fig. 12**. The amount of demethylated nobiletin metabolites including 3'-DMN, 4'-DMN and 3',4'-DDMN was significantly higher than the administered nobiletin in the first 12 hours. After 12-hour digestion, the amount of demethylated metabolites was less than nobiletin in the feces. Although most of nobiletin and its metabolites excreted within 24 hours after oral administration, a small amount of nobiletin could be detected in feces within 24-48 hours. It indicated that it took more than 24 hours for the colon to eliminate

the orally administered nobiletin.

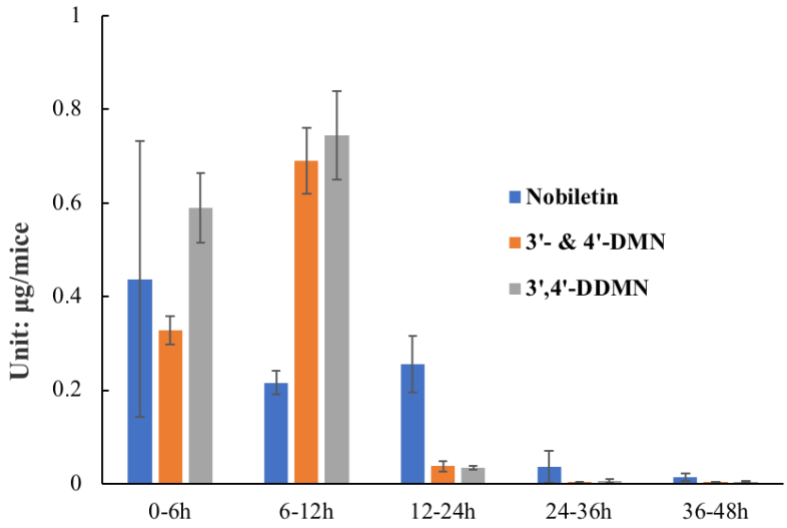

Figure 12 : The amount of nobiletin and its metabolites in feces within 48 hours.

3.3.3 Nobiletin metabolism in the feces in the 8-week study

As shown in **Fig. 13A**, the concentration of nobiletin in feces increased with the feeding time. It indicated that nobiletin had an accumulation effect in feces for the 8-week feeding. This result was consistent with our previous 48-hour study, which implied that the digestion time for daily administered nobiletin in the colon exceeded 24 hours. Most biotransformation of nobiletin occurred on the B-ring of flavone skeleton. By comparing the concentration change over 8 weeks, B-ring metabolites in feces had much more dramatical increase than nobiletin (**Fig. 13B & 13C**). The increasing ratio of metabolites to nobiletin along the time indicated that the biotransformation capacity of gut microbiota was enhanced gradually. Moreover, the concentration of 3',4'-DDMN (≈300 μg/g) in feces was much higher than 3′-DMN and 4′-DMN (≈50 μg/g), as well as nobiletin (≈0.45 μg/g) after 8 weeks. It indicated that gut microbiota could extensively biotransform nobiletin into

hydroxy metabolites.

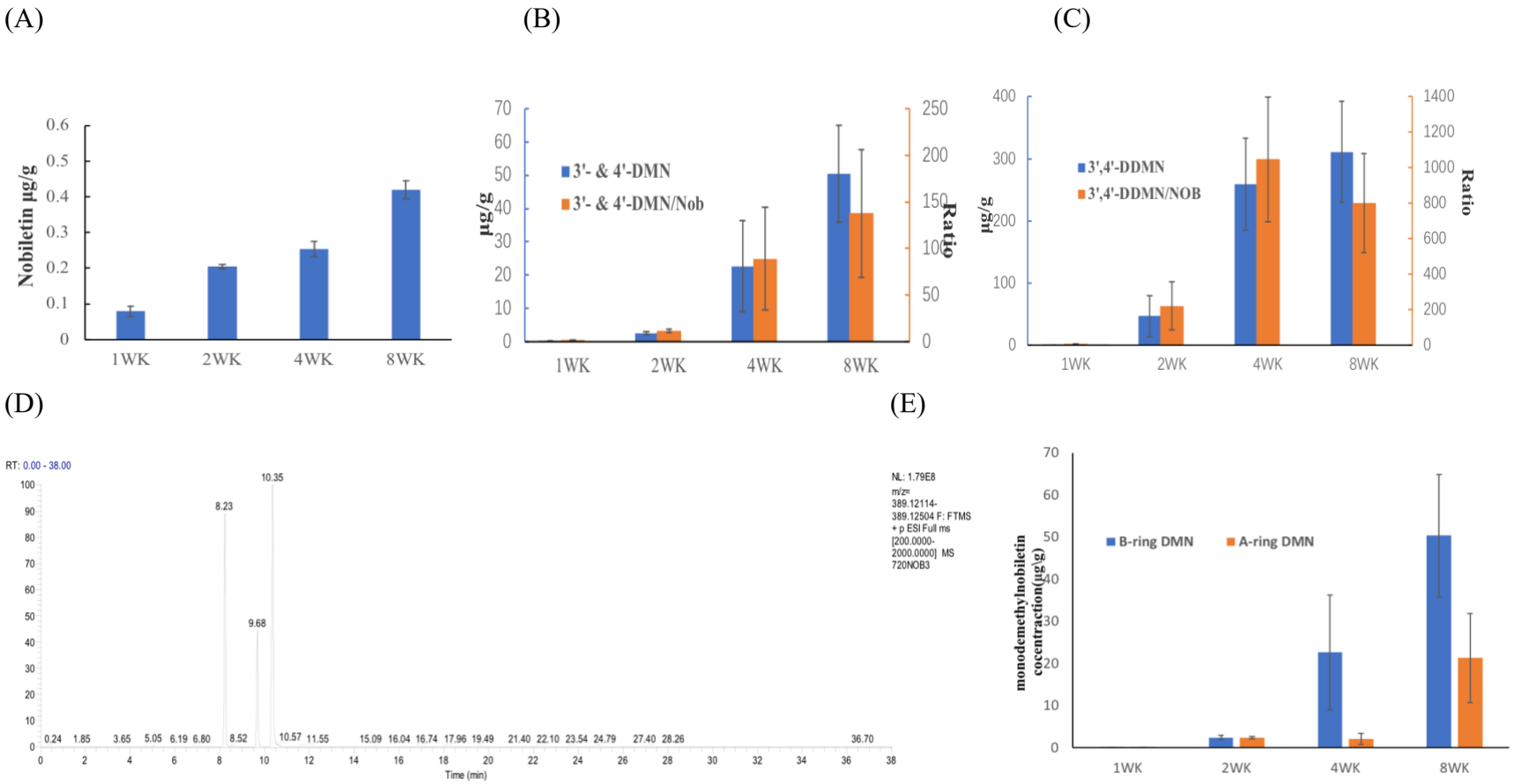

Figure 13: The concentration change of nobiletin and its metabolites in feces during 8-week consecutive feeding study: (A) nobiletin, (B) B-ring monodemthylnobiletin, (C) 3′,4′-didemethylnobiltin, and (E) A-ring monodemethylnobiletin. (D) LC-MS profile of monodemethylnobiletin in feces collected after 8-week feeding.

Another evidence of the improved biotransformation activity of gut microbiota was the generation of more diversified demethylated metabolites. **Fig. 13D** demonstrated the mono-demethylated metabolites identified in feces using selective ion model. The first two peaks corresponded to metabolites demethylated on A-ring position. As shown in **Fig. 13F**, the concentration A-ring MDN increased with the feeding time.[1] The increased concentration of A-ring MDN would lead to the generation of more diversified demethylated metabolites, as demethylation reaction would keep moving forward on the skeleton of nobiletin.

3.3.4. Nobiletin metabolism in mice liver and brain.

Table 3: The concentration of nobiletin and its metabolites in the mouse livers and brains.

Concentration & Ratio	Nobiletin (ng/g)	3'-DMN & 4'-DMN (ng/g)	3',4'-DDMN (ng/g)	DMN/NOB (Ratio)	DDMN/NOB (Ratio)
liver	14.67±6.25	1279.08±1787.68	886.40±1520.00	60.87±57.66	37.84±60.27
Brain	16.26±4.95	3.89±4.42	1.5±0.42	0.23±0.19	0.11±0.08

Liver and brain were selected as the representative tissues to study the metabolism of nobiletin in the host after 8-week study. As demonstrated in **Table. 3**, the concentration of nobiletin in liver and brain was comparable, i.e. 14.67±6.25 ng/g and 16.26±4.95 ng/g. Similar with previous studies (*215, 216*), this finding suggested that nobiletin had a good permeability across the blood-brain barrier (BBB). However, these two organs had quite different profiles for the demethylated metabolites. The liver was found to contain much

[1] Due to the lack of standard compound for A-ring metabolites, the concentration of A-ring metabolites was calculated using the B-ring metabolite with the same m/z.

more metabolites than nobiletin, while the brain contained much less metabolites than nobiletin. Moreover, the concentration of MNB in the liver was higher than 3',4'-DDMN. It indicated that livers might have weaker demethylation activity as compared to gut microbiota, since 3',4'-DDMN dominated in the metabolites profile in the feces (**Fig. 13B & 3C**).

3.3.5 The influence of nobiletin on fecal SCFA

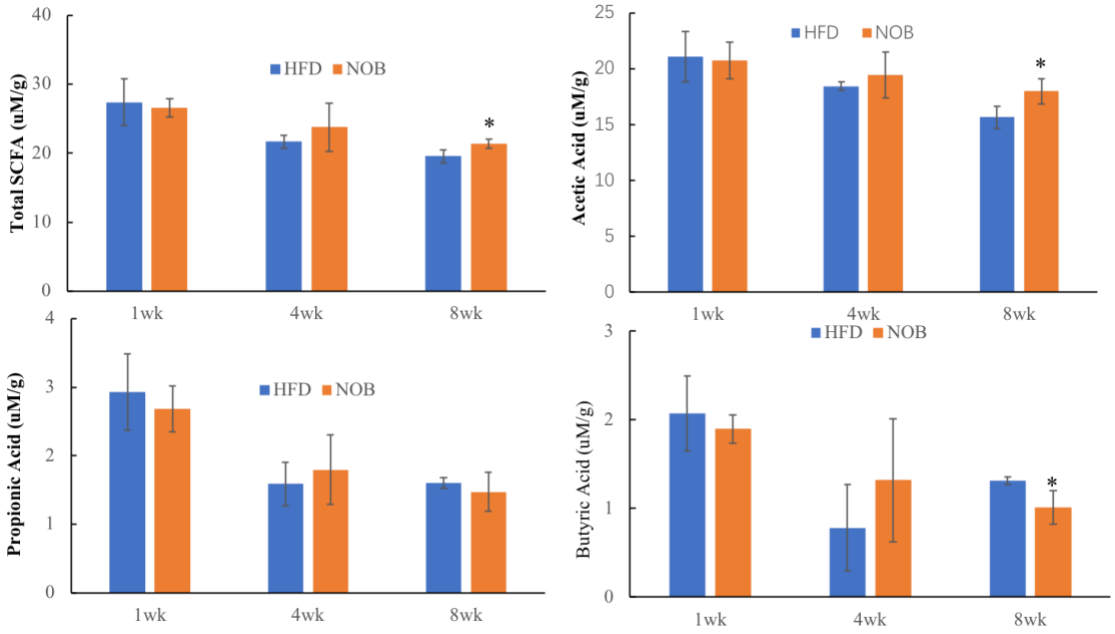

Figure 14: Nobiletin affected the fecal short-chain fatty acids (SCFA) profiles in mice fed with high-fat diet (HFD). Statistical differences compared to relative abundance in the HFD group were presented as * if $p < 0.05$.

The fecal SCFA of mice in two groups (NOB vs. HFD) were measured at the 1st, 4th, and 8th week (**Fig. 14**). The total SCFA represented for the sum of acetic acid, propionic acid, butyric acid, isobutyric acid, valeric acid and isovaleric acid. In general, the fecal SCFA decreased along the time for each group, and this phenomenon might be resulted

from the supplement of HFD for both groups. In the first 4 weeks, the fecal SCFA between two groups did not have significant difference. After 8-week regimen, the concentrations of total SCFA and acetic acid in mouse feces from the NOB group were significantly higher than that from the HFD group. The propionic acid from the two groups showed no significant difference. Even though the butyric acid produced in the NOB group was less than that in the HFD group, the decrease of butyric acid was negligible in terms of the total SCFA change.

3.3.6 Nobiletin modulated the fecal gut microbiota

The mice feces from the NOB and HFD groups at the 4th and 8th week were collected to examine the structural change of gut microbiota. The alpha diversity of gut microbiota from the four groups was shown in **Table. 4**. At the 4th week, the higher Shannon, Simpson and Chao1 indexes in NOB group indicated that the colonic microbial community was more diversified in the NOB group than that in the HFD group. However, these three indexes for NOB and HFD groups at the 8th week showed no significant difference. It indicated that the intake of nobiletin for 8 weeks did not significantly influence the microbial diversity.

Table 4: The indexes of Shannon, Simpson, and Chao1 for gut microbiota from the high fat diet control group (HFD) and nobiletin treatment group (NOB) at the 4th- and 8th- week. Oneway anova and Bonferroni post-test was used to examined for the significance level.

	Shannon	Simpson	Chao1
HFD_4wk	6.24 ± 0.18^{a}	0.95 ± 0.00^{a}	1337.94 ± 93.88^{a}
NOB_4wk	6.92 ± 0.14^{b}	0.97 ± 0.00^{b}	1910.93 ± 75.41^{b}

HFD_8wk	6.94±0.37[b]	0.96±0.01[a]	1737.34±165.78[b]
NOB_8wk	6.50±0.24[ab]	0.95±0.00[a]	1792.80±217.96[b]

Different letters (i.e., a, b, c) in superscript in the same column indicated the statistical significance level $p<0.05$

The structural change of gut microbiome between NOB and HFD groups at the 4th week (**Fig. 15A**) and 8th week (**Fig. 15B**) was analyzed by LEfSe at the same significance level (LDA=3.5). The enriched bacteria at different time intervals demonstrated different phenotypes. For example, nobiletin enriched Firmicutes and Bacteroidetes and inhibited Actinobacteria and Proteobacteria at the 4th week (**Fig. 15A**) at the phylum level. Meanwhile nobiletin enriched Firmicutes and Actinobacteria, and inhibited Bacteroidetes at the 8th week (**Fig. 15B**). Similar phenomenon was observed on the order-, family- and genus-level. In particular, *Erysipelotrichale* at the order level and *Erysipelotrichaceae* at the family level were found to keep enriched by nobiletin at both time points.

(A)

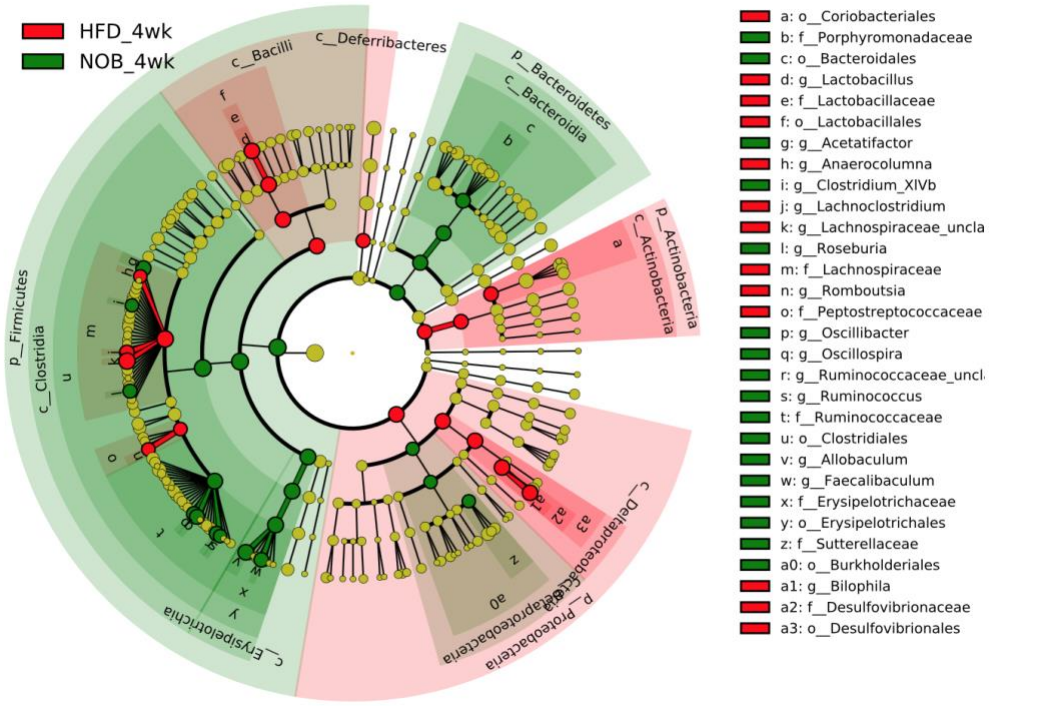

(B)

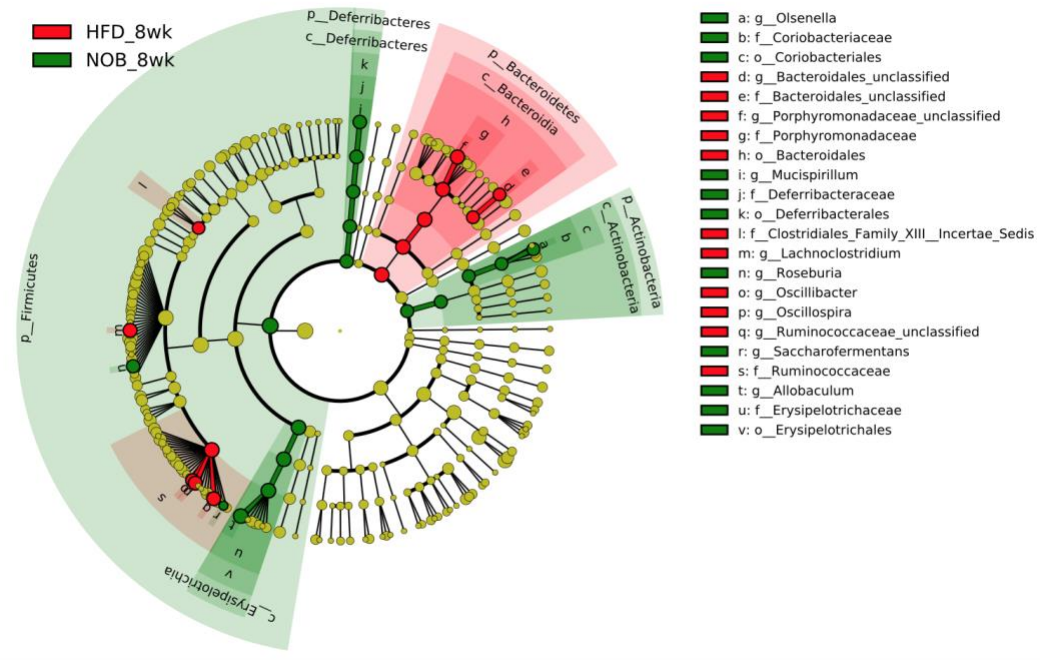

Figure 15: The influence of nobiletin on the compositional change of gut microbiota(A)at the 4th week and (B)at the 8th week.

(A)

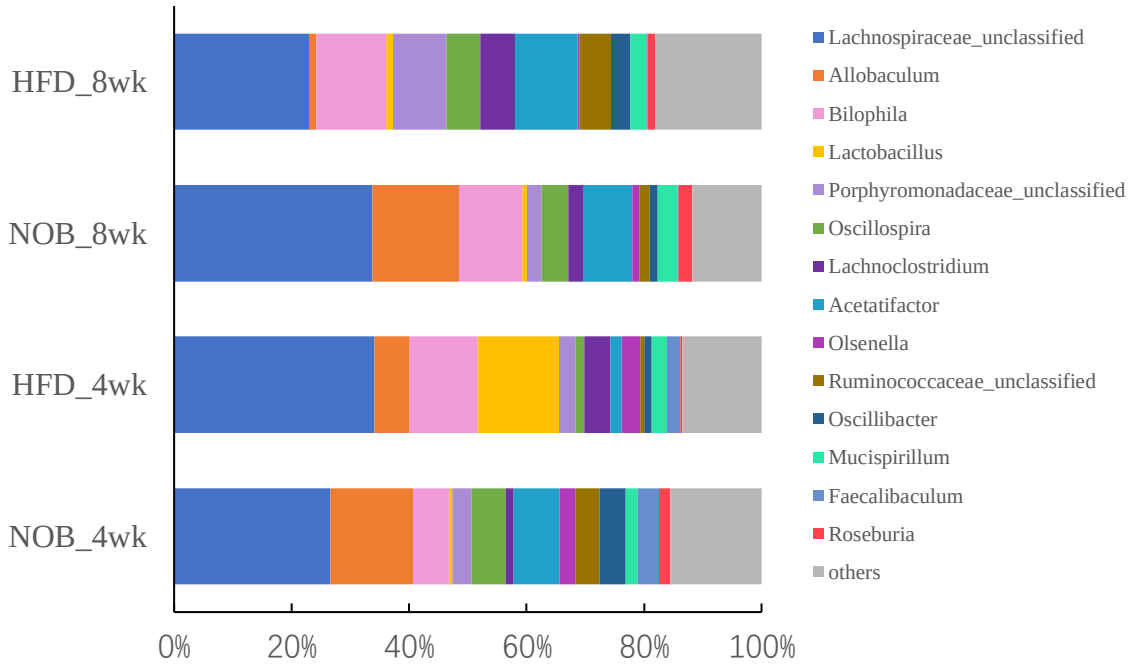

(B)

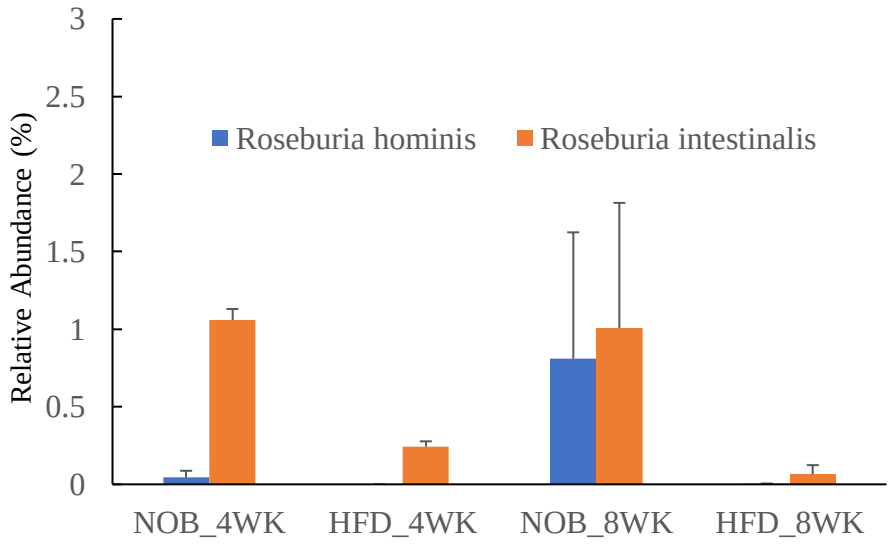

Figure 16: (A)The averaged colonic bacteria at the genus level in the high fat diet control group (HFD) and nobiletin treatment group (NOB) at the 4th- and 8th- week. (B) The relative abundance of *Roseburia hominis* and *Roseburia intestinalis* in the two groups at each time interval.

The averaged bacterial profiles at the genus level for the four groups were presented

in Fig. 16. *Allobaculum* and *Rosebuira* were consistently enriched by nobiletin at both time points (**Fig. 16A**). The relative abundance of *Allobaculum* was 14.11±0.60% for NOB group and 5.98±0.23% for HFD group at the 4th week; and 14.67±8.78% for NOB group and 1.24±0.81% for HFD at the 8th week. As *Allobaculum* prevalence was decreased along the time in the HFD group, it indicated that HFD would inhibit the abundance of *Allobaculum* in the colonic microbes. However, the similar abundance of *Allobaculum* in the NOB group at the 4th and 8thweek suggested that nobiletin significantly promoted *Allobaculum*, and even compensated the inhibitory effect caused by HFD. Another enriched bacterium—*Roseburia* demonstrated different dynamic pattern with *Allobaculum*. The relative abundance of *Roseburia* was 1.98±0.59% for NOB group and 0.38±0.06% for HFD group at the 4th week; 2.43±0.4% for NOB group and 1.26±0.18% for HFD at the 8th week. The amplification fold of *Roseburia* in the NOB group between the two time points seemed lower than that in the HFD group. Whereas, the influence of nobiletin on the species level of *Roseburia* was more significant, especially for *R. hominis* and *R. intestinalis* (**Fig. 16B**). The relative abundance of *R. hominis* in the NOB group at the 8th week was 17.69 times higher than that at the 4th week; while *R. hominis* in the HFD group remained a very low level at both intervals. The dynamic change of *R. intestinalis* looked similar with *Allobaculum*. The magnification of *R. intestinalis* by nobiletin was about 4.35 folds at the 4th week and 15.51 folds at the 8th week, compared with the control group at each time interval. Together, these results indicated that nobiletin kept promoting the prevalence of *R. hominis* and *R. intestinalis* along the time.

3.4 Discussion

In the present study, we investigated the directional interaction of nobiletin and gut microbiota using mice fed with HFD.

The biotransformation of nobiletin by gut microbiota was studied in the single dose study within 48 hours as well as the 8-week consecutive dosing study. From the 48-hour excretion study for feces, it showed that most of nobiletin was excreted within 24 hours after oral administration. The total recovered amount of metabolites was higher than nobiletin within 48 hours. In detail, the concentration of 3',4'-DDMN was highest, followed by the MNB and nobiletin in the feces excreted within first 12 hours. However, another excretion study found that the concentration of MNB was 6 times higher than 3',4'-DDMN in the mouse urine excreted within first 12 h (*78*). The different metabolites profiles in feces and urine indicated that the biotransformation activity of nobiletin varied between the host and gut microbiota. Through 8-week consecutive dosing study, two ratios- 3'- & 4'-DMN/NOB and 3',4'-DDMN/NOB increased along the time (**Fig. 13**). It suggested that the oral administration of nobiletin for a long time would change the gut microbiota, and the altered microbes had a stronger metabolizing ability on nobiletin. Similar phenomenon was discovered in previous literatures. For example, Asian people who regularly consumed soy were more likely to produce equol, a beneficial colonic metabolites of isoflavones, compared with western populations (*217*). Similarly, a specific microbiota-encoded enzyme system for porphyrin, a polysaccharide from marine red algae were more frequently discovered in seaweed-consumed population, compared with populations who seldom consumed seaweeds (*218*). These findings suggested that gut microbiota might be

a reservoir of selectable functions, and certain metabolic input could select specific pathways or microbes that harbored these pathways (*160*).

The mouse brain and liver were selected to study the metabolic profiles of nobiletin in the host, considering the important role of gut-brain and gut-liver axis in obesity signaling (*34*). The concentration of nobiletin in the brain and liver was found quite comparable, indicating that nobiletin had a very good permeability across the BBB. Recent studies illustrated neuroprotective effect of nobiletin, including the improvement of neuroinflammation, memory impairment and dementia (*9*). These beneficial effect of nobiletin might partially derive from its rapid penetration across BBB (*215*). In terms of metabolites profile, liver was very active for nobiletin biotransformation, but little demethylated metabolites were detected in the brain. Two reasons might explain this phenomenon: 1) the metabolic activity in the brain was deficient; 2) due to the changed polarity, the demethylated metabolites had weaker capacity to cross BBB than nobiletin.

The modulate effect of nobiletin on gut microbiota were accessed through two aspects--fecal SCFA and microbial compositional change. SCFA were often used as the biomarkers for gut health due to their anti-inflammation activity. In the present study, acetic acid was significantly elevated by nobiletin after 8 weeks and served as the main driving factor for the elevated total SCFA (Fig. 14). SCFA could function locally in the colon, such as feeding colonocytes; protecting intestinal barriers by stimulating mucin production; and inhibiting pathogenic microbe proliferating by lowing the pH condition (*100*). In addition, SCFA, especially acetic acid could enter the portal circulation, and

actively participate in the host energy homeostasis regulation (*34*). Therefore, the SCFA pathway might be one possible mechanism underlying the anti-obesity activity of nobiletin.

Nobiletin could dynamically change the composition of gut microbiota, and the altered microbes could affect the energy homeostasis of the host. The enriched colonic bacteria at different time intervals were not necessarily the same through LEfSe analysis. In this study, two bacteria at the genus level -*Allobaculum* and *Roseburia*- were found to promote by nobiletin at both time intervals. Considering the increased demethylation activity of gut microbiota (**Fig. 13**) and the similar trend of these two bacteria, it suggested that *Allobaculum* and *Roseburia* correlated with the enhanced metabolic activity on nobiletin.

Previous studies have investigated the health implications for these two bacteria. *Allobaculum* was identified as the active glucose assimilator through the RNA-based stable isotope probing analysis. Besides, acetates, propionates and lactates were found as the major fermented metabolites of the ^{13}C-labled glucose by *Allobaculum* (*219*). The abundance of *Allobaculum* was relatively lower in HFD-fed mice compared to mice fed with normal diets (*187*). According to the correlation analysis, *Allobaculum* abundance was associated with higher plasma HDL concentrations, lower circulating leptin concentration and higher gene expression for energy homeostasis (*187*). Similar to our finding, *Allobaculum* was also reported to promote by several phytochemicals, such as PMFs in citrus peels (*72*) and berberine (*188*). Another typically enriched bacteria by nobiletin, *Roseburia*, had received increasing attentions due to its positive role on metabolic diseases, such as atherosclerosis, obesity, and type 2 diabetes (*220*). In addition, *Roseburia* was

found to involved in the SCFA production (*92*). In this study, two species were responded to nobiletin administration: *R. hominis* and *R. intestinalis*. Both species demonstrated multiple beneficial effects on the host through the colonization studies (*221, 222*). For example, the treatment of *R. hominis* on mice was suggested to protect against DSS-induced colitis, enhance the gut barrier function, and promote Treg population expansion in the host (*221*). Another study also found that the colonization of *Roseburia intestinalis* could lower the level of inflammatory markers and inhibit atherosclerosis, and these effects might come from its metabolite—butyrate (*222*). The improved abundance of these functional bacteria could contribute to the anti-obesity effect of nobiletin.

3.5 Conclusion

In summary, this study investigated the bidirectional interaction between nobiletin and gut microbiota by analyzing the colonic metabolites and compositional change of gut microbiota. Results showed that this interaction played an important role on the anti-obesity effect of nobiletin. For the excretion study, more demethylated metabolites with higher biological activity was found in feces than nobiletin. Moreover, oral administration of nobiletin for a long period would alternate gut microbiota with improved demethylation activity and enhanced production for SCFA. Gut microbiota might have higher biotransformation activity of nobiletin than the host, since higher ratio of DDMN were detected in feces rather than mouse livers and brains. Two bacteria, *Allobaculum* and *Roseburia*, were found to correlate with nobiletin biotransformation through analyzing the dynamical change of gut microbiota composition. As many health benefits had been

recorded for *Allobaculum* and *Roseburia*, it indicated that the enrichment of functional bacteria should be one of the pathways for the anti-obesity activity of nobiletin.

CHAPTER IV: COMPARATIVE ANALYSES OF BIOAVAILABILITY, BIOTRANSFORMATION AND EXCRETION OF NOBILETIN IN LEAN AND OBESE RATS

4.1 Introduction

Citrus fruits have high consumer demand for their delicious taste, attractive aroma, and high nutritional values (*223*). The citrus peels, which account for about 44% of the whole fruit mass, are the by-products in citrus juice industry (*224*). Various bioactive compounds such as dietary fibers, essential oils, and flavonoids have been identified in citrus peels (*225*). Polymethoxyflavones (PMF) are important constituents in citrus flavonoids, especially in the citrus peels. About 80 PMF have been reported so far (*9*). Nobiletin is one of the most prevalent PMF in citrus peels, and has been widely studied for its pronounced bioactivities, including anti-inflammatory, anti-obesity, anti-carcinogenic, and anti-atherogenic properties (*11*).

The studies about the bioavailability and biotransformation of nobiletin *in vivo* remain limited. The bioavailability of phytochemicals is an overall consequence influenced by their bioaccessibility, absorption and metabolism (*51*). Nobiletin has poor water solubility but high membrane permeability due to the existence of multiple methoxy groups in the chemical structure. Singh, Tewari (*216*) found that the maximum concentration of nobiletin was 1.78 μg/mL in the plasma observed 1 hour after single oral dosage (50 mg/kg). The common metabolic pathway of nobiletin is demethylation. Manthey, Cesar (*55*) identified 8 demethylated metabolites in the aglycone- and conjugated forms in the rat serum after

oral administration of nobiletin. In our previous work, we chemically synthesized the demethylated nobiletin and found that the demethylated metabolites demonstrated better anti-inflammation and anti-cancer effects than nobiletin (*37, 38, 214*). In addition, the chemopreventive effect of nobiletin *in vivo* against colon carcinogenesis was suggested to strongly associate with the demethylated metabolites (*81*). Overall, it indicates that the biotransformation is an important pathway to influence the bioefficacy of nobiletin *in vivo*. However, few pharmacokinetic studies of nobiletin have quantitatively investigated the biotransformation in the blood (*55, 64, 65, 216*).

The colon was recently studied as an important organ for the metabolism and reabsorption of flavonoids, since numerous microorganisms harbor in this site. The orally administered flavonoids that are not absorbed by the small intestine will enter the colon, where they undergo biotransformation by gut microbiota before reabsorption (*75*). The common colonic bioconversion of flavonoids includes: deglycosylation, C-ring cleavage, hydrolysis of ester, demethylation, etc. (*68, 75, 76*). The demethylation of PMF by gut microbiota have been observed using the *in vitro* fermentation model (*76, 80*). However, few studies have investigated the microbial biotransformation of nobiletin *in vivo*. The comparative study of the demethylation of nobiletin in the host and by gut microbiota is helpful to gain in-depth understanding of the biological fate of nobiletin *in vivo*.

The recent obesity epidemic receives increasing attentions. Our previous studies have shown that PMF have a very good anti-obesity effect as the dietary supplement using the high fat diet (HFD) induced obese mouse model (*73, 150*). PMF could attenuate obesity via preventing lipid accumulation in the host bodies (e.g. in the adipose tissue and liver) as well as modulating the composition of gut microbiota (*73, 136, 150*). Interestingly, the

obesity is found to in turn influence the absorption and metabolism of phytochemicals *in vivo* (*226*). Since HFD has been reported to decrease the protein expression for tight junction (*98*), the increased intestinal epithelium permeability in obese individuals might influence the absorption of phytochemicals. Besides, the composition of gut microbiota in obese individuals is structurally different from their lean counterparts for both rodents and humans (*34, 67*). It indicates that the colonic biotransformation of phytochemicals may vary depending on weight status. For example, the producers of equol, a bioactive colonic metabolite of isoflavones, are more relevant in normal-weight participants than the obese ones (*227*). A recent study finds that nobiletin attenuates obesity in mice fed with HFD, but not significantly affect the weight status in mice fed with normal diets (*106*). The linkage between the metabotypes and specific health benefit of polyphenols/flavonoids is very interesting but poorly investigated (*227*). To our knowledge, this is the first study exploring the influence of the obesity on the bioavailability and biotransformation of nobiletin *in vivo*.

To quantitatively investigate the absolute bioavailability and biotransformation of nobiletin, this study conducted the excretion and pharmacokinetic studies via oral administration and intravenous injection, and 15-day consecutive dosing study using the HFD induced obese rats and their lean counterparts. In particular, the demethylation is focused on the biotransformation of nobiletin. This comparative study about nobiletin metabolism was presented in three approaches: 1) via host body and gut microbiota; 2) in the lean and obese rats; and 3) in single-dose pharmacokinetic study and 15-day consecutive dosing study. Our results will provide scientific insights for the biological fate of nobiletin as well as its bioavailability-bioactivity relationship.

4.2 Materials and Methods

4.2.1 Reagents and Chemicals

Nobiletin with 97% purity was purchased from Qiongge Biochemicals Inc (Wuhan, China). Organic solvents including methanol and acetonitrile were all HPLC grade and obtained from MilliporeSigma (Burlington, MA, USA). Tween 80 and dimethyl sulfoxide (DMSO) were analytical grade and obtained from Sinopharm Chemical Reagent Co., Ltd (Shanghai, China). Two types of animal diets were obtained from Guangdong Medical Laboratory Animal Center (Guangzhou, China), including normal diets (ND, 10% calories from fat, D12450B) and HFD (60% calories from fat, D12492). Carboxymethyl cellulose (CMC) was obtained from Yuanye Bio-Technology Co., Ltd (Shanghai, China). β-glucuronidase and Sulfatase were purchased from Sigma-Aldrich (St. Louis, MO, USA).

4.2.2 Synthesis of Nobiletin Metabolites

The demethylated metabolites of nobiletin were synthesized according to our previous methods (*214*). Briefly, the B-ring metabolites were synthesized from the 5-step reactions, and the replacement of hydroxyl group on the 5-position methoxy group was obtained through one-step process in acidic condition. Overall, three mono-demethylated nobiletin (DMN) and two di-demethylated nobiletin (DDMN), i.e., 3′-DMN, 4′-DMN, 5-DMN, 3′,4′-DDMN and 5,4′-DDMN were obtained. The chemical structures for nobiletin and its demethylated metabolites are shown in **Fig. 17**. All the synthesized metabolites were purified by silica gel column chromatography and their chemical structures were

confirmed by NMR. These synthesized metabolites were used to quantify the metabolites of nobiletin in the urine, plasma and feces.

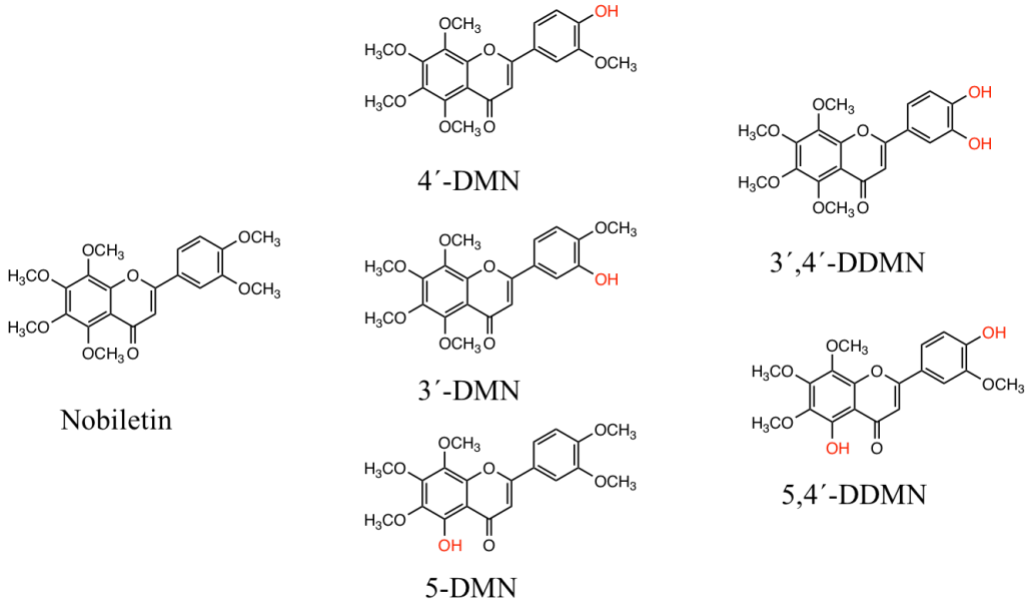

Figure 17: The chemical structures of nobiletin, mono-demethylated nobiletin (DMN) and di-demethylated nobiletin (DDMN): 3′-DMN, 4′-DMN, 5-DMN, 3′,4′-DDMN, and 5,4′-DDMN.

4.2.3 Animals and Diets

5-week-old male Sprague-Dawley rats were purchased from Southern Medical University (Guangzhou, China) and housed in a specific pathogen free, temperature-/humidity-controlled room with 12 h light/dark cycles. The experimental protocol was approved by the Institutional Animal Care and Use Committee in South China Agricultural University (protocol number: 2019048). After one-week adaptation to the environment, rats were randomly assigned to two groups and then received ND and HFD *ad libitum* for another 10 weeks, respectively. After 10-week feeding, the body weights of rats were recorded and the serum indexes of rats were determined using chemical analyzer (Mindray BS-380, Shenzhen, China). The serum indexes included aspartate aminotransferase (AST,

U/L), alanine aminotransferase (ALT, U/L), fasted glucose (mmol/L), total cholesterol (mmol/L) and total triglycerides (mmol/L). In total, 42 rats (21 lean rats and 21 obese rats) were recruited in the following excretion, pharmacokinetics and 2-week consecutive dosing study.

4.2.4 Excretion Experiment

Five obese rats and five lean rats were housed in the metabolic cages individually for the excretory study. They were treated with 100 mg/kg nobiletin suspended in 0.5% CMC solution. Urine and feces samples were collected after oral gavage during the following intervals: 0-12 h, 12-24 h, 24-36 h, 36-48 h. The feces samples were freeze-dried before pulverization. The volume of urine samples and the weight of freeze-dried feces were recorded before extraction. 100 μL urine samples were treated with sulfatase and β-glucuronidase, and incubated at 37 ℃ for 45 min after well mixing. Then, the mixture was mixed with 20 μL tangeretin (100 μg/mL) as the internal standard, extracted by 300 μL ethyl acetate using a shaker for 5 min, then centrifugated at 9500*g* for 3 min to obtain the supernatant. After repeating the extraction process, the combined supernatant was evaporated by a flow of nitrogen. The residues were dissolved by 80% methanol aqueous solution containing 0.2% acetic acid and diluted 10 times before measurement. The feces samples were pulverized by bead homogenizer (Servicebio, Wuhan, China). Fifty mg pulverized feces samples were added to tangeretin solution as the internal standard, extracted by 1 mL 80% methanol with 0.2% acetic acid, and subsequently centrifuged at 9500*g* for 3 min. After twice extraction, the combined supernatant was properly diluted and filtered through a 0.22 μm nylon filter before measurement.

4.2.5 Pharmacokinetics Experiment

The animals for this study were divided into 4 groups (5 rats/group) by the weight status and administration routes: lean rats with oral administration, lean rats with intravenous injection, obese rats with oral administration, and obese rats with intravenous injection. For the oral administration, nobiletin was suspended in 0.5% CMC solution and given to rats by oral gavage at the dose of 100 mg/kg. For the intravenous injection, nobiletin was dissolved in 5% DMSO and 20% Tween 80 and given to rats via tail vein injection at the dose of 4 mg/kg. Blood samples were collected in heparin-coated tubes at the 0.5, 1, 2, 4, 6, 10 and 24 h after the administration of nobiletin. After centrifugation at 2400*g* for 10 min, the plasma was collected by removing the residues. 100 μL plasma was treated with sulfatase and β-glucuronidase; incubated at 37 ℃ for 45 min; and extracted by 300 μL ethyl acetate with tangeretin as the internal standard. After centrifugation at 9500*g* for 3 min, the supernatant was collected. The extraction was conducted twice. After evaporating the combined supernatant, the residue was dissolved by 200 μL 80% methanol with 0.2% acetic acid and filtered through 0.22 μm nylon filter before LC-MS measurement.

The pharmacokinetic indexes were estimated using Phoenix WinNonlin 8.1 software (Certara, NJ, USA). The area under the curve (AUC) in the pharmacokinetics study was the integral of the plasma concentration of nobiletin against the definite time. The subscript abbreviation *po* referred to oral administration, and *iv* corresponded to intravenous injection. The absolute bioavailability of nobiletin was calculated according to the following equation (*52*):

$$F(\%) = (AUC_{po} * Dose_{iv})/(AUC_{iv} * Dose_{po)} * 100 \quad (1)$$

4.2.6 15-day Consecutive Dosing Study

Six lean rats and six obese rats were used to investigate nobiletin metabolism in the 2-week consecutive dosing study. All rats were allowed to freely access the diets/water and given 100 mg/kg nobiletin daily by oral gavage. Blood samples were collected at the 6 h after oral administration of nobiletin at the 1st, 3rd, 6th, 9th, 12th, and 15th day. The preparation of blood samples for analysis was the same as the pharmacokinetics study. Fresh feces samples were collected at the 12 h after oral administration at the 2nd, 5th, 8th, 11th, and 14th day. 100 mg feces were weighted and subjected to the subsequent extraction process the same as that in the excretion study.

4.2.7 Determination of Nobiletin Metabolites using UPLC-MS/MS

The concentrations of nobiletin and its demethylated metabolites in bio-samples were quantified by using UPLC-MS/MS consisting of UPLC (model: LC-30AD) (Shimadzu, Kyoto, Japan) and Triple Quadrupole Linear Ion Traps mass spectroscopy (model QTRAP 4500) (AB SCIEX, Concord, Canada). The Poroshell 120 PFP column (4.6*150 mm, 2.7 μm) (Agilent, Santa Clara, CA, USA) was utilized and the column temperature was set at 40 ℃. The injection volume was set as 5 μL. The mobile phases included 0.1% formic acid (v/v) in water (A) and acetonitrile (B). The flow rate was 1 mL/min. The following elution program was used: 0-2 min, 35%-35% B; 2-7 min, 35%-50% B; 7-10 min 50%-95% B; 10-12 min, 95% B, 12.01 min-13 min, 35% B (maintaining 35% B for another 2 min for post-measurement). Following global MS parameters were used: Turbo ion spray source temperature 550 ℃, ion spray voltage 5500 V, curtain gas 40 psi, ion source gas 60 psi. The quantification of nobiletin and its metabolites were carried out in the positive mode

with multiple reaction monitoring (MRM). The MRM transition, declustering potential and collision energy for each compound were optimized and shown in the supplementary materials (**Table 5**).

Table 5： MRM conditions for determination of nobiletin and its demethylated metabolites by LC-MS.

Analyte	Precursor ion (m/z)	Product ion (m/z)	Declustering potential (V)	Collision energy (eV)
nobiletin	402.80	373.00	135.00	35.06
3′-DMN	389.00	359.10	137.89	35.25
4′-DMN	389.20	359.10	130.92	34.00
5-DMN	389.20	359.10	108.05	37.78
3′,4′-DDMN	375.20	345.10	89.20	34.16
5,4′-DDMN	375.20	345.10	89.20	34.16
tangeretin	372.80	343.00	145.40	34.80

DMN is the abbreviation for mono-demethylated nobiletin and DDMN is the abbreviation for di-demethylated nobiletin

4.2.8 Statistical Analysis

All experimental results were presented as means ± standard deviations. The statistical difference between the lean and obese rats was examined by the one-way ANOVA followed by Bonferroni multiple-comparison test or the unpaired student t-test using StataSE v15. The significance was reported if P-value<0.05.

4.3 Results

4.3.1 Development of the obese/lean rat model

Table 6: The body weight, serum aspartate aminotransferase (AST, U/L), serum alanine

aminotransferase (ALT, U/L), serum fasted glucose (mmol/L), serum total cholesterol (mmol/L) and total triglycerides (mmol/L) for lean- and obese-rats after the 10-week feeding.

	Body weight(g)	AST(U/L)	ALT(U/L)	fasted glucose (mmol/L)	Total cholesterol (mmol/L)	Total triglycerides (mmol/L)
Lean rats	490.4±48.3	144.6±17.0	75.7±12.0	6.38±2.2	1.9±0.3	1.5±0.8
Obese rats	586.3±36.4***	152.0±18.4	85.0±8.1	6.8±0.9	2.8±0.1**	1.1±0.4

The asterisks, *, **, and ***, indicate the statistically significance levels at $P<0.05$, $P<0.01$ and $P<0.001$

Before conducting the experiment, the rats were supplied with ND or HFD for 10 weeks to initiate the development of obesity. As shown in **Table 6**, the body weight of rats fed with HFD (586.3±36.4 g) was significantly higher ($P<0.001$) than those fed with ND (490.4±48.3 g). The total cholesterol concentration in the serum was significantly higher ($P<0.01$) in the obese rats than lean rats. The concentrations of AST, ALT, fasted glucose and total triglycerides in the serum did not shown statistically significant difference between the lean and obese rats (**Table 6**). For all bio-samples, the quantification of nobiletin and its demethylated metabolites was carried out by LC-MS/MS and internal standard (tangeretin) calibration. The LC-MS/MS profiles of the standard compounds of nobiletin and its metabolites are shown in **Fig. 18**.

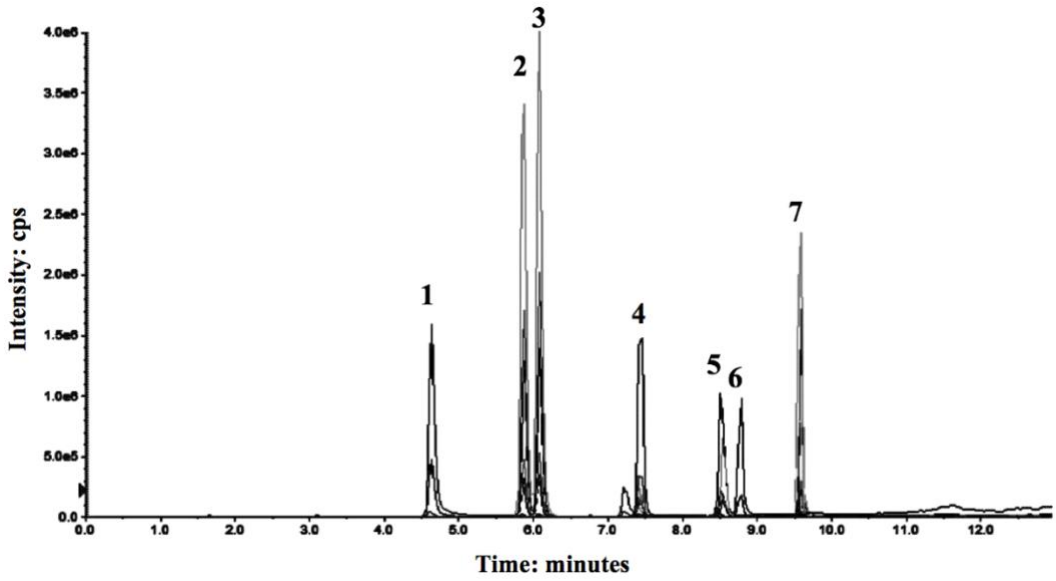

Figure 18: The LC-MS/MS profiles of standard compounds of nobiletin, mono-demethylated nobiletin (DMN) and di-demethylated nobiletin (DDMN): Peak 1 represents 3′,4′-DDMN; peak 2 represents 3′-DMN; peak 3 represents 4′-DMN; peak 4 represents nobiletin, peak 5 represents tangeretin (internal standard); peak 6 represents 5,4′-DDMN, and peak 7 represents 5-DMN.

4.3.2 Urinary and fecal Excretion Study

The quantities of nobiletin and its demethylated metabolites excreted from the urine of lean rats and obese rats are listed in **Table 7**. As the quantities of metabolites were much larger than nobiletin, it indicated that nobiletin underwent significant biotransformation in the host body. Most metabolites were excreted within 12-24 h for lean rats or within 12-36 h for obese rats. 4′-demethylnobiletin (4′-DMN) had the highest concentration among demethylated metabolites in the urine, and its amount accounted for about 5% of the intake. In general, the rank order for the concentration of DMN in the urine was: 4′-DMN>3′-DMN>5-DMN. For the DDMN, the concentration of 4′,5-DDMN was higher than 3′,4′-DDMN in the urine. The concentrations of the metabolites to nobiletin in the urine did not

show significant difference regarding rats' weight status ($P<0.05$).

The excreted quantities of nobiletin and its demethylated metabolites via feces from lean and obese rats are shown in **Table 8**. Similar with urinary metabolites, the concentrations of metabolites in feces were much higher than nobiletin. In general, the recovered quantity of metabolites excreted via feces increased along with the time, which indicated that the extent of demethylation on nobiletin depended on the incubation time in the colon. For the lean rats, the amount of 3′,4′-DDMN was the highest among demethylated metabolites in feces and accounted for about 3.35±2.88% of the intake. For the obese rats, the quantities of 4′-DMN and 3′,4′-DDMN were the highest in the fecal metabolites profile and totally accounted for about 5% of the intake. Moreover, the content ratio of total demethylated metabolites over nobiletin in feces excreted from obese rats (60.16±19.67) was significantly higher ($P< 0.05$) than that (27.75±15.43) from lean rats.

Table 7: The Excreted Quantity of Nobiletin and its Metabolites from Urine[1] (Unit: μg).

	Parent compound nobiletin	Mono-demethylated metabolites			Di-demethylated metabolites	
		3′-DMN	4′-DMN	5-DMN	3′,4′-DDMN	4′,5-DDMN
Lean rats						
0-12 h	24.92±7.61[a]	46.16±32.78[a]	461.69±209.01[b]	18.22±6.21[a]	1.62±1.33[a]	67.87±27.00[a]
12-24 h	18.73±9.19[a]	103.76±92.84[a]	792.41±396.74[b]	13.3±6.10[a]	4.92±3.49[a]	102.6±58.40[a]
24-36 h	12.50±4.87[a]	63.73±63.14[a]	524.98±196.89[b]	8.98±2.64[a]	1.84±1.08[a]	65.06±36.73[a]
36-48 h	21.18±8.55[a]	171.06±116.59[a]	558.63±207.77[b]	5.39±1.54[a]	1.84±31.16[a]	75.03±31.33[a]
total amount	77.34±13.57[a]	384.71±221.44[a]	2337.71±833.38[b]	45.89±9.64[a]	52.83±35.35[a]	310.56±130.87[a]
%intake [2]	0.17±0.03[a]	0.87±0.50[a]	**5.22±1.86**[b]	0.10±0.02[a]	0.12±0.09[a]	0.69±0.28[a]
Content Ratio of metabolites/nobiletin				39.95±12.56		
Obese rats						
0-12 h	96.43±124.86[a]	33.50±23.36[a]	668.56±305.25[b]	18.43±10.53[a]	1.19±0.80[a]	139.4±50.78[a]
12-24 h	21.51±12.78[a]	44.46±36.40[a]	827.98±523.58[b]	10.66±9.70[a]	2.99±1.00[a]	155.47±145.53[a]
24-36 h	18.73±9.19[a]	103.76±92.84[a]	792.41±396.74[b]	13.3±6.10[a]	4.92±3.49[a]	102.6±58.40[a]
36-48 h	12.50±4.87[a]	63.73±63.14[a]	524.98±196.89[b]	8.98±2.64[a]	1.84±1.08[a]	65.06±36.73[a]
total amount	145.65±152.31[a]	306.87±259.48[a]	2725.06±1163.83[b]	45±25.68[a]	61.29±59.87[a]	520.16±300.81[a]
%intake [2]	0.27±0.30[a]	0.52±0.39[a]	**4.80±2.13**[b]	0.08±0.05[a]	0.10±0.10[a]	0.93±0.59[a]
Content Ratio of metabolites/nobiletin				40.79±27.21		

[1] Data was expressed as the mean ± standard deviation. The oral dosage of nobiletin was 100 mg/kg. Statistical analysis was conducted among nobiletin and its metabolites in the same time intervals. Different letters in superscript indicated the statistically significant level $p<0.05$.

[2] % intake was the amount (μg) of recovered compound in the urine divided by the oral intake (μg) of nobiletin

Table 8: The Excreted Quantity of Nobiletin and its Metabolites from Feces[1] (Unit: μg).

	Parent compound nobiletin	Mono-demethylated metabolites			Di-demethylated metabolites	
		3′-DMN	4′-DMN	5-DMN	3′,4′-DDMN	4′,5-DDMN
Lean rats						
0-12 h	16.92±20.15^{a}	7.93±15.68^{a}	29.54±57.21^{a}	12.96±24.14^{a}	7.08±13.81^{a}	21.27±42.54^{a}
12-24 h	27.89±24.58^{a}	22.57±22.55^{a}	79.99±72.80^{a}	51.57±43.53^{a}	88.54±93.57^{a}	69.19±59.85^{a}
24-36 h	27.26±26.87^{a}	90.53±110.33^{a}	76.66±91.80^{a}	29.86±38.87^{a}	237.24±377.83^{a}	64.88±77.38^{a}
36-48 h	41.98±42.63^{a}	252.80±78.80^{a}	227.95±71.73^{a}	53.52±36.48^{a}	1141.87±1181.62^{a}	147.25±35.40^{a}
Total amount	114.06±35.37^{a}	373.83±168.49^{ab}	414.15±167.87^{ab}	147.91±48.87^{a}	1474.74±1197.52^{b}	302.59±134.11^{a}
%intake [2]	0.25±0.07^{a}	0.83±0.37^{ab}	0.92±0.37^{ab}	0.33±0.12^{a}	3.35±2.88^{b}	0.67±0.29^{ab}
Content Ratio of metabolites/nobiletin				**27.75±15.43**		
Obese rats						
0-12h	7.96±7.18^{a}	0.03±0.04^{a}	0.15±0.15^{a}	1.06±1.04^{a}	0.22±0.23^{a}	0.00±0.00^{a}
12-24h	26.19±23.62^{a}	47.99±57.75^{a}	204.98±164.27^{a}	53.03±38.22^{a}	147.22±106.85^{a}	231.21±221.50^{a}
24-36h	37.46±32.72^{a}	306.24±160.94^{ab}	597.67±251.95^{b}	70.40±37.05^{ac}	520.74±232.00^{bc}	454.44±162.13^{abc}
36-48h	20.38±8.13^{a}	722.55±634.55^{a}	766.55±454.52^{a}	38.26±14.37^{a}	673.19±70.74^{a}	477.68±215.21^{a}
Total amount	92.00±20.86^{a}	1076.81±745.00^{ab}	1569.35±541.28^{b}	162.76±43.82^{a}	1341.37±271.62^{b}	1163.33±254.4^{ab}
%intake [2]	0.16±0.03^{a}	1.80±1.09^{bc}	2.69±0.78^{b}	0.28±0.06^{ac}	2.30±0.29^{b}	1.99±0.29^{b}
Content Ratio of metabolites/nobiletin				**60.16±19.67**		

[1] Data was expressed as the mean ± standard deviation. The oral dosage of nobiletin was 100 mg/kg. Statistical analysis was conducted among nobiletin and its metabolites in the same time intervals. Different letters in superscript indicated the statistically significant level $p<0.05$.

[2] % intake was the amount (μg) of recovered compound in the feces divided by the oral intake (μg) of nobiletin

4.3.3 The Pharmacokinetics Study via Intravenous Injection

The concentration-time profiles of nobiletin in the plasma after intravenous injection are shown in **Fig. 19A**. The area under the curve (AUC) within 0.5-24 h for lean rats and obese rats was 4.96 ± 0.97, and 5.63 ± 1.71, respectively (**Fig. 19C**). The AUC did not have statistically significant difference between the two groups. The metabolites profile in the plasma was similar with that in the urine, in which the quantity of DMN was higher than DDMN. In particular, 4′-DMN had the highest concentration among metabolites. Moreover, the AUC of total metabolites was quite similar between lean and obese rats.

(A)

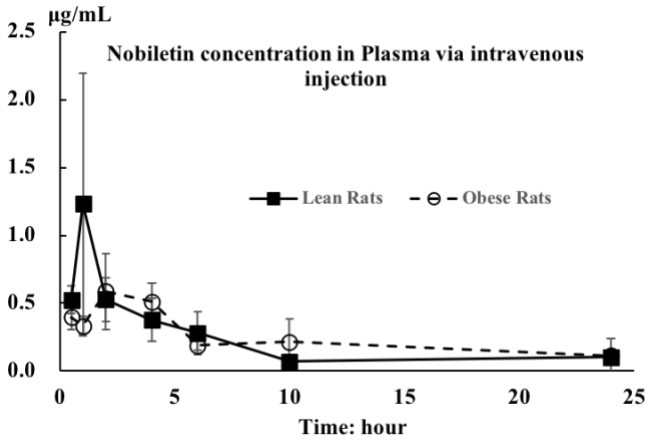

(B)

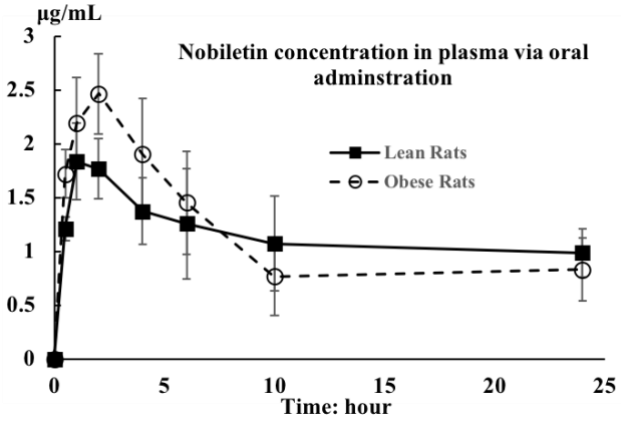

(C)

Parameters	Intravenous injection		Oral administration	
	lean rats	obese rats	lean rats	obese rats
Dosage (mg/kg)	4	4	100	100
Tmax (hour)	1.40±0.49[a]	2.75±1.30[a]	2.00±2.00[a]	2.40±0.80[a]
Cmax (µg/mL)	1.30±0.91[ac]	0.67±0.24[a]	1.93±0.37[bc]	2.49±0.35[b]
kel	0.07±0.04[a]	0.07±0.05[a]	0.02±0.02[a]	0.04±0.04[a]
AUC (hour*µg/mL)	4.96±0.97[a]	5.63±1.71[a]	27.74±5.61[b]	26.28±6.76[b]
F%	-	-	22.37±4.52%[a]	18.67±4.80%[a]

Different letters in superscript in the same raw indicated the statistically significant level $p<0.05$

Figure 19: Concentration-time profiles of nobiletin in rat plasma via intravenous injection of 4 mg/kg nobiletin(A), via oral administration of 100 mg/kg nobiletin (B) and the pharmacokinetic indexes (C).

4.3.4 The Pharmacokinetics Study via Oral Administration

The concentration changes of nobiletin in the plasma via oral administration are shown in **Fig. 19B**. The AUC of nobiletin in obese rats (11.48 ± 2.17) was larger than that in lean rats (8.65 ± 1.30) during the first 6 hours after oral administration. The AUC within 10-24 h for lean rats was higher than obese rats. Due to this compensation, the AUC within 24 h for lean rats (27.74 ± 5.61) and obese rats (26.28 ± 6.76) did not significantly vary from each other ($P<0.05$). The pharmacokinetic parameters of nobiletin in the lean and obese rats are summarized in **Fig. 19C**. According to the equation (1), the bioavailability of nobiletin was calculated as 22.37% ± 4.52% for lean rats and 18.67% ± 4.80% for obese rats, respectively. The bioavailability of nobiletin did not show statistically significant difference ($P<0.05$) regarding to rats' weight status.

Similar to the metabolite profile in the urine, the concentration of DMN in the plasma was much higher than that of DDMN. Specifically, the AUC of three DMN followed the order: 4′-DMN>3′-DMN>5-DMN, as shown in **Figs. 20A, 20B and 20C**. The dynamic concentration pattern of 3′,4′- DDMN (**Fig. 20D**) looked very similar to 3′-DMN (**Fig. 20B**). The reason might be that the demethylation in the 3′-position was more difficult than in 4′- position, and thus the 3′-position demethylation became the limiting step for the generation of 3′,4′-DDMN in the plasma. Similar phenomenon was also observed in the demethylation on 4′-and 5-positions, by comparing the concentration-time profiles of 4′-DMN (**Fig. 20A**), 5-DMN (**Fig. 20C**) and 5,4′-DDMN (**Fig. 20E**). **Fig. 20F** demonstrated the AUC ratio of demethylated metabolites to nobiletin in the plasma. Except for 3′,4′-DDMN, all metabolites in the plasma from obese rats had a significantly higher ($P<0.05$) AUC ratio than that from lean rats.

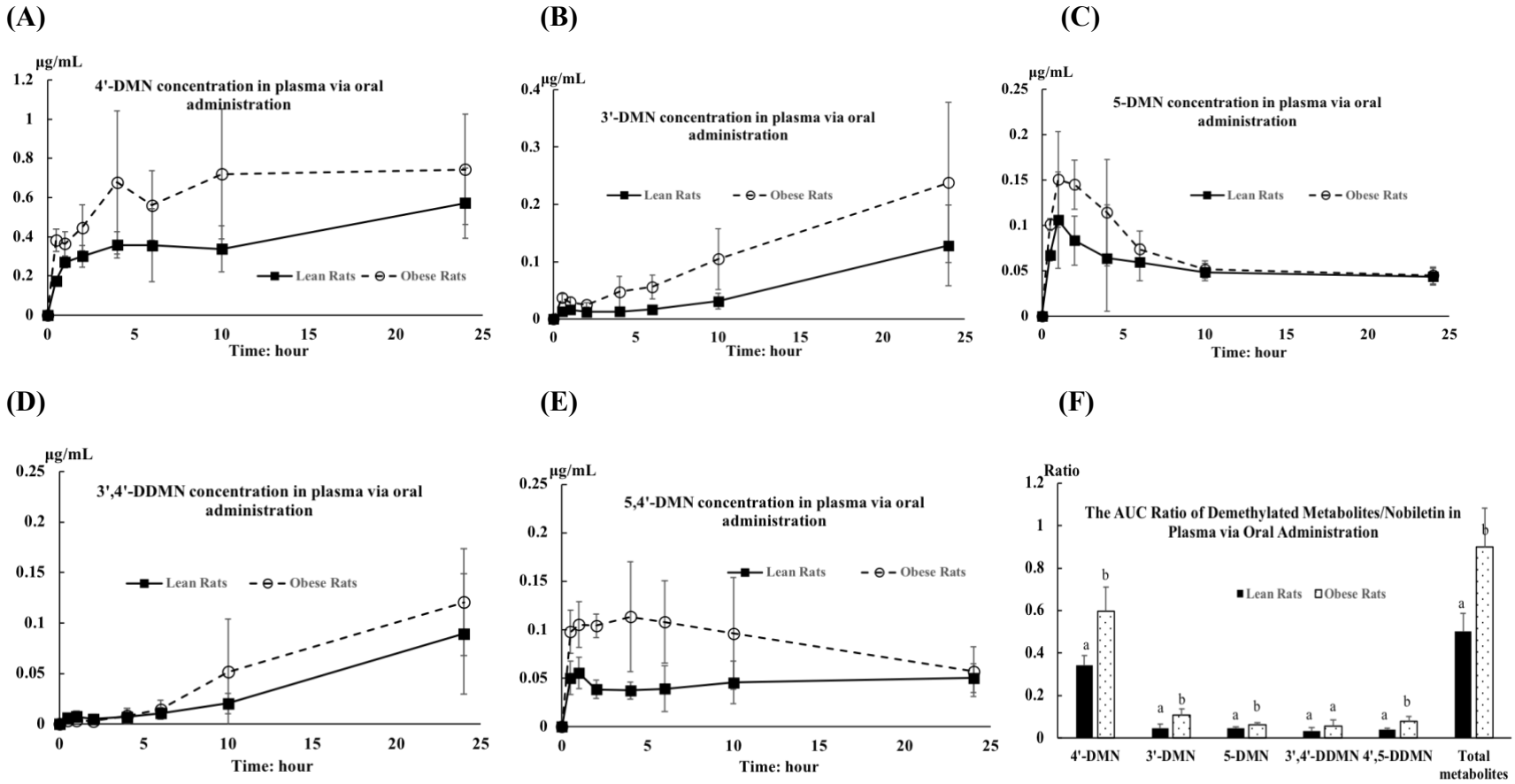

Figure 20: After oral administration of 100 mg/kg nobiletin, the concentration-time profiles of mono-demethylated nobiletin (DMN) and di-demethylated nobiletin (DDMN) in rat plasma: 4′-DMN (A), 3′-DMN (B), 5-DMN (C), 3′,4′-DDMN (D), 5,4′-DDMN (E). The 24-hour AUC ratio of demethylated metabolites/nobiletin in the plasma (F).

4.3.5 The Consecutive Dosing Study

Fig. 21A demonstrated the concentration change of nobiletin in the plasma at the 6^{th} hour after daily intake of nobiletin during the 2-week consecutive dosing study. The concentration of nobiletin increased in the first 3 days, decreased slightly within 3^{rd}-9^{th} days, and finally remained a plateau between 9^{th}-15^{th} days. However, the concentrations of nobiletin at these time intervals did not show statistically significant difference ($P<0.05$). Furthermore, we summed the concentrations of total monitored demethylated metabolites in the plasma and divided the sum by nobiletin plasma concentration in order to access the biotransformation level in the host body. As shown in **Fig. 21B**, this ratio increased with the feeding time. Two reasons leading to this phenomenon might be: 1) the accumulation effect of metabolites due to their slow elimination rate from the plasma; and 2) increased biotransformation activity on nobiletin, as nobiletin experienced decrease after 3-day consecutive intake (**Fig. 21A**). The concentration ratio of each metabolite to nobiletin in the plasma from lean- and obese-rats are shown in **Fig. 21C** and **Fig. 21D**, respectively. The profile of plasma metabolites had a similar pattern with the urinary metabolites: 4′-DMN dominated among demethylated metabolites during the 15-day consecutive dosing study. The metabolites profile for lean- and obese rats did not have significant difference at the selected time points.

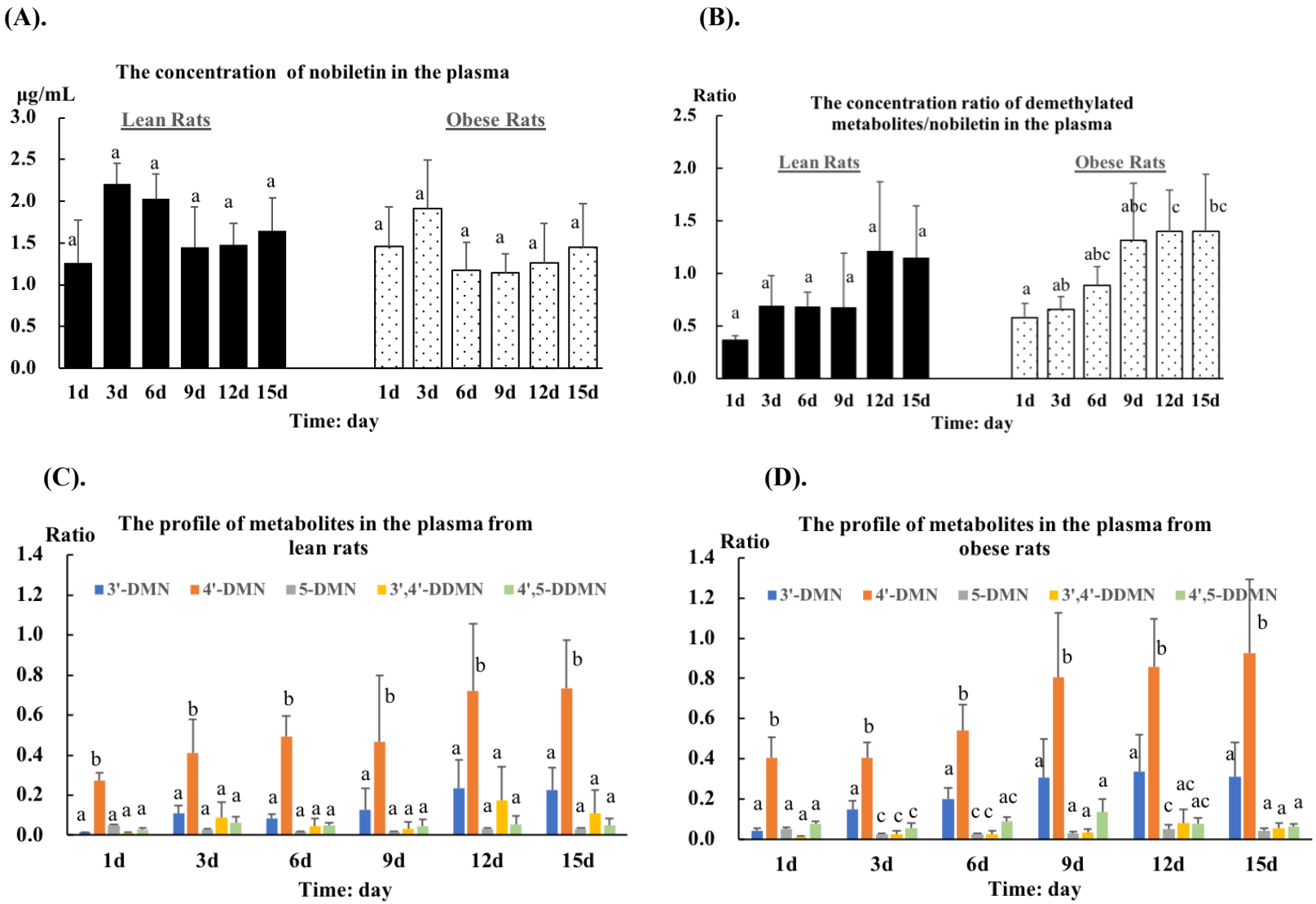

Figure 21: The concentration change of nobiletin (A) in the plasma during the 2-week consecutive dosing study, as well as the ratios of demethylated metabolites/nobiletin (B) and the metabolite profile in the lean rats (C) and obese rats (D).

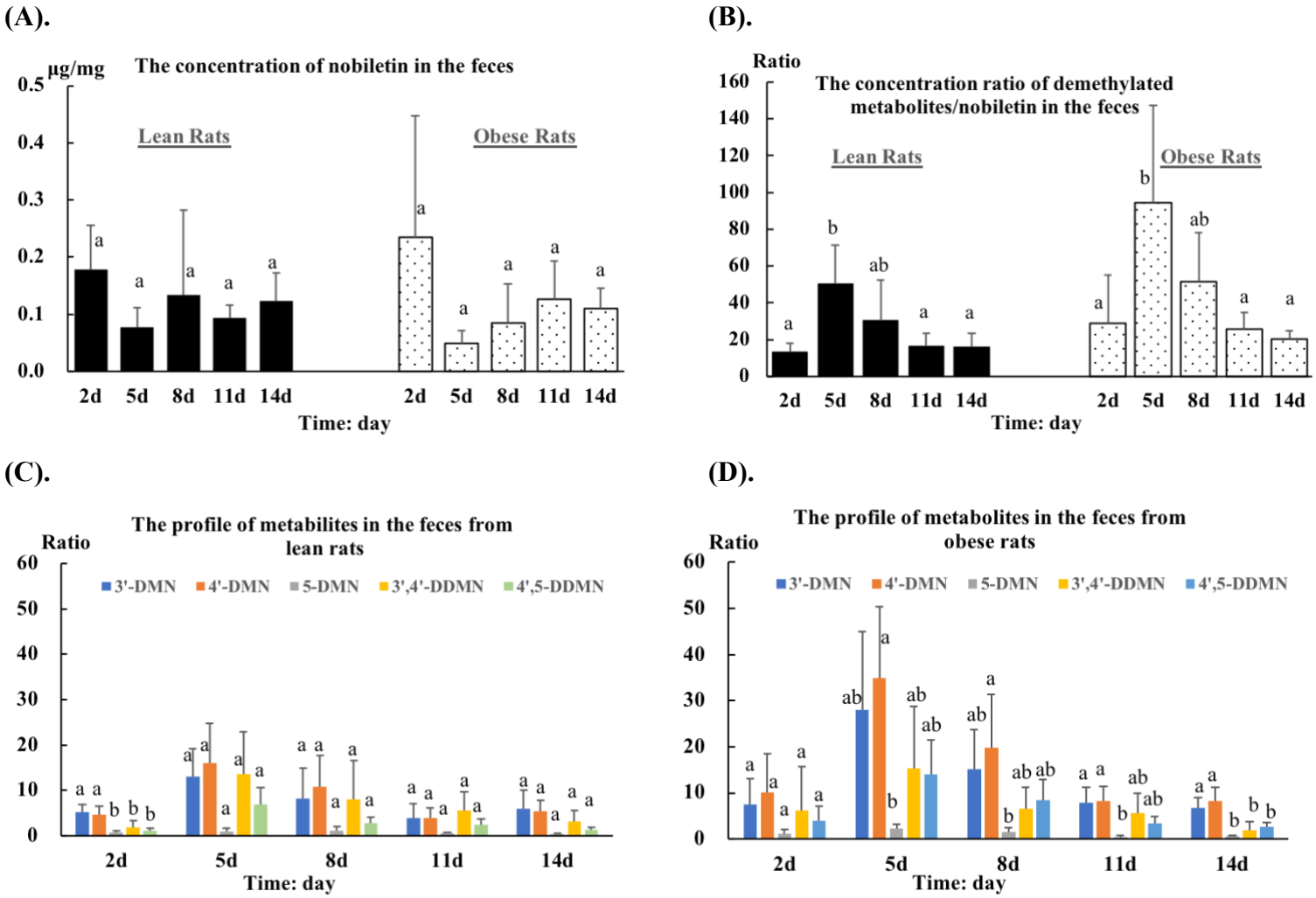

Figure 22: The concentration change of nobiletin (A) in the feces during the 2-week consecutive dosing study, as well as the ratios of demethylated metabolites/nobiletin (B) and the metabolite profile in the lean rats (C) and obese rats (D).

The concentration of nobiletin in feces excreted at the 12th hour after daily intake of nobiletin is shown in **Fig. 22A**. During the 2-week study, the concentration of nobiletin in feces did not show statistically difference during the 2-week feeding. In general, the metabolite ratios in feces from lean rats were lower than those from obese rats (**Fig. 22B**). The metabolite ratios increased significantly ($P<0.05$) in the first 5 days and then decreased to the initial level gradually in the following days (**Fig. 22B**). It indicated that the biotransformation activity of gut microbiota was enhanced during the first 5 days. During the 5th-14th day, the concentration of nobiletin in feces was similar while the concentration of monitored metabolites decreased. Possible explanation could be that gut microbiota with enhanced biotransformation activity might yield more diversified demethylated metabolites (not monitored in this study). The profiles of colonic metabolites are presented as their concentration ratio to nobiletin in feces from lean rats (**Fig. 22C**) and obese rats (**Fig. 22D**), respectively. Different from the profile of plasma demethylated metabolites (**Fig. 22C & Fig. 22D**), the demethylation on nobiletin by gut microbiota seemed more random. In most cases, 3′-DMN, 4′-DMN, 3′,4′-DDMN and 4′,5 -DDMN had similar concentrations in feces during the 2-week feeding.

4.4 Discussion

Phytochemicals after oral administration would undergo absorption/digestion in the gastrointestinal tract (GIT) and excreted from human body through two routes—urine and feces. The absorption of phytochemicals mainly occurred in the small intestine (*46*). The absorbed phytochemicals would be metabolized by phase I and phase II biotransformation

enzymes in the intestinal cells and liver, then delivered to targeted organs by the circulation system, and finally excreted by urine (*77*). The unabsorbed phytochemicals would enter the colon where harbored great numbers of microorganisms (*68*). After colonic biotransformation and reabsorption, the phytochemicals and their metabolites would be excreted via feces. To follow the biological fate of phytochemicals, we investigated the excretion, bioavailability and biotransformation of nobiletin using the HFD-induced obese rats and their lean counterparts. Demethylation activity was emphasized for the biotransformation in this study. In order to quantitatively investigate the overall demethylation in the host, all urine and plasma samples were treated with sulfatase and β-glucuronidase to deconjugate the phase II metabolites.

From excretion study, the first observation was that the content of demethylated metabolites were much higher than nobiletin in both urine and feces. Besides, the metabolite profiles indicated that gut microbiota had higher demethylation activity than the host, because a higher ratio of DDMN was found in the feces as compared to urine. Moreover, the demethylation on nobiletin skeleton was position-specific in the host, since 4′-DMN dominated in the profile of urinary metabolites (**Table 7**). This result was consistent with previous report, which showed that the demethylated biotransformation mostly occurred on the 4′-position of nobiletin, followed by 3′- and 5- position in mouse urine.(*78*) On the contrary, the demethylation position of nobiletin was more random by gut microbiota. For example, the amount of 4′-DMN and 3′-DMN in feces was quite similar (**Table 8**). The distinctive metabolite profiles indicated that the demethylation enzymes in gut microbiota were more complicated than that in the host. The demethylation reaction was important to influence the lifetime and bioactivity of nobiletin. Host

demethylation was thought to liberate polar groups for further conjugation and excretion from bodies, while demethylation by microbes could provide carbon source for their growth (*228*). In the host body, the liver microsome and cytochrome P450 enzymes have been reported to demethylate nobiletin (*213*). Gut microbiota also carries out demethylation reaction on polyphenols (*75*). In particular, several specific colonic microbes are reported to have the demethylase activity for flavonoids, such as *Eubacterium limosum* and *Blautia* sp. MRG-PMF1, etc. (*75, 76, 80*). An *in vitro* enzyme inhibition study suggested that the demethylation of PMF depended on the Co-corrinoid demethylase system in the bacteria (*76*). In-depth work is calling attentions for exploring the metabolism of nobiletin, such as the identification of organ-specific metabolism in the host, the discovery of more responsive colonic microbes and the mechanic study of demethylases.

The absolute oral bioavailability of nobiletin suspended in 0.5% CMC aqueous solution was estimated to be about 20% for both lean and obese rats in this study. Likewise, the absolute bioavailability of tangeretin (another typical citrus PMF) was about 27%, when rats were orally administered 50 mg/kg tangeretin in the dissolved state (*52*). The bioavailability of PMF was quite high as compared to flavonoids with multiple hydroxyl groups. For example, the bioavailability of tea polyphenols and anthocyanins were less than 2% estimated using the rat model (*229-231*). The high bioavailability of PMF was supposed to derive from their multiple methoxy groups, which enable PMF good intestinal membrane permeability. Given the bioavailability of nobiletin (≈20%), it indicated that most of the administered nobiletin would enter the colon, interact with gut microbiota and excrete from feces. However, the amount of urinary excreted nobiletin and the detected metabolites accounted for about 7% of the administered dosage (**Table. 7**), while the

amount of fecal nobiletin and metabolites was about 8% (**Table. 8**) from our 48-hour excretion study. The similar recovery rate for nobiletin and metabolites in the urine and feces again suggested that the biotransformation by gut microbiota was more extensive than the host. The biotransformation of nobiletin by gut microbiota might yield more diversified demethylated metabolites or ring-fission metabolites, which were not monitored in this study. Besides, the elimination of nobiletin and its metabolites from the rats might need longer time exceeding 48 hours. Overall, those might be the reasons for the limited recovery rate in the excretion study, especially in the feces.

The difference of nobiletin metabolism between lean and obese rats was mainly represented in two aspects. Firstly, the content ratio of demethylated metabolites to nobiletin in feces was significantly higher for obese rats than lean rats ($P>0.05$). It indicated that the microbiome in obese rats had higher biotransformation activity. This result might be derived from the microbial compositional difference between the lean and obese individuals. For example, studies reported that greater ratio of Firmicutes to Bacteroidetes was identified in obese mice than their lean counterpart (*185*). The structural change of gut microbiota caused by HFD was reported to influence the generation of microbiota-derived metabolites, such as bile acids, short chain fatty acids and lipopolysaccharides (*67*). In addition, a recent study found that the long-term administration of HFD would change the colonic metabolism of tea polyphenols as compared to ND (*226*). Secondly, the 24-hour AUC of demethylated metabolites in the plasma of was greater for obese rats than lean rats, when nobiletin was orally administered (**Fig. 19**). The metabolites in the plasma were either from the biotransformation in the host or reabsorption from the colon. Previous study reported that HFD could inhibit the protein expression for intestinal tight junction and thus

increase membrane permeability (*98*). The increased intestinal permeability might be the reason that more nobiletin was absorbed into the blood in obese rats within 0-6 hours after oral administration (**Fig. 18B**). The higher concentration of nobiletin in plasma would promote the generation of metabolites. In addition, as the microbiome of obese rats was found to have higher demethylation activity (**Table. 8**), more metabolites might be reabsorbed from the colon into their circulation system. Therefore, the increased intestinal permeability and the microbiome of obese rats were considered as the two important factors for the comparatively high ratio of plasma metabolites in obese rats after oral administration of nobiletin.

From the consecutive dosing study, it seemed that the biotransformation activity was enhanced for both the host and gut microbiota. Some demethylated metabolites were found to be more biological active. For example, 4′-DMN and 3′,4′-DDMN possessed much stronger anti-inflammation activity as compared to nobiletin in RAW264.7 cell studies (*38*). 5-DMN was reported to more effectively inhibit the colon cancer cells than nobiletin (*182*). Thus, the enhanced biotransformation activity by long-term administration of nobiletin should be associated with better bioactivity. Wu, Song (*81*) also found that the health benefit of nobiletin might strongly come from its metabolites in the DSS-induced colitis mice.

4.5 Conclusion

In summary, the excretion, bioavailability and biotransformation of nobiletin in lean and obese rats were investigated. By comparing the demethylated metabolite profiles in the urine and feces, gut microbiota demonstrated greater biotransformation activity on

nobiletin than the host. The absolute oral bioavailability of nobiletin in lean (22.37% ± 4.52%) and obese (18.67% ± 4.80%) rats has negligible statistically significant difference ($P>0.05$). However, higher extent demethylated metabolites was found in the feces and plasma of obese rats than lean rats ($P<0.05$). The greater biotransformation activity in the microbiome and the increased intestinal permeability of obese rats were considered as the leading factors to explain this difference. Moreover, the consecutive dosing of nobiletin might lead to higher extent of demethylated metabolites in the plasma as well as in feces. These results suggested that gut microbiota played important roles on nobiletin metabolism and its demethylation activity was impacted by HFD and consecutive dosing of nobiletin.

CHAPTER V: ASSESSMENT OF ORAL BIOAVAILABILITY AND BIOTRANSFORMATION OF EMULSIFIED NOBILETIN USING *IN-VITRO* AND *IN-VIVO* MODELS

5.1 Introduction

Many phytochemicals have demonstrated promising chemopreventive effects in cell line studies, but their bioefficacy *in vivo* is often limited due to the low oral bioavailability (*232*). The limiting factors for the oral bioavailability of phytochemicals are classified into three major categories: bioaccessibility, absorption, and biotransformation(*51*). Bioaccessibility is the prerequisite for bioavailability and is defined as the potentially absorbable amount of phytochemical in the lumen after the gastrointestinal digestion (*233*). The absorption refers to the fraction of phytochemical transported across the intestinal epithelium. It is associated with the physicochemical properties of the phytochemical molecules, including their lipophilicity, hydrogen bonding capacity, molecular size, etc. (*234, 235*). The biotransformation of phytochemicals *in vivo* yields extensive metabolites by gut microbiota and the host. The generation of metabolites plays an important role on the bioavailability and bioactivity of phytochemicals *in vivo* (*50, 51, 77*).

Nobiletin, one of the most prevalent citrus polymethoxyflavones (PMFs), has received much attention for its promising biological activities, such as anti-obesity, anti-inflammation, and anti-cardiovascular disease, etc. (*9-11, 106*). Nobiletin has six methoxy groups on the 5,6,7,8,3',4'-positions of the flavone skeleton (*11*). The multiple methoxy

groups enable nobiletin good membrane permeability but poor bioaccessibility due to the limited water solubility (*10*). Different encapsulation strategies, using emulsion systems (*60, 61*), hydrogels (*236*), nanoparticles (*56, 57*) and amorphous solid dispersions (*64, 65*), have been developed to enhance the bioaccessibility of PMFs. *In vitro* models are often utilized as the screening method for numerous delivery systems, even though these models are criticized for their oversimplified conditions mimicking the gastrointestinal environment.

The common *in vitro* models evaluating the bioaccessibility of phytochemicals include static- and dynamic digestion models, such as the pH stat model and TNO gastro-intestinal model (*46, 237*). To assess the intestinal absorption, the commonly used methods are parallel artificial membrane assay (PAMA) or cell cultures (e.g. Caco-2 monolayers) (*238, 239*). Recent studies have found that the *ex vivo* permeability method using isolated intestinal tissues from animals, and measured using a Franz diffusion cell, is highly correlated with the *in vivo* absorption results (*240*). Compared to the Caco-2 cell model, the Franz diffusion cell is easier to handle and more cost-effective. The Franz cell is widely used for skin permeability and has been used in several recent studies to investigate intestinal absorption (*240-242*). Currently, there is no report using a Franz cell to assess the absorption behavior of PMFs. Compared with single-factor models, the *in vitro* models with the combination of bioaccessibility and absorption would better mimic the oral bioavailability of nobiletin in different delivery systems.

Few studies have validated the results from *in vitro* models with *in vivo* data in terms of evaluating the oral bioavailability of nobiletin. In addition, our understanding of the bioavailability and biotransformation of nobiletin *in vivo* remains limited. The delivery

vehicle was considered as a key factor for the bioavailability *in vivo*. Manthey, Cesar (*55*) found that the maximum concentration (C_{max}) of nobiletin in the rat serum was 9.03 μg/mL following oral gavage of 50 mg/kg nobiletin dissolved in corn oil, whereas the C_{max} was decreased to 3.21 μg/mL when the same dosage of nobiletin was given to rats by gavage as solid precipitate suspended in corn oil (*55*). Compared to crystalline nobiletin, an amorphous solid dispersion of nanosized nobiletin was found to increase its bioavailability and concentration in the brain 13- and 7-fold, respectively (*65*). A subsequent study found that the improved bioavailability of nanosized nobiletin might lead to better attenuation effect on the hepatic damage than crystalline nobiletin in the acute liver injury rat model (*64*). However, for the limited *in vivo* studies, few of them have investigated the biotransformation of nobiletin quantitatively. As the metabolism is an important aspect of the overall bioavailability and some of the nobiletin metabolites were reported to deliver higher bioactivity (*77*), in-depth exploration of biotransformation will help us better understand the biological fate of nobiletin influenced by delivery systems.

To fulfill the knowledge gap between the *in vitro* and *in vivo* models for evaluating the bioavailability of nobiletin, this study compares the results from the combined *in vitro* models (pH stat lipolysis and Franz diffusion cell) and the rat study (illustrated in **Fig. 23**). The objectives of this study include: 1) to develop emulsion as a convenient vehicle to improve nobiletin bioavailability; 2) to explore the oral bioavailability and biotransformation of nobiletin *in vivo* in the unformulated/formulated forms; and 3) to develop a combined *in vitro* model as a robust and rapid-screening method to evaluate oral bioavailability. For the biotransformation, this study focuses on the demethylation kinetics of nobiletin in the blood. This work provides scientific insights for rational design and

screening of delivery systems for the bioavailability enhancement of the lipophilic phytochemicals, especially for PMFs.

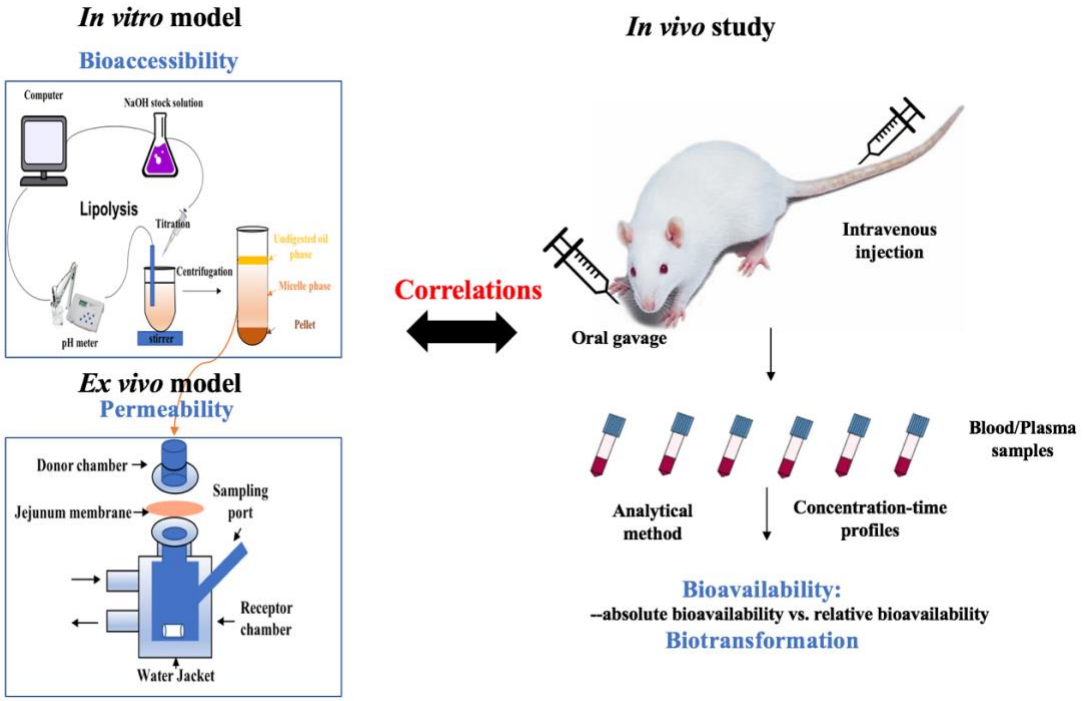

Figure 23: Illustrative scheme for the models evaluating the oral bioavailability.

5.2 Materials and Methods

5.2.1 Materials

Nobiletin with more than 95% purity was purchased from Qiongge Biochemicals Inc (Wuhan, China). Medium-chain triacylglycerols (MCT) were a gift from Stepan Company (Northfield, IL, USA). Lecithin (PC75, AlCOLEC) was a gift from the American Lecithin Company (Oxford, CT, USA). Lecithin (Biolipon 95) used for lipolysis buffer was obtained from Perimondo, LLC (Florida, NY, USA). Pancreatin with 8x USP, sulfatase, β-

glucuronidase, Tris maleate and sodium taurodeoxycholate (Na TDC) were purchased from Sigma-Aldrich (St. Louis, MO, USA). HPLC grade organic solvents including ethanol, methanol and acetonitrile were purchased from Greenfield (Brookfield, CT, USA). Analytical grade sodium chloride, sodium hydroxide and calcium chloride dihydrate were purchased from VWR (Radnor, PA, USA).

5.2.2 Synthesis of Nobiletin Metabolites

Demethylated metabolites were synthesized according to our previous method (*38, 214*). 5-Demthylnobiletin (5-DMN) was synthesized by one-step reaction of nobiletin in the acidic ethanol condition. Three B-ring metabolites with the demethylation on the 3′-, 4′- and 3′,4′- positions were obtained after 5-step reactions. Briefly, pure nobiletin underwent C-ring fission hydrolysis and yielded 2′-hydroxy-3′,4′,5′,6′-tetramethoxyacetophenone (Step.1). Aldol condensation of 2′-hydroxy-3′,4′,5′,6′-tetramethoxyacetophenone with 3-benzyloxy-4-methoxybenzaldehyde/4-benzyloxy-3-methoxybenzaldehyde/3,4-benzyloxybenzaldehyde yielded corresponding methoxychalcones (Step.2). These methoxychalcones were transformed to corresponding flavanones after cyclization under phosphoric acid and acid condition (step.3); then yielded benzylated nobiletin on the 3′-, 4′- and 3′,4′- positions (step.4) and finally formed the B-ring demethylated nobiletin after debenzylation (step.5). All the metabolites were purified by silica gel column chromatography (VWR, Radnor, PA, USA) and confirmed by NMR.(*214*) The chemical structures for nobiletin, 3′-demethylnobiletin (3′-DMN), 4′-demethylnobiletin (4′-DMN), 5-DMN and 3′,4′-didemethylnobiletin (3′,4′-DDMN) are illustrated in the supplementary information (**Fig. 17**).

5.2.3 Preparation of Nobiletin Emulsion

Nobiletin emulsion was prepared according to our previous published method with minor modification (*60*). Briefly, 3% (w/v) lecithin (PC 75) was dissolved in water phase in 50 °C water bath and 2% (w/v) nobiletin was dissolved in the MCT in the boiling water bath. The water phase was mixed with oil phase at the ratio of 1:1 (v/v). The mixture was subjected to high speed homogenization (Ultra-Turrax T25, IKA Works Inc., Wilmington, NC, USA) at 20,000 rpm for 3 minutes and then passed through high-pressure homogenization (EmulsiFlex-C6, AVESTIN Inc., Ottawa, ON, Canada) at least three times.

5.2.4 Particle Size Measurement

Nobiletin emulsion was diluted about 200 times with deionized water before measurement. The averaged droplet size of the emulsion and its polydispersity index (PDI) were measured by dynamic scattering light using particle sizing analyzer (NanoBrook 90Plus, Brookhaven Instrument, Holtsville, NY, USA) at the fixed scattering angle of 90° at room temperature.

5.2.5 Polarized Light Microscopy (PLM)

The crystalline nobiletin in emulsion was observed by Nikon TE-2000-U inverted microscope equipped with a polarizer and a CDD camera (Retiga EXi, QImaging).

5.2.6 Rheological Measurement

Both static and dynamic rheological measurements of blank- and nobiletin-loaded

emulsion were carried out at room temperature using an ARES Rheometer (TA instruments, New Castle, DE, USA). The parallel plate with 50 mm diameter was used and the gap was set at 0.7 mm for all measurements. The viscosity under shear rate ranging from 0.01 to 100 s^{-1} was recorded using the static mode. In order to find the linear viscoelastic region, the dynamic strain test was performed and set as 0.5% for all the dynamic frequency sweep test. During the dynamic frequency sweep test, the storage modulus G' and loss modulus G" were recorded with the angular frequency ranging from 0.05 to 100 rad/s.

5.2.7 In Vitro Lipolysis

Before conducting lipolysis experiment, the freshly prepared delivery systems were stored for 24 hours at the room temperature to reach the equilibrium for nobiletin crystal formation. The *in vitro* lipolysis was carried out according to our previous published method (*239, 243*). Briefly, 0.25 g oil for each sample (0.255 g in total for nobiletin oil suspension and 0.529 g in total for nobiletin emulsion) was digested by pancreatin in the fasted-state lipolysis buffer for 2 hours in the 37 °C oil bath. During the lipolysis process, the pH of the buffer was manually maintained at 7.5 ± 0.02 by adding 0.25 N NaOH solution. The volume of added NaOH solution over time was recorded to estimate the extent of lipolysis. After 2-hour digestion, the buffer was centrifuged at 12000 rpm (Beckman Coulter, Brea, CA, USA) for 40 min. The micelle phase (illustrated in **Fig. 23**) was filtered subsequently using 0.22 μm filter. The filtrate was diluted by 4 volumes of methanol and passed through the 0.22 μm filter again before the concentration measurement by high performance liquid chromatography (HPLC). The bioaccessibility of nobiletin in oil suspension or emulsion was calculated as:

$$\%bioaccessibility = \frac{mass\ of\ nobiletin\ in\ the\ micelles}{mass\ of\ nobiletin\ in\ the\ oil\ phase} * 100 \quad (1)$$

The mass of nobiletin in the micelles was the product by multiplying the volume of aqueous phase after digestion and the concentration of nobiletin measured by HPLC. The mass of nobiletin in the oil phase was the loaded nobiletin in the oil suspension or emulsion before digestion.

5.2.8 Franz Diffusion Cell

The small intestine of pig used for the permeability study was provided by a local slaughterhouse. The porcine jejunum was carefully opened after removing the adipose tissue and cut into suitable segments for the size of the Franz cell. Before the experiment, jejunum segments were immersed in PBS buffer for 15 min to get the equilibrium condition. The jejunum segment was mounted between the donor- and receptor- compartments with the mucosal side facing the donor medium. The contacted area between the two compartments was 0.64 cm^2. The receptor compartment was filled with 5 mL 50% (v/v) ethanol aqueous solution as the receiving medium and maintained stirred at 37 °C in a water bath (*244*). 1 mL filtered lipolysis buffer after digestion was added in the donor compartment which was subsequently sealed by parafilm to prevent water evaporation. During the diffusion experiment, sampling was conducted from the receptor compartment at the 1^{st}, 2^{nd}, 3^{rd} and 4^{th} hour. The same volume of fresh receiving medium was reintroduced in the receptor after each sampling point. The absorption process was maintained for 4 hours in total. To assess the permeability of nobiletin delivered by emulsion and oil suspension, each experiment was conducted triply. The receiving medium collected at each time interval was diluted by methanol properly before measuring nobiletin

concentration by HPLC. The jejunum segments after each 4-hour permeation study were washed by flowing tap water, extracted by methanol, and then measured for the content of nobiletin by HPLC. For the combined *in vitro* models, the relative bioavailability of nobiletin delivered by emulsion versus oil suspension is estimated by the amount ratio of nobiletin in the receptor cell delivered by emulsion to oil suspension.

5.2.9 Pharmacokinetics Study Using Rats

Male Sprague-Dawley rats used for the pharmacokinetic study were purchased from Southern Medical University (Guangzhou, China). Rats were housed in a specific pathogen free, 12 h light/dark cycle, temperature (20-23 °C)- and humidity-controlled (relative humidity: 50%-60%) environment. The experimental protocol (protocol number: 2019048) was approved by the Institutional Animal Care and Use Committee in South China Agricultural University. After 2-week adaptation to the environment, the body weight of rats was around 250-300 g. Rats were randomly assigned to three groups (n=6/group) and fed with nobiletin either by oral gavage or intravenous injection. For the oral administration, mice were given nobiletin delivered by oil suspension (2% w/v) or emulsion (1%, w/v) at the dosage of 100 mg/kg. For the intravenous injection, nobiletin was dissolved in 5% DMSO and 20% Tween 80 and given to rats via tail vein injection at the dose of 5 mg/kg. Blood samples were collected in heparin-coated tubes at the 0.5, 1, 2, 4, 6, 10 and 24 h after the administration of nobiletin. The plasma samples were obtained by centrifuging blood samples at 5000 rpm for 15 min. To assess the concentration of nobiletin in the plasma, 200 μL plasma was treated with sulfatase and β-glucuronidase and incubated at 37 °C for 45 min. The treatment of enzymes was to release the conjugated demethylated

metabolites, which allows us estimated the overall demethylation biotransformation of nobiletin in the blood. Then, the mixture was spiked with tangeretin solution as the internal standard and extracted by ethyl acetate twice. After centrifugation at 10000 rpm for 3 min, the supernatant was combined and evaporated by flowing nitrogen. 200 μL 80% methanol with 0.2% acetic acid was used to re-dissolve the residue and filtered through 0.22 μm nylon filter before further measurement.

The absolute bioavailability of nobiletin was calculated according to the following equation:(*52*)

$$F(\%) = (AUC_{po} * Dose_{iv})/(AUC_{iv} * Dose_{po}) * 100 \quad (2)$$

Where AUC is the abbreviation for the area under the curve of the concentration-time profile, which represented for the integral of nobiletin concentration in the plasma against the definite time. The subscript abbreviation, *po* and *iv* refer to oral administration and intravenous injection, respectively. The relative bioavailability *in vivo* was calculated according to following equation:

$$Relative\ bioavailability = AUC_{emulsion}/AUC_{oil\ suspension} \quad (3)$$

The maximum concentration (C_{max}) of nobiletin in the plasma after intravenous injection was calculated as the concentration at t=0 hour according to the first-order elimination kinetics. The elimination rate constant (K_e) was determined by the fitted slope of the concentration-time profile on the semi-log scale.

5.2.10 HPLC Analysis

The quantification of nobiletin and its metabolites was carried out using Agilent 1100 series HPLC system (Santa Clara, CA, USA) with the UV detector (320 nm). A Poroshell

120 PFP column (4.6*150 mm, 2.7 μm) (Agilent, Santa Clara, CA, USA) was used for separation. The injection volume for tested samples was 20 μL. The mobile phases included water (A) and acetonitrile (B). The flow rate was 0.7 mL/min. The following elution program was used: 0-2 min, 35%-35% B; 2-7 min, 35%-60% B; 7-13 min 60%-95% B; 13-15 min, 95% B, 15.01 min-18 min, 35% B.

5.2.11 HPLC-MS/MS Analysis

The quantification of nobiletin and its metabolites in the rat plasma after intravenous injection was carried out by UPLC-MS/MS due to the low given dosage and low concentration in the plasma. The UPLC-MS/MS consisted of UPLC (model: LC-30AD) (Shimadzu, Kyoto, Japan) and Triple Quadrupole Linear Ion Traps mass spectroscopy (model QTRAP 4500) (AB SCIEX, Concord, Canada). The column for LC-MS/MS was the same as the above HPLC measurement. The injection volume for tested samples was 5 μL. The mobile phases included 0.1% formic acid water (A) and acetonitrile (B). The flow rate was 1 mL/min. The following elution program was used: 0-2 min, 35% B; 2-7 min, 35%-50% B; 7-10 min 50%-95% B; 10-12 min, 95% B, 12.01 min-13 min, 35% B (maintaining 35% B for another 2 min for post-measurement). The global MS parameters were as follows: turbo ionspray source temperature 550 ℃, ionspray voltage 5500 V, curtain gas 40 psi, ion source gas 60 psi. The quantification of nobiletin and its metabolites was carried out in the positive mode with multiple reaction monitoring (MRM). The MRM transition, delustering potential and collision energy for each compound were optimized and are shown in the supplementary materials (**Table. 5**).

5.2.12 Statistical Analysis

All experimental results are shown as means ± standard deviations. The statistical difference between the oil suspension and emulsion was examined using the unpaired student t-test via StataSE v15. The significance was recorded if P-value<0.05.

5.3 Results

5.3.1 Characterization of Nobiletin Emulsion

In order to test its stability, nobiletin emulsion was stored at room temperature for one week. As illustrated **in Fig. 24A**, the emulsion remained quite stable: no significant phase separation or precipitation was observed. Even though the appearance of emulsion was homogenous (**Fig. 24A**), nobiletin crystals could still be observed under polarized microscope (**Fig. 24B)**. This indicated that the conventional emulsion could not completely prevent the formation of nobiletin crystals at such a high loading rate (1%) (*60*). The droplet size distribution of nobiletin emulsion is shown in **Fig. 24C**. The averaged droplet size was 325.7 ± 28.1 nm and the PDI was 0.11± 0.03. Both the blank emulsion and nobiletin emulsion were very viscous at the low shear rate and had shear-shinning behavior (**Fig. 24D**). In addition, the emulsions had an elastic and gel-like structure, indicated by the larger G' as compared to G" (**Fig. 24E**). The addition of nobiletin led to a higher viscoelastic property of the emulsion (**Figs. 24D & 24E**). This phenomenon might be related to the formation of crystals that engaged in the network of the gel-like structure (*60*).

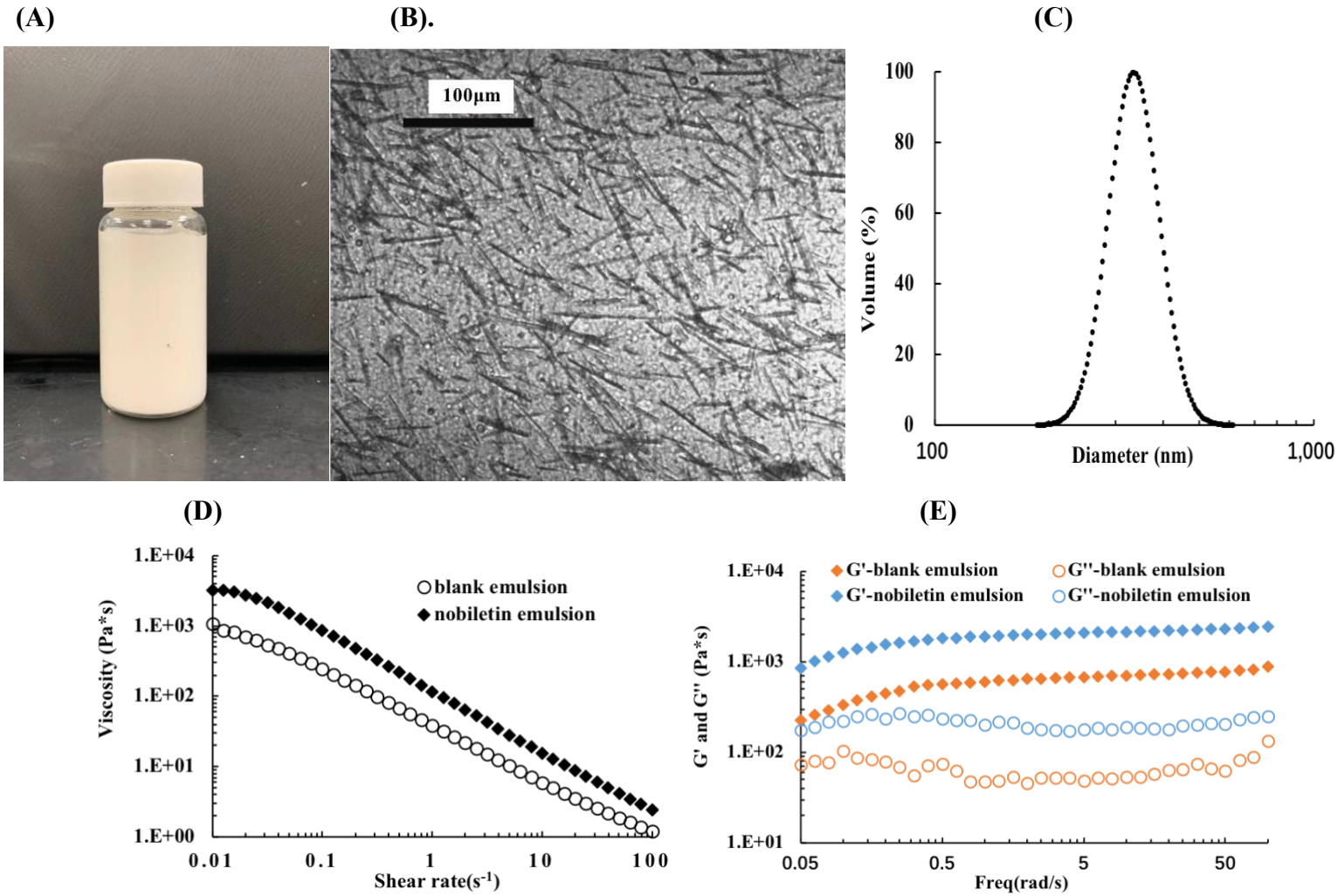

Figure 24: (A) The photograph of nobiletin emulsion; (B) the morphology of nobiletin emulsion under polarized optical microscopy; (C) the droplet size distribution of nobiletin emulsion; (D) the viscosity of emulsions versus shear rate (0.01-100 s^{-1}); (E). the storage modulus (G') and loss modulus (G'') of emulsions at the fixed strain (0.5%) versus frequency (0.05-100 rad/s).

5.3.2 *In Vitro* Lipolysis Profile between Oil Suspension and Emulsion

To assess the relative bioaccessibility, nobiletin oil suspension (2% nobiletin, w/v) was selected as the control delivery system as compared to nobiletin emulsion. The lipolysis titration profiles for oil suspension and emulsion were recorded and are shown in **Fig. 25A**. The volume of consumed sodium hydroxide solution for nobiletin emulsion was 1.6 times higher than that for the oil suspension. As more free fatty acids were released from the emulsion after lipolysis, more nobiletin could be trapped into micelles consisting of fatty acids. According to the equation (1), the bioaccessibility of nobiletin delivered by oil suspension and emulsion was calculated as 17.9 ± 1.8% and 81.3 ± 3.0%, respectively (**Fig. 25B**).

(A)

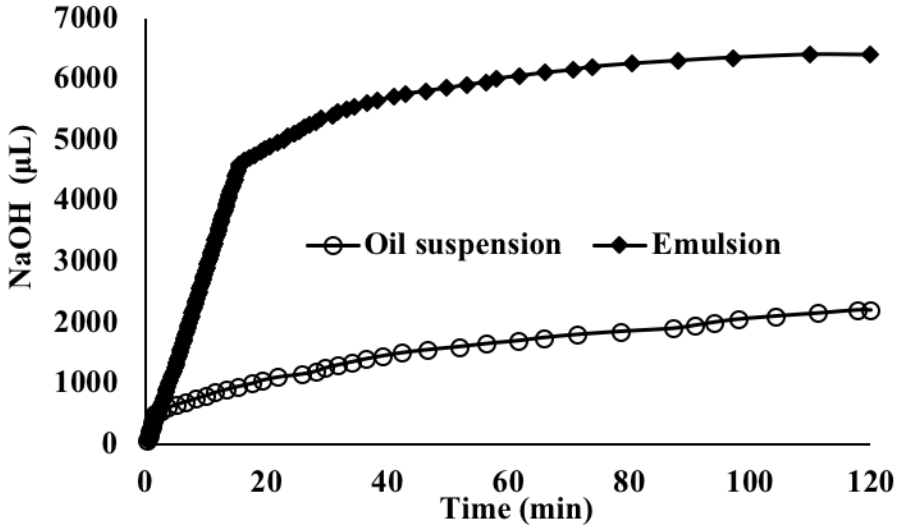

(B)

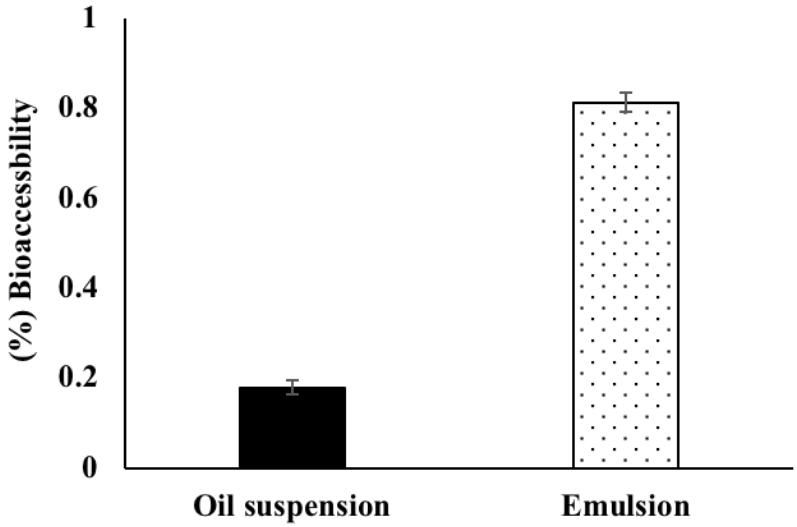

Figure 25: The comparison of pH-stat lipolysis between nobiletin emulsion and oil suspension: (A) the lipolysis profile; (B) the bioaccessibility (%) of nobiletin after 2-hour lipolysis.

5.3.3 Intestinal Absorption via Franz Diffusion Cell

1 mL micelle layer solution after lipolysis was transferred to the Franz cell as the donor medium for intestinal absorption (illustrated in **Fig. 23**). The concentration of nobiletin dissolved in the micelle was 245.7 ± 6.4 μg/mL for emulsion and 68.9 ± 6.1 μg/mL for oil suspension (**Fig. 26A**). The diffusion kinetics in the receptor are shown in **Fig. 26B**. The accumulated quantity of the trans-membrane nobiletin increased with the diffusion time for both groups. Moreover, the difference of accumulated nobiletin between the two groups increased with time. After 4-hour diffusion, 21.9 ± 2.3 μg nobiletin was found to transport across the membrane for emulsion samples, which accounted to about 2.31 times that for the oil suspension. The trapped amount of nobiletin in the jejunum segment after 4-hour diffusion is shown in **Fig. 26C**. The trapped amount of nobiletin in

the membrane was about 25-35% of that in the receptor for both groups. This indicated that most of the absorbed nobiletin was released into the circulation system rather than being trapped in the membrane. The trapped nobiletin content in the membrane for digested emulsion was about 2.72 times that for the oil suspension. The quantity of nobiletin in the membrane and receptor cell after 4-hour diffusion was summed and its ratio to the initial quantity of nobiletin before diffusion was defined as the absorption ratio. The absorption ratio was 17.34% ± 0.39% for oil suspension and 11.70% ± 0.71% for emulsion. This indicated that the absorption ratio was not linearly driven by concentration, as the initial nobiletin concentration was 68.9 ± 6.1 and 245.7 ± 6.4 μg/mL for oil suspension and emulsion, respectively.

(A)

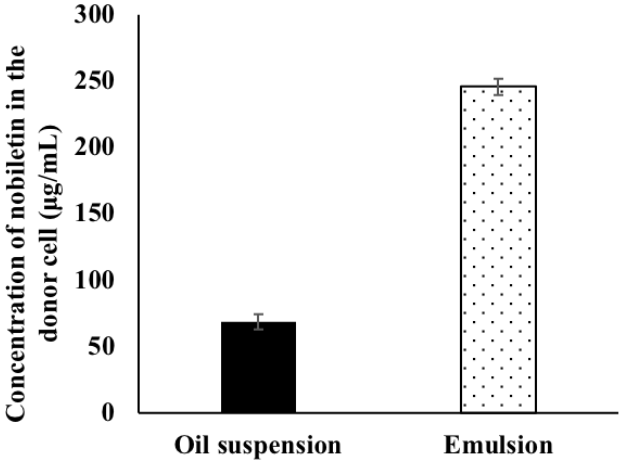

(B)

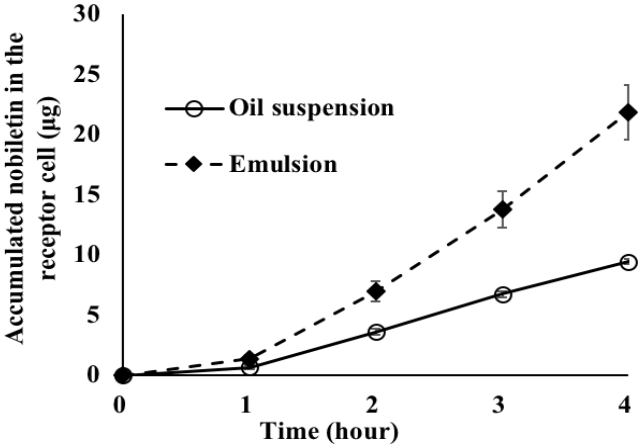

(C)

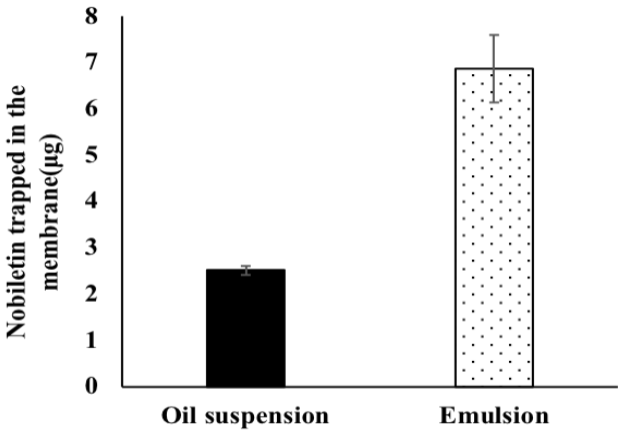

Figure 26: The comparison of intestinal diffusion between nobiletin emulsion and oil suspension using Franz cell: (A) The concentration of nobiletin in the donor cell before diffusion; (B) the accumulated amount of nobiletin in the receptor part during the 4-hour permeation; (C) the quantity of nobiletin trapped in the intestinal membrane after 4-hour permeatio

5.3.4 Pharmacokinetics and Biotransformation of Nobiletin in Rats After Intravenous Injection

The concentration-time profile of nobiletin in plasma after intravenous injection is shown in **Fig. 27A**. The concentration of nobiletin decreased significantly during the first 6 hours. It was 9 ng/mL in the 6th hour, which was about 1.3% of that in the 0.5th hour after intravenous injection. In terms of the biotransformation, 4′-DMN had the highest concentration of all demethylated metabolites, i.e. higher than 3′-DMN, 5-DMN and 3′,4′-DDMN (**Fig. 27B**). As 4′-DMN was identified as the major metabolite in the plasma, the concentration ratio of 4′-DMN to nobiletin in the plasma was further investigated (**Fig. 27C**). The concentration ratio of 4′-DMN to nobiletin increased significantly during the first 6 hours after injection. In particular, the ratio was 0.92 ± 0.23 in the 2nd hour and 3.00 ± 1.18 in the 4th hour. The ratio reached a peak during the 6th -10th hour and decreased to 0.10 ± 0.06 in the 24th hour.

(A)

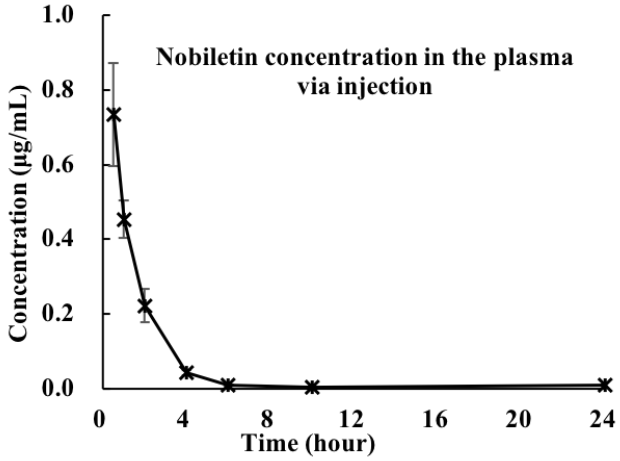

(B)

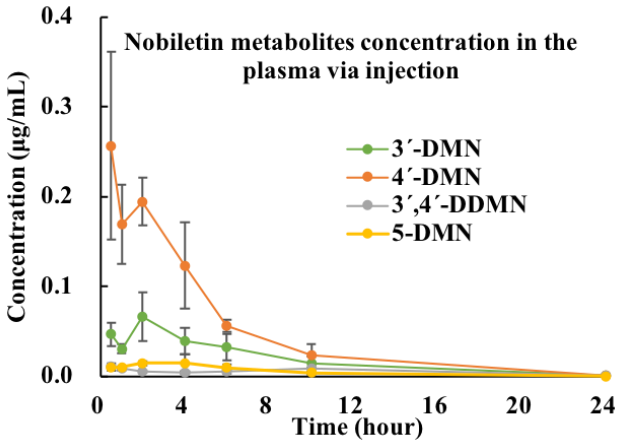

(C)

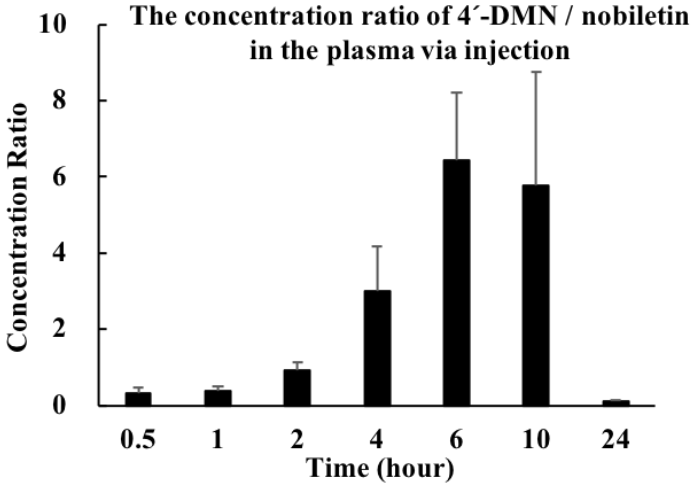

Figure 27: The dynamic concentration change in the plasma after intravenous injection of 5mg/kg nobiletin for nobiletin(A), major demethylated metabolites (B), and concentration ratio of 4′-demethylnobiletin (DMN)/nobiletin (C).

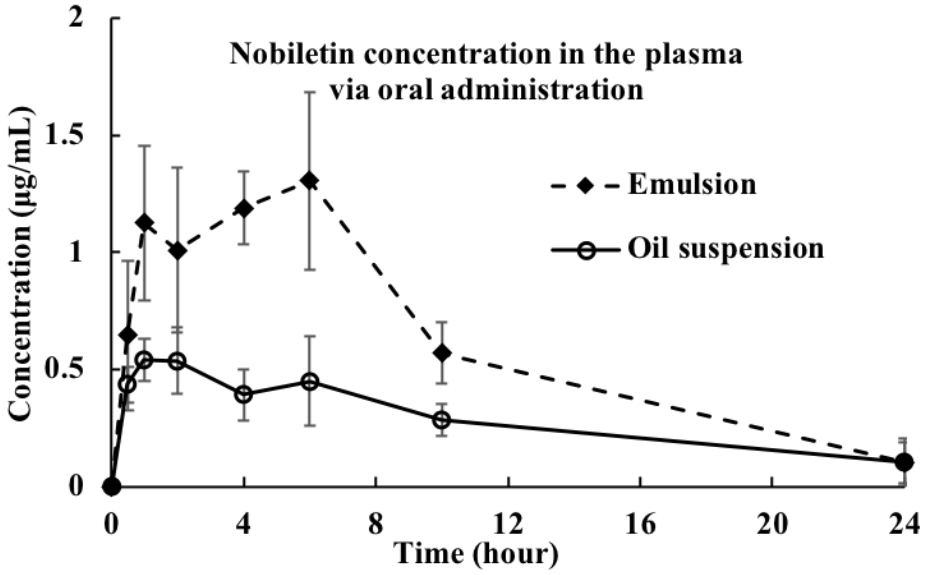

Figure 28: The concentration-time profile of nobiletin in the plasma after oral administration of nobiletin emulsion and oil suspension at the dosage of 100mg/kg nobiletin.

Table 9: The pharmacokenetic parameters of nobiletin in rats after intravenous and oral administration

	Administration Routes		
Parameters	Intravenous	Oral-Oil suspension	Oral-Emulsion
Dosage (mg/kg)	5	100	100
T_{max} (hour)	-	3.00±2.16	4.00±2.24
C_{max} (µg/mL)	0.73±0.14	0.63±0.10	1.45±0.32
K_e	0.79	-	-
AUC (hour*µg/mL)	1.54±0.12	6.14±1.21	14.23±1.55
Bioavailability (F%)	-	19.93±3.93	46.20±5.03
Relative bioavailability	-	2.32	

5.3.5 Evaluation of the Oral Bioavailability of Nobiletin in Emulsion

The time-concentration profiles of nobiletin in the rat plasma after oral administration of nobiletin emulsion and oil suspension are shown in **Fig. 28**. The pharmacokinetic indexes are summarized in **Table. 9**. The T_{max} and C_{max} of nobiletin in the plasma was 3.00±2.16 hour and 0.63±0.10 μg/mL for oil suspension and 4.00±2.24 hour and 1.45±0.32 μg/mL for emulsion. The bioavailability of nobiletin in oil suspension and emulsion was estimated as 19.93±3.93% and 46.20±5.03%, respectively. The relative bioavailability of nobiletin in emulsion was thus 2.32 as compared to oil suspension. The concentration-time profile of the major metabolite 4′-DMN is shown in **Fig. 29A**. The AUC of 4′-DMN in the plasma delivered by emulsion was about 1.95 times that delivered by oil suspension (**Fig. 29B**). This suggested that the delivery systems had a similar effect on the AUC of nobiletin and its major metabolite. Moreover, the AUC of 4′-DMN accounted for 60%-75% of nobiletin for both oil suspension and emulsion (**Fig. 29B**). **Fig. 29C** illustrates the concentration ratio of 4′-DMN to nobiletin within 24 hours. The ratio was less than 1 during the first 10 hours after oral administration and was greater than 1 in the 24th hour. Considering the quick biotransformation (about 2 hours for nobiletin and 4′-DMN to reach the concentration equivalent in the plasma) after intravenous injection (**Fig. 27C**), the longer equivalent time (about 10 hours, shown in **Fig. 29C**) indicated that the absorption rate of nobiletin was larger than the biotransformation rate in the rat plasma during the first 10 hours after oral administration. In addition, this result suggested that the reabsorption from the colon also contributed to the overall bioavailability of nobiletin.

(A)

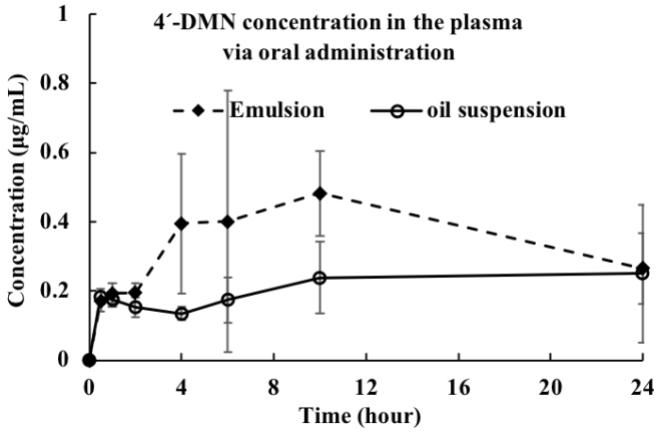

(B)

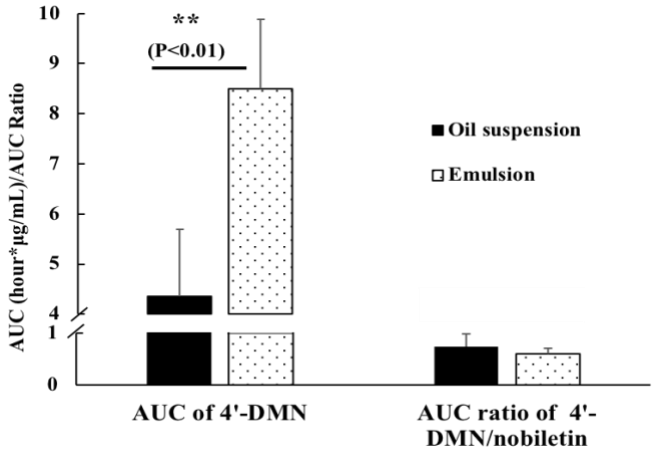

(C)

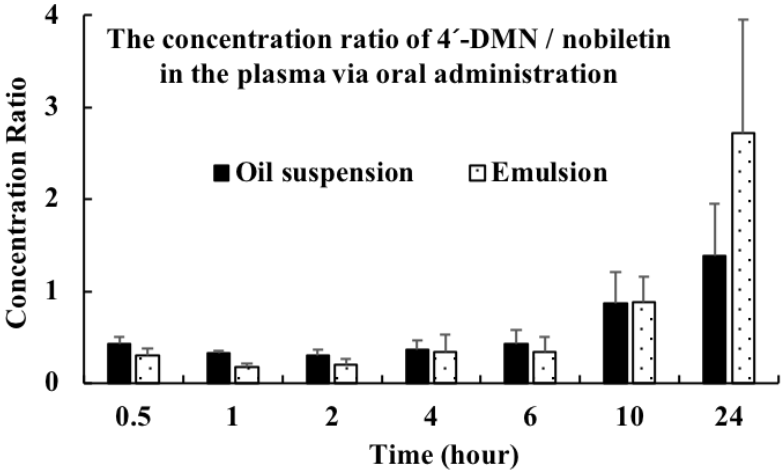

Figure 29: After oral administration 100mg/kg nobiletin delivered by emulsion and oil suspension, the concentration-time profile of 4′-DMN in the plasma(A); the area under the curve(AUC) of 4′-DMN and the AUC ratio of 4′-DMN to nobiletin(B); the concentration ratio of 4′-DMN/nobiletin at different time intervals(C).

5.4 Discussion

Table 10: The advantages/disadvantages of *in vitro* and *in vivo* models to estimate the bioavailability of nobiletin delivered by different delivery systems.

Advantages/disadvantages	The combined *in vitro* models	*In vivo* study
Incorporating factors for bioavailability		
-bioaccessibility	√	√
-absorption/permeability	√	√
-biotransformation	×	√
The estimation of absolute oral bioavailability	×	√
Cost-effective and rapid screening method	√	×
Ethical concerns	×	√

Table. 10 shows the comparisons of the *in vitro* and *in vivo* models in terms of their advantages/disadvantages. The solubility and permeability are considered fundamental to define the extent of intestinal absorption for bioactive ingredients according to the biopharmaceutics classification system developed by the FDA (*245*). Due to the poor water solubility of PMFs, most studies aimed to enhance their bioaccessibility by different formulations and evaluated via *in-vitro* digestions models, such as the pH-stat lipolysis and TIM-1 models (*41, 61*). In addition, the permeability of PMFs has been investigated by PAMA and Caco-2 cell studies (*10, 246*). Ours is the first study using an *ex vivo* Franz diffusion cell to evaluate the intestinal permeability of PMFs. We have tailored the receiving medium (e.g. PBS buffer, Tween solutions and ethanol solutions) in the Franz cell (data not shown), and finally chose ethanol solution to better correlate the in *vivo* results. Even though PMFs were considered to have good permeability, the diffusion in the real intestinal membrane was not linearly associated with the preabsorbed solubilized

concentration of PMFs (**Fig. 26**). The relative bioaccessibility was about 4.5 indicated by *in vitro* lipolysis, and the relative bioavailability was estimated as 2.3 after *ex vivo* intestinal absorption. This overall value was very close to the relative bioavailability calculated from the time-concentration profiles using the rat model. As both solubility and permeability were taken into consideration for our combined models, this might be the reason for the good correlation with the *in vivo* data. Importantly, the *in vitro* models were easy to use and time efficient. Thus, the combined *in vitro* models developed in this study could readily be used to predict the relative bioavailability of PMFs *in vivo* and to screen various delivery systems.

One of the advantages of *in vivo* studies over *in vitro* models was to assess the absolute bioavailability (F%) when intravenous administration was used as the comparison for oral administration. This study found that the absolute bioavailability of nobiletin was about 20% for oil suspension and 46% for emulsion. Nobiletin had a high bioavailability even delivered by oil suspension, compared to other typical flavonoids. For example, the absolute bioavailability of anthocyanins ranged from 0.26% to 1.8% (*53*); and absolute bioavailability of (-)-epigallocatechin-3-gallate (EGCG) from green tea was about 1.6% in rats (*54*). The high bioavailability of nobiletin may result from the properties of the methoxy groups which provide 1) chemical stability against the harsh gastrointestinal environment, and, 2) high intestinal permeability (*247*). Moreover, the number of methoxy groups had an important effect on the pharmacokinetic parameters of PMFs. With an additional methoxy group on the 3'-position, nobiletin was found to have nearly 10-fold greater AUC in the serum than tangeretin with the identical dosage using the rat model (*55*).

Biotransformation is important for the bioavailability and bioactivity of

phytochemicals *in vivo* (*51, 77*). The major drawback of the *in vitro* models is in them not realistically mimicking the biotransformation *in vivo*. For the orally administered phytochemicals, the small intestine is the major site for absorption after digestion (*46*). Once absorbed, the phytochemicals are metabolized in the host body (*77*). On the contrary, the unabsorbed phytochemicals would enter the colon and be biotransformed by the gut microbiota (*68*). Moreover, the colonic metabolites could be reabsorbed into the circulation system from the colon. The major metabolite of nobiletin in the plasma was 4′-DMN via either oral or intravenous administration of nobiletin. This finding was consistent with previous results (*78, 81*). The demethylation on the B-ring position is the major pathway for the biotransformation of nobiletin in the mouse urine (*38, 78*). Moreover, the demethylated metabolites were found to have higher bioactivities than nobiletin, including the anti-inflammation, anti-obesity, anti-cancer, etc. (*15*). The AUC of 4′-DMN was about 60%-75% of nobiletin after oral administration of nobiletin within 24 hours. Considering the high extent of biotransformation and greater bioactivities of metabolites, it is suggested that the metabolite formation might be an important pathway for the bioactivity of nobiletin *in vivo*. Compared to oil suspension, nobiletin emulsion improved the AUC of nobiletin and 4′-DMN to about the 2.32- and 1.95-fold higher levels, respectively. The similar amplification rates indicated that the biotransformation to its major metabolite in the host might be driven by the concentration of nobiletin delivered into the blood system. From our previous studies, PMFs could attenuate obesity by two routes: 1) inhibiting the adipogenesis/lipogenesis of preadipocyte cells after entering the circulation system (*136, 150*); 2) modulating the gut microbiota in the colon (*73*). This study found that the oral bioavailability and biotransformation of nobiletin in the host could be remodeled by

delivery formulations. In our ongoing work, the influence on gut microbiota and colonic metabolism will be investigated by unformulated/formulated nobiletin. Furthermore, the association between bioavailability and obesity-related metabolic syndromes will be explored.

5.5 Conclusion

In summary, a high loading nobiletin emulsion (1%) was developed in order to enhance the oral bioavailability of nobiletin. To better evaluate the oral bioavailability of PMFs, this study developed an *in vitro* model for the first time with the combination of *in vitro* lipolysis and Franz cell permeation. This model was easy to use, cost-efficient and highly correlated with the *in vivo* data in terms of the relative bioavailability. Thus, it was considered as a rapid and reliable screening method for various delivery systems. The *in vivo* pharmacokinetic study provided us more insights for the absolute bioavailability and biotransformation of nobiletin. Nobiletin had a high oral bioavailability due to the stability of its chemical structure and high intestinal permeability. The AUC of its major metabolite 4′-DMN accounted for about 60%-75% of nobiletin within 24 hours after oral administration. The emulsion could improve the AUC of nobiletin and its major metabolite in the plasma by about 2-fold as compared to oil suspension. This work provides scientific insights for a rapid screening method for delivery systems and better understanding of the biological fate of nobiletin *in vivo*.

CHAPTER VI: DEVELOPMENT OF ORGANOGEL-BASED EMULSION TO ENHANCE THE SOLUBILITY AND BIOACCESSIBILITY OF 5-DEMETHYLNOBILETIN

6.1 Introduction

Polymethoxyflavones (PMFs) are identified as the functional ingredients in citrus peels and have shown profound biological activities, such as anti-obesity, anti-inflammation, neuroprotection and anti-cancer properties (*9, 10, 73*). Nobiletin and tangeretin are the two predominant PMFs in citrus peels. Moreover, 5-demethylnobiletin (5-DMN) is identified and accumulated in the aged citrus peels during the long-period storage after drying procedures. 5-demethylnobiletin has shown better bioactivities than nobiletin especially for the anti-obesity effect (*136, 159*). However, due to the hydrophobic and highly crystalline structure, 5-DMN has very poor water solubility which becomes the limiting factor for its bioaccessibility.

Many strategies have been developed to improve the bioaccessibility of PMFs, such as nanoparticles (*57*), emulsion systems (*59, 61*), self-emulsifying systems (*62*) and amorphous solid dispersion (*65*). The emulsion-derived delivery systems have been proven as the efficient and convenient way for bioaccessibility enhancement using both *in vitro* and *in vivo* models (*59, 61*). Before preparing emulsions, PMFs are either dissolved or

suspended in the oil phase. PMFs in the dissolved state are found to have significantly higher oral bioavailability in the rat pharmacokinetic study as compared to those in the suspended state in the same oil (*55*). However, the solubility of PMFs in the oil is also quite low, which limits the loading capacity of emulsion with dissolved PMFs in the oil phase. For example, the solubility of nobiletin and 5-demethytangeretin in the medium chain triglycerides (MCT) is about 4.4 mg/g and 2.3 mg/g, respectively, in the room temperature (*40, 41*). Therefore, it is a challenge for traditional emulsion-derived delivery systems to reduce the crystallinity and improve the loading capacity of PMFs.

The organogel-based emulsion is considered as an effective tool to improve the solubility of nutraceuticals in the oil phase and greatly increase their oral bioavailability *in vivo*, according to our previous report (*239, 243*). The gel can be classified into organogel and hydrogel. The organogel is obtained when the gelled liquid phase is oil, while the hydrogel is obtained when the gelled liquid phase is water (*248*). However, compared with hydrogel, the studies on organogel are quite limited (*248*). Most gelation process is thermoreversible for organogel: the gelation can be induced by the temperature reduction after the dissolution of gelator in the oil (*249*). The organogel has been widely explored to structure liquid oil and use as the replacement of solid/hydrogenated fat in food industry (*249*). In recent years, using organogel as the delivery system for hydrophobic bioactives has received increasing attentions. The gel structure is found to prevent the crystal precipitation and control the release of bioactives after digestion (*250*). However, the

exploration and application of organogel are still in its infancy (*248, 249*).

This is the first study using organogel-based emulsion to encapsulate PMFs. PMFs are suitable for the organogel-based emulsion, as they are heat stable (resistant to the heating during gelator dissolution), hydrophobic and highly crystalline (interacted with the gel structure). 5-DMN was selected as the representative of PMFs due to its promising bioactivity. This study aims to develop organogel-based emulsion with two distinctive characteristics: 1) high loading of amorphous 5-DMN; 2) enhanced bioaccessibility compared with conventional emulsion. By carefully engineering the gelator and surfactants in the oil, the organogel can increase the solubility of 5-DMN to about 3.5 times higher level as compared to that in the MCT. Furthermore, the organogel-based emulsion was developed by systemically investigating the phase behaviors and rheology properties. In the end, the organogel-based emulsion demonstrated greater enhancement for the bioaccessibility of 5-DMN than oil suspension and conventional emulsion evidenced by the *in vitro* lipolysis.

6.2 Materials and Methods

6.2.1 Materials

5-DMN was synthesized from pure nobiletin according to our previously published method (*214*). MCT was a gift from Stepan company (Northfield, IL, USA). The

surfactants with analytic grade was purchased from Sinopharm Chemical Reagent Co., Ltd (Shanghai, China), including Span 20 (sorbitan monolaurate), Span 40 (sorbitan monopalmitate), Span 60 (sorbitan monostearate), Span 80 (sorbitan monooleate) and Tween 80 (polyoxyethylene sorbitan monooleate). Sugar ester (sucrose stearic acid ester, S370) was provided from Mitsubishi Chemical Corporation (Tokyo, Japan). Water, acetonitrile and methanol with HPLC-grade were purchased from Greenfield (Brookfield, CT, USA). Pancreatin with 8x USP, Tris maleate and sodium taurodeoxycholate (Na TDC) were purchased from Sigma-Aldrich (St. Louis, MO, USA). Sodium chloride, sodium hydroxide and calcium chloride dihydrate were purchased from VWR (Radnor, PA, USA). Lecithin (Biolipon 95) was a gift from Perimondo, LLC (Florida, NY, USA).

6.2.2 Determination the solubility of 5-DMN

The solubility of 5-DMN in the MCT was carried out according to previous report with minor modification (*58*). Briefly, 1% (w/v) 5-DMN was added to the MCT under stirring in the boiling water bath for 10 minutes. After fully dissolution, the samples were stored in the room temperature for 24 hours to ensure equilibrium. The oil samples were centrifuged 10,000 rpm for 10 minutes and the supernatant was passed through 0.22 μm nylon filter. The filtered supernatant was diluted about 400 times by acetonitrile and analyzed by high performance liquid chromatography (HPLC). To estimate the metastable solubility of 5-DMN in the MCT/Span mixture, saturated Span oil solution was prepared

by adding 1 g Span in 9 g MCT under stirring and heating. The measurement of metastable solubility was carried out after 24-hour and 120-hour (5 days) storage in the room temperature. The procedures were the same as described above.

6.2.3 Polarized light microscopy

The crystal formation of 5-DMN in the MCT, oil/Span mixture and organogel was observed by Olympus CX41 microscope (Tokyo, Japan) equipped with a polarizer and Cannon camera for recording images.

6.2.4 Preparation of 5-DMN organogel and organogel-based emulsion

1% (w/v) 5-DMN and different concentrations of sugar ester (5%, 10%, 15%, 20%, w/v) were added in the Span 20-saturated MCT. The mixture kept stirred in the boiling water bath for 10 minutes to fully dissolve the 5-DMN and sugar ester (SE). The oil solution would transform to organogel within few hours after the oil solution was set to the room temperature.

To prepare the organogel-based emulsion, Tween 80 with different concentrations (0%, 5%, 10%, 20%, 30%, w/w) was firstly dissolved in the water phase. The water phase was added into the oil solution in the boiling water bath at different ratios (30%, 50%, 60%, 70%, 80%, 90%, w/w). The mixture was kept stirred in the boiling water for another 2 minutes, homogenized at 15,000 rpm for 3 minutes using high speed homogenizer (IKA

Works Inc. Wilmington, NC, USA), and sonicated for 5 min using a tip sonicator at about 200W.

6.2.5 Rheology measurement

The rheology properties of the organogel and organogel-based emulsion after 24-hour storage were measured using the parallel plate at the room temperature by ARES Rheometer (TA instruments, New Castle, DE, USA). The viscosity was measured using the static model under the shear rate ranging from 0.1 to 100 s^{-1}. The dynamic strain test was performed before the dynamic frequency sweep test in order to get the linear viscoelastic region. For the dynamic frequency sweep test, the strain was fixed as 1%. The G' (storage modulus) and G" (loss modulus) were recorded as the function of the frequency ranging from 0.1 to 100 rad/s.

6.2.6 Particle size measurement

The organogel-based emulsion was diluted properly by deionized water before analysis. The droplet size and its distribution of organogel-based emulsion was determined by dynamic light scattering and measured using particle sizing analyzer (NanoBrook 90Plus, Brookhaven Instrument, Holtsville, NY, USA). The fixed scattering angle was set as 90°. The samples for each formulation were measured in triplicate in the room temperature.

6.2.7 *In vitro* lipolysis of 5-DMN in lipid-based delivery systems

The oil suspension and conventional emulsion with the same loading of 5-DMN (1%) in the oil phase were prepared, as the comparison of organogel-based emulsion. The conventional emulsion had the same ratio of oil phase (40%, v/v) and Tween 80 (6%, w/v) with organogel-base emulsion but did not contain Span and SE. The preparation procedures were the same for both conventional emulsion and organogel-based emulsion. The *in vitro* lipolysis of 5-DMN in different delivery systems was conducted using our method as previously described (*239, 243*). Briefly, 0.25g MCT equivalent from the oil suspension, conventional emulsion and organogel-based emulsion was digested by pancreatin in the fasted/fed buffer in the 37 °C oil bath, respectively. The contents of fast/fed-state buffer were listed in our previous work (*243*). During the 2-hour digestion process, the pH of the buffer was kept at 7.5 ± 0.02 by manually adding 0.25 N sodium hydroxide (NaOH) solution. The volume and adding time intervals of NaOH solution were recorded in real-time. After lipolysis, the buffer was centrifuged at 12000 rpm for 40 minutes (Beckman Coulter, Brea, CA, USA) and the micelle phase was passed through 0.22 μm filter to get rid of possible crystals. The filtrate was dilute 2 times by methanol and filtered by 0.22 μm filter again before HPLC measurement. The bioaccessibility of 5-DMN in the lipid-based delivery systems was calculated as:

$$\%\text{bioaccessibility} = \frac{\text{mass of } 5-\text{DMN in the micelles}}{\text{mass of } 5-\text{DMN in the oil phase}} * 100$$

The mass of 5-DMN in the oil phase was the loading amount of 5-DMN in 0.25 g MCT equivalent for each formulation at the starting point of lipolysis. The mass of 5-DMN in the micelles was calculated by multiplying the concentration of 5-DMN estimated by

HPLC and the aqueous volume after 2-hour lipolysis.

6.2.8 HPLC analysis

The determination of 5-DMN concentration was carried out using Agilent 1100 series HPLC system (Santa Clara, CA, USA) equipped with the UV detector (320 nm) and a Poroshell 120 PFP column (4.6*150 mm, 2.7 μm) (Agilent, Santa Clara, CA, USA). The injection volume was 20 μL and the flow rate was 0.7 mL/min. The mobile phases were composed of the water (A) and acetonitrile (B). The elution program was: 0-2 min, held at 35% B; 2-7 min, linear gradient from 35% B-60% B; 7-13 min, linear gradient from 60% B-95% B; 13-15 min, held at 95% B, 15.01 min-18 min, held at 35% B.

6.2.9. Statistical test

StataSE v15. was used for the statistical significance test. Student t-test and One-Way Analysis of Variance (ANOVA) followed by Bonferroni multiple-comparison test were utilized to examine the difference among groups and the significance level was set as 0.05 for P-value.

6.3 Results and Discussion

6.3.1 The development of organogel with improved solubility of 5-DMN

(A)

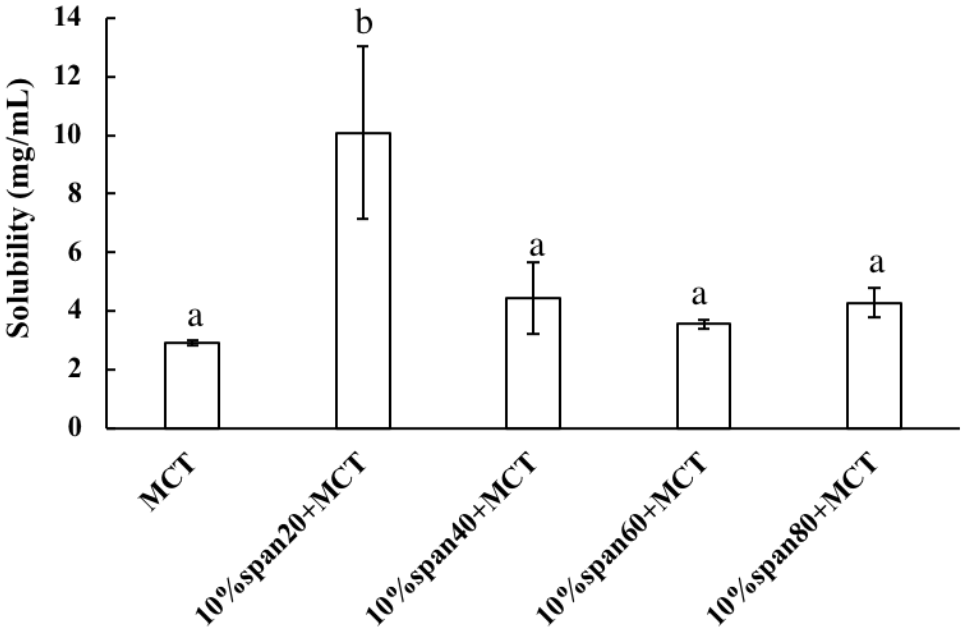

(B)

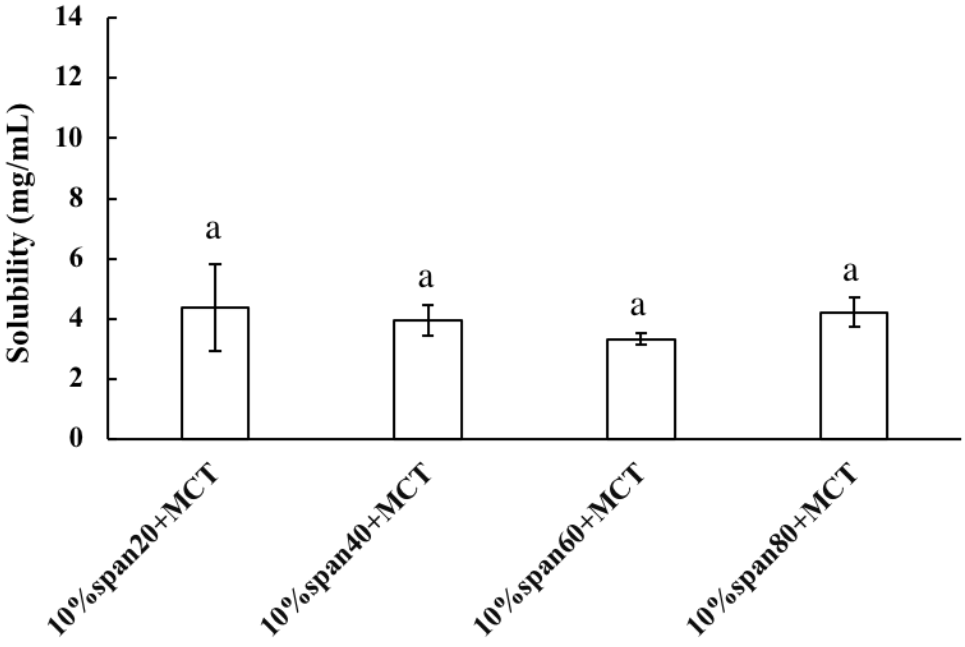

Figure 30: The stability/metastable stability of 5-demethylnobiletin in oil/structured oil after (A) 24-hour and (B) 120-hour storage in the room temperature.

In this study, a series of food-grade surfactants Span were selected to structure the oil phase, including Span 20, Span 40, Span 60 and Span 80. The solubility of 5-DMN in

the oil/structured oil after 24-hour storage was demonstrated in **Fig. 30A**. The solubility of 5-DMN in the MCT was 2.92±0.10 mg/mL. The addition of Span could increase the metastable solubility of 5-DMN in the oil after 1-day storage. Among the Span surfactants, Span 20 had the best promotional effect as the co-solvent to dissolve 5-DMN. The solubility of 5-DMN in Span 20-saturated MCT was 10.09±2.94 mg/mL, which was about 2.46 times higher than that in the pure MCT. The major difference of Span-20, 40, 60, and 80 is the chain length of the fatty acid ester. The laurate side chain might be more effective to prevent the crystallinity of 5-DMN as compared to palmitate-, stearate-, and oleate- side chains. Therefore, Span 20 was chosen for the following study. However, the solubility of 5-DMN in the span-saturated MCT after 5-day storage decreased to the similar level of its solubility in the MCT (**Fig. 30B**). Besides, no significant difference was observed for different types of span surfactants after 5-day storage (**Fig. 30B**). It indicated that the excessively dissolved 5-DMN promoted by Span in the MCT was metastable and 5-DMN crystals would gradually precipitate within 5 days.

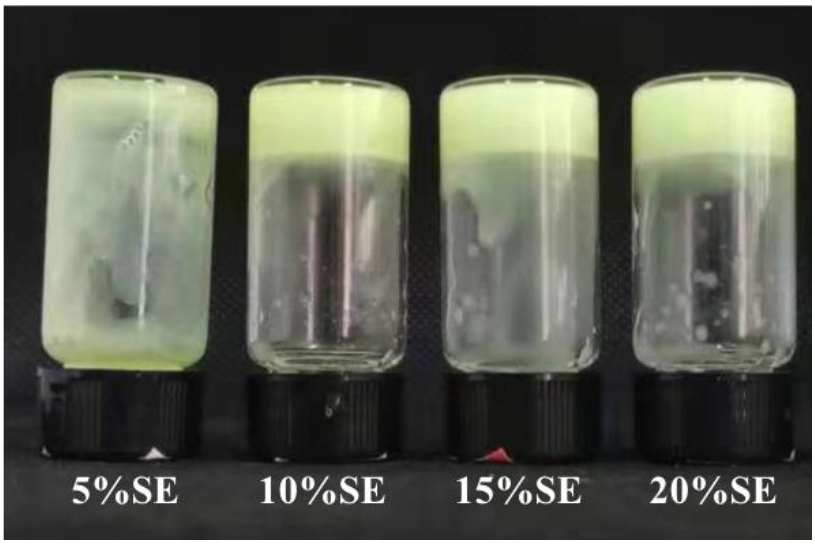

Figure 31: The photograph of the 5-demethylnobiletin loaded organogel with different concentrations of sugar ester (SE).

Different concentrations (5%, 10%, 15% and 20%) of SE were added to the Span 20-saturated MCT with 1% (w/v) 5-DMN and heated for 10 minutes to ensure the dissolution of SE and 5-DMN. **Fig. 31** showed the gel formation after 24-hour storage in the room temperature. The gel was formed if the concentration of SE was no less than 10%. In order to investigate the influence of SE on the 5-DMN crystal formation, 5-DMN (1%, w/v) in the different structured oils was observed by polarized light microscopy after 5-day storage in the room temperature (**Fig. 32**). From **Figs. 32A, 32B, 32C,** the supersaturated 5-DMN precipitated and had the need-like crystals in the pure MCT, MCT with 10% Span 20, and MCT with 20% SE. It indicated that MCT, saturated Span 20 and high concentration of SE alone could not completely prevent the crystal formation at such a high loading of 5-DMN. However, the combination of the three agents could achieve this result: the addition of 10-

20% SE in the Span-saturated MCT kept the 5-DMN amorphous during the 5-day storage as shown in **Figs, 32E, 32F, 32G.** For the addition of 5% SE, few crystals were observed in the structured oil (**Fig. 32D**). As 5% SE did not reach the minimum gelling concentration (MGC, **Fig. 31**), it suggested that the gel network was very crucial in terms of crystal prevention. For the small molecular gelators for organogel, the common gelling mechanism was through particle or fibril crystallization. These gelator molecules could self-assembly during the cooling process, potentially mimic the triglycerides crystallization and therefore forming the 3D organogel network (*249*). The MGC of SE in the 5-DMN loaded MCT was 10% in this study, while it was 15% for the blank MCT and capsaicin-loaded MCT according to our previous report (*251, 252*). The reduction of SE concentrations in this study indicated that 5-DMN and Span might also participated in the gel network formation.

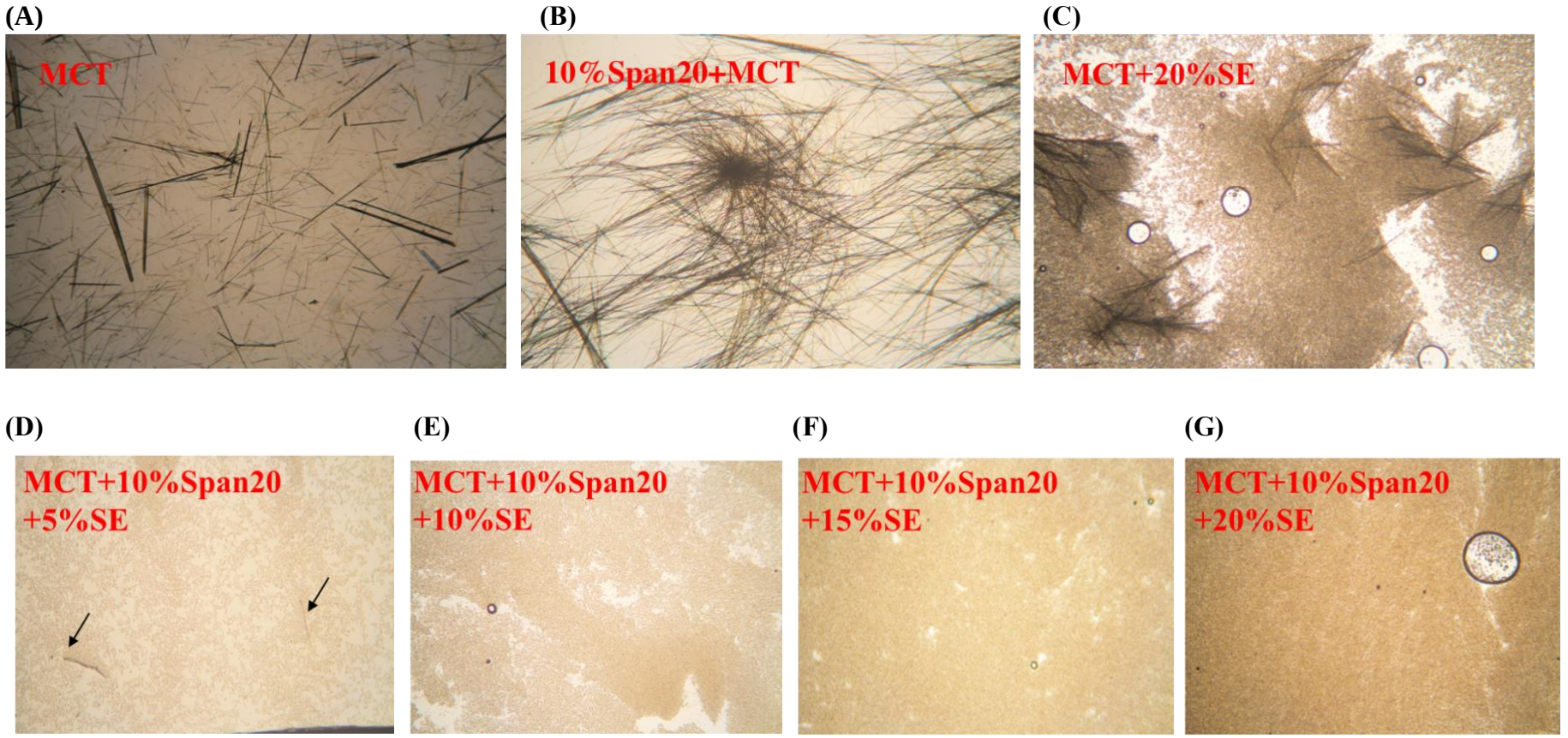

Figure 32： The images of 5-demethynobiletin (1%, w/v) in different structured oils observed by polarized microscope after 5-day storage in the room temperature: (A)in the pure medium chain triglycerides (MCT), (B)in the Span20-saturated MCT, (C) in the MCT containing 20% sugar ester(SE), (D)in the MCT containing 10% span20 and 5% SE; (E) in the MCT containing 10% span20 and 10% SE, (F)in the MCT containing 10% span20 and 15% SE; (G)in the MCT containing 10% span20 and 20% SE.

Our results demonstrated that the structure of organogel could increase the solubility of 5-DMN to 3.46 times as compared to that in the oil. The loading capacity of organogel was determined by the metastable solubility of 5-DMN in the span-statured MCT after 24-hour in the room temperature. As the supersaturated 5-DMN would keep amorphous for 24 hours, it provided enough time for SE to from the 3D network. Higher loading of 5-DMN (e.g. 1.5%) than the metastable solubility would lead to the precipitation of crystals in the organogel, as shown in **Fig. 33**.

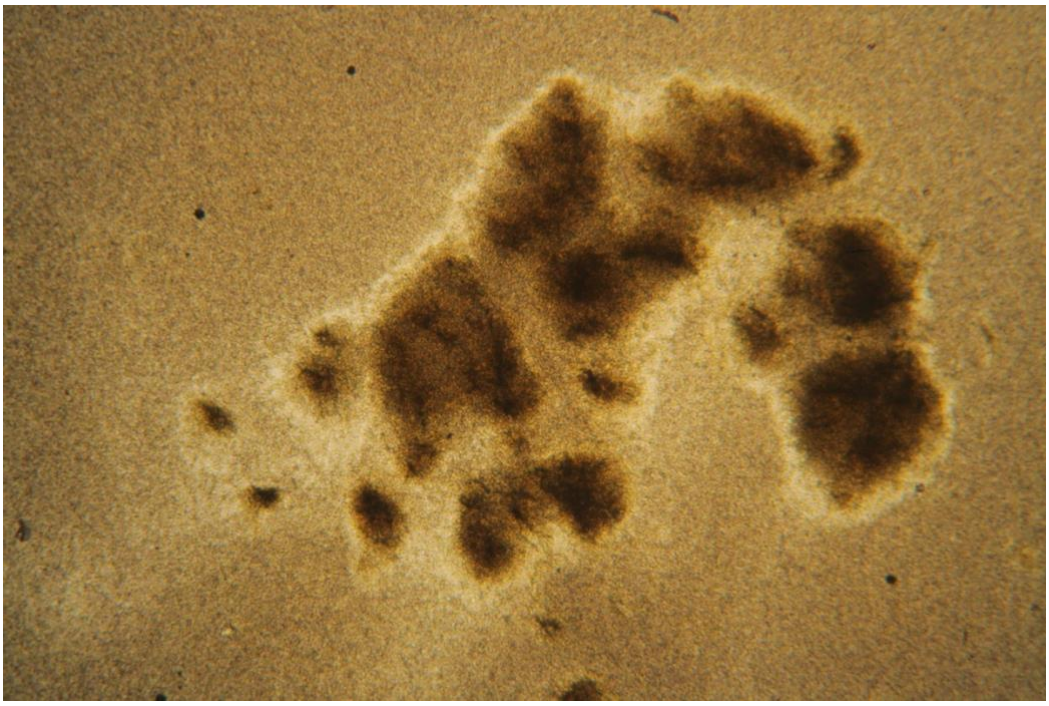

Figure 33: The PLM images of 5-demethynobiletin (1.5%, w/v) in the structured oil containing 10% span 20 and 10% sugar ester, after 1-day storage in the room temperature.

6.3.2 The development of organogel-based emulsion

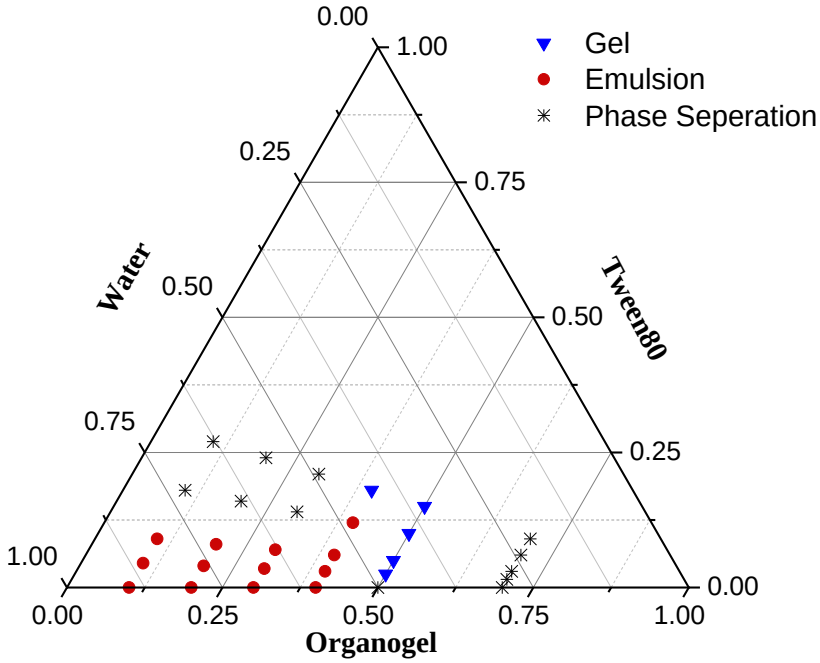

Figure 34: The ternary phase diagram of organogel-based emulsion consisting of organogel, water and Tween 80.

The phase behaviors were investigated under conditions with different organogel ratios and surfactant concentrations. Tween 80 was selected as the emulsifier in the water phase due to its outperformance than Tween 20, Tween 40 and Tween 60 for the emulsification ability (*251*). To obtain the stable emulsion, the ternary phase diagram for the blank organogel, water and Tween 80 was measured after the samples were prepared and stored for a week in the room temperature, as shown in **Fig. 34**. When the weight ratio of the organogel increased to 50%, the emulsions formed the physical gel with the

participation of Tween 80. They would stick to the top of inverted bottle without gravitational flow for at least 5 minutes. Further increasing the organogel ratios to 70%, the phase separation was observed for all samples. Therefore, the maximum ratio of organogel for the fluidic emulsion was around 40%. From **Fig. 34**, the emulsion could be formed without Tween 80. In the absence of Tween 80, the emulsification among the two phases was achieved by the Span 20 and SE in the organogel. The hydrophilic-lipophilic balance (HLB) value for Span 20 and SE was about 8.6 and 3, respectively (*253, 254*). Moreover, the high concentration of Tween 80 (HLB≈15) could even disturbed the emulsion stability when the organogel phase ratio was no more than 30%. The disturbance of emulsion stability might be resulted from the imbalance of the three surfactants in the bi-phase in these scenarios.

40% (v/v) organogel was chosen to prepare the emulsion, as the higher ratio of organogel referred to higher loading of 5-DMN. The emulsion samples after 24-hour storage were shown in **Fig. 35A**. The average droplet size of organogel-based emulsion was measured for the emulsion with different concentrations (w/v) of Tween 80 (**Fig. 35B**). The increase of Tween 80 concentration led to the decrease of average droplet size of the emulsion. In particular, the droplet size was less than 200 nm with the small polydispersity index (PDI<0.2), when the concentration of Tween 80 equated/ exceeded to 6% (**Figs. 5B&5C**). There was no statistical difference among the four groups for PDI. This might be resulted from the large difference within the groups containing 0%- and 3%- Tween 80.

Moreover, all emulsions loading 5-DMN kept homogenous and stable after 7-day storage in the room temperature.

(A)

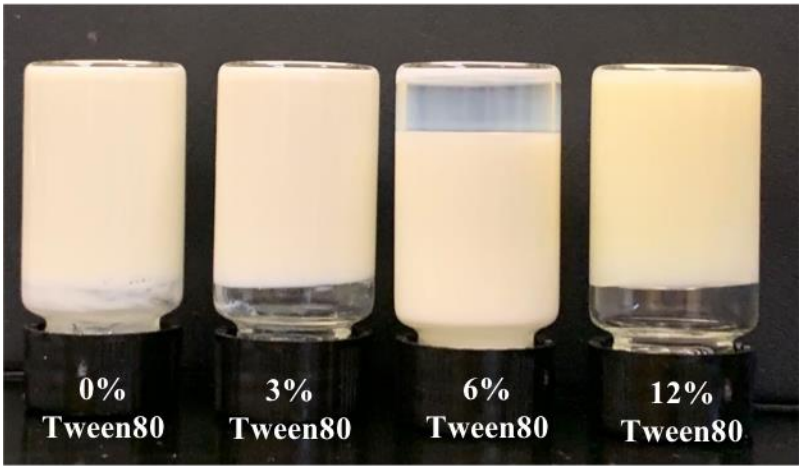

(B)

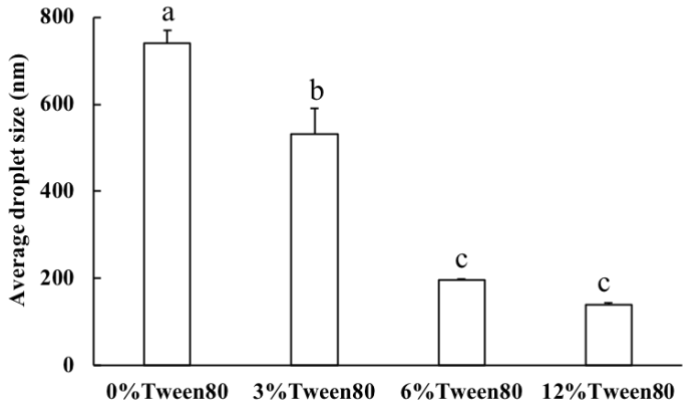

(C)

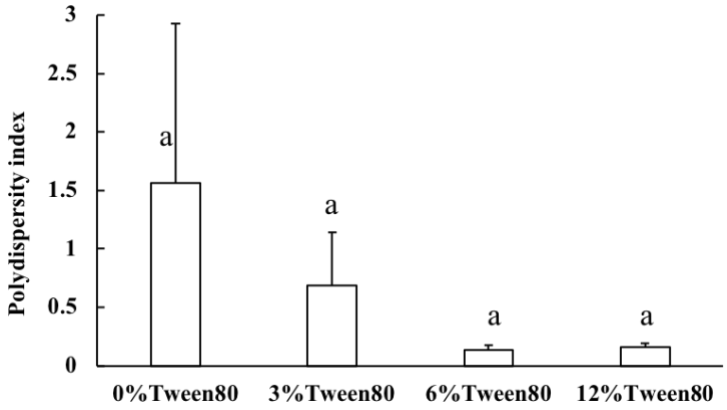

Figure 35: The characteristics of organogel-based emulsions with different concentrations of Tween 80: (A) the formation of physical gel, (B)average droplet size, (C)polydispersity index of the emulsions.

6.3.3 The rheological properties of organogel and organogel-based emulsion

The rheological characteristics of the organogel and organogel-based emulsion showed great importance for the applications in the food and cosmetic industry(*249*). Therefore, we firstly looked into the impact of SE on the formation of organogel loaded with 1% 5-DMN (**Figs. 6A&6B**). As shown in **Fig. 36A**, all samples demonstrated the shearing-thinning behaviors. The viscosity was increased by the concentration of added SE, when the shear rate was larger than 0.4 s^{-1}. Irrespective of the SE concentrations, the G' was larger than G" when the frequency was less than 30 (**Fig. 36B**). It indicated that all samples had the gel-like structure, but none of them belonged to “strong gel (G'/ G">10)” (*255*). These gel network could be destroyed by high shear rate, since the G' and G" tended to intersect at high frequency. Overall, the gel structure was enhanced by the increasing concentration of SE. The higher concentration of gelators led to higher extent of supersaturation and more nucleation site, which in-turn promoted the gelator crystallization and 3-D network formation (*256*).

The addition of Tween 80 significantly influenced the rheological properties of the organogel-based emulsion. As shown in **Fig. 35A**, all emulsion samples formed the physical gel, except the emulsion with 6% Tween 80. This phenomenon was consistent with the viscosity change illustrated in **Fig. 36C**. The viscosity of emulsion was firstly decreased by the Tween80 with the concentration increased from 0% to 6%. And then, the

viscosity of emulsion with 12% Tween 80 increased to the highest level among all emulsions. All the emulsion samples demonstrated the gel-like structure (G'> G''), as shown in **Fig. 36D**. The gel structure of organogel-based emulsion seemed stronger than that of the organogel, since no intersection was observed for the emulsion under the wide range of frequencies. The dynamic pattern of G' and G'' was similar for emulsions with 0%- 3%- and 12% Tween 80, while the G' and G'' of the emulsion with 6% Tween were significantly lower than those for the other emulsions. The surfactants-Span and Tween were reported to have synergistic effect on the interfacial properties and stability of emulsion (*257, 258*). The decreased viscosity and droplet size of emulsions might be resulted from the reduced interfacial tension by the increased concentration (0-6%) of Tween 80. Further increase the Tween 80 concentration might led to more intermolecular interaction, and thus promoting the gel structure. As the liquid form of emulsion was more convenient to fortify the nutraceuticals in the downstream food application, we selected 6% Tween for the following studies.

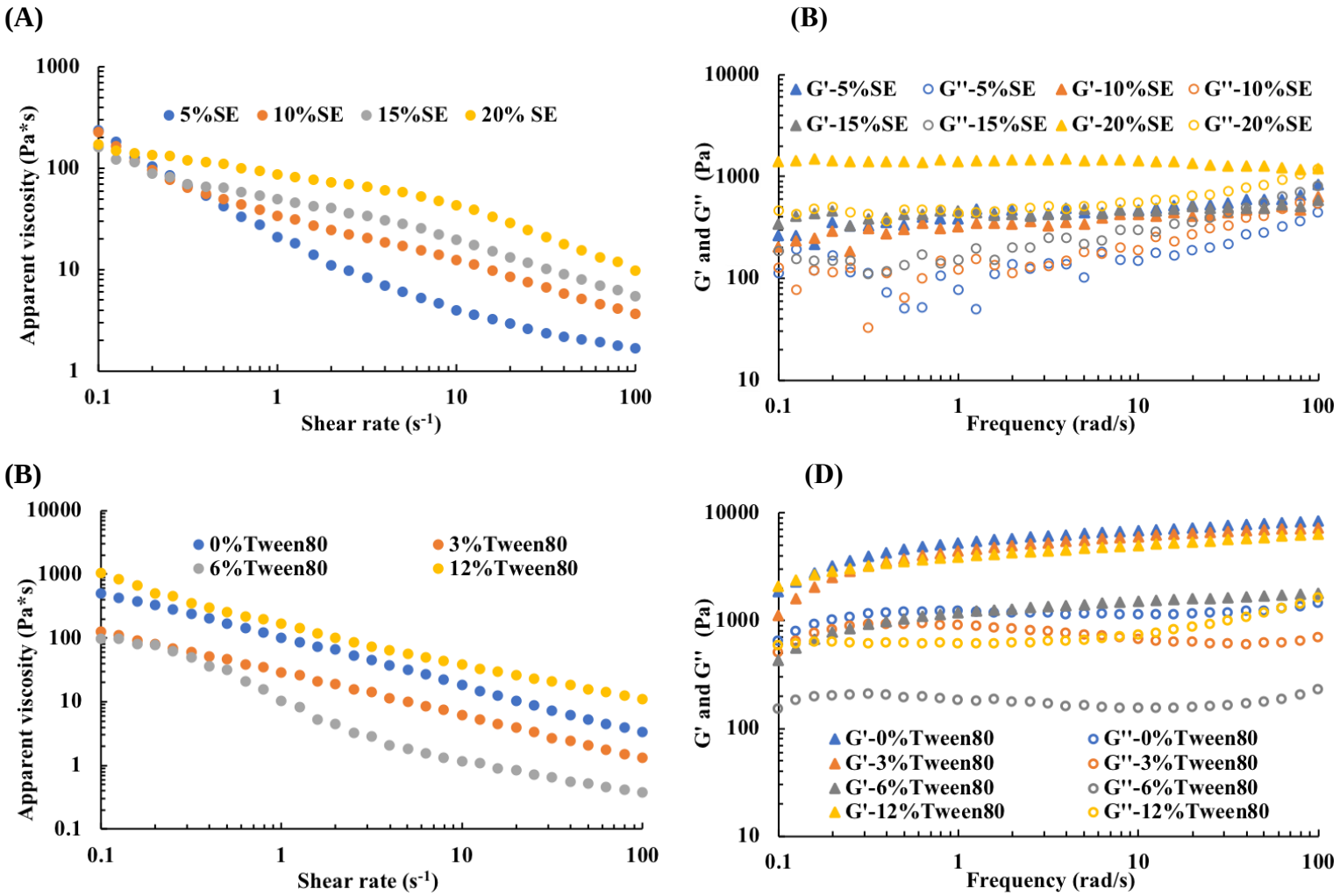

Figure 36: The rheological properties of 5-demethylnobiletin loaded organogel and organogel based emulsions: (A)the apparent viscosity of organogels versus shear rate (0.1-100s-1); (B)the storage modulus (G') and loss modulus (G") of organogels versus frequency (0.1-100 rad/s); (C) the apparent viscosity of organogel-based emulsions versus shear rate (0.1-100s-1); (D) the G' and G" of the organogel-based emulsions versus frequency (0.1-100 rad/s).

6.3.4 The bioaccessibility of 5-DMN in the lipid-based delivery systems

The bioaccessibility of nutraceuticals refers to the fraction that the nutraceutical is released from the food matrix after digestion and entrapped by mixed micelles in the gastrointestinal juice (*237*).The pH-static lipolysis is the widely used *in vitro* model to evaluate the bioaccessibility of nutraceuticals in lipid-based delivery systems (*59, 237*).

(A)

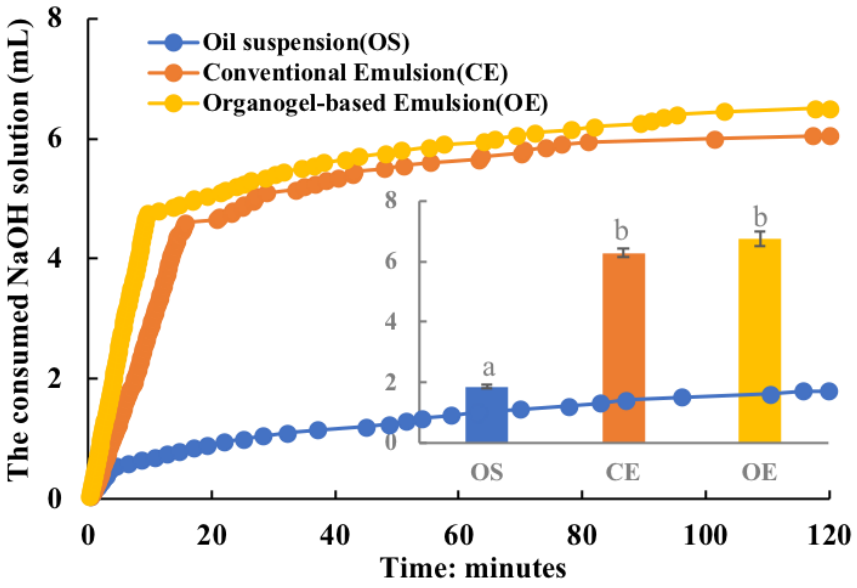

(B)

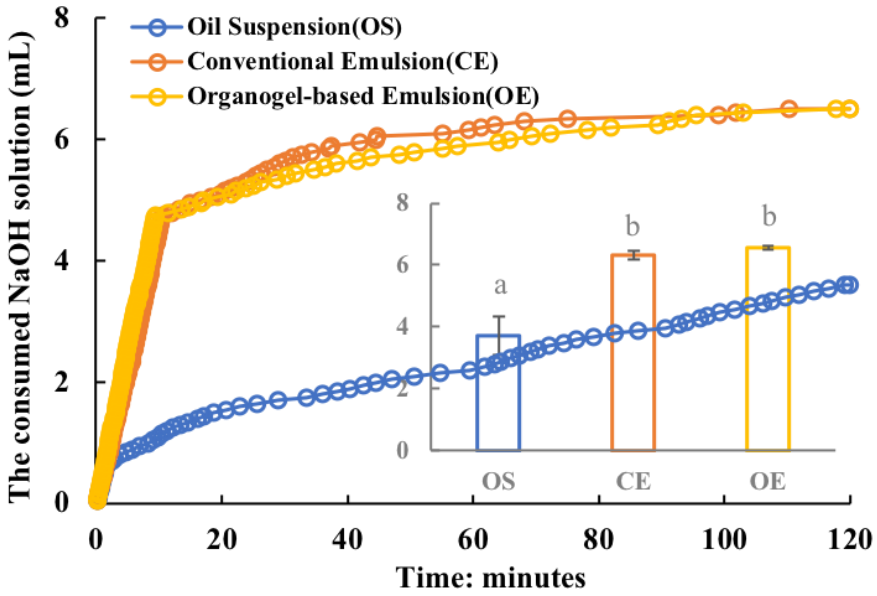

Figure 37: The digestion kinetics of the three lipid-based delivery systems expressed by the real-time consumed NaOH solutions and their total consumed volume (inner bar chart) after 2-hour (A) fast-state and (B) fed-state lipolysis.

In this study, three lipid-based delivery systems were prepared with the same loading of 5-DMN (1%, w/v) in the oil/organogel phase, including oil suspension, conventional emulsion and organogel-based emulsion. To compare the effect of these three delivery vehicles, 5-DMN bioaccessibility was evaluated using both fast- and fed-state lipolysis methods. The consumed NaOH solution as the function of time in the fast- and fed-state lipolysis is shown in **Fig. 37A** and **Fig. 37B**, respectively. In the fast-state lipolysis, the consumed NaOH solutions for oil suspension, conventional emulsion and organogel-based emulsion were 1.85±0.05, 6.28±0.13, 6.75±0.24 mL, respectively (inner picture in **Fig. 37A**). The digestion of organogel-based emulsion was faster than conventional emulsion. In the fed-state lipolysis, the consumed NaOH solution for oil suspension increased to

3.7±0.61 mL due to the greater concentrations of emulsifiers (e.g. Na TDC and lecithin) in the fed-state buffer than the fast-state buffer. Moreover, the volume of consumed NaOH solution was similar for conventional emulsion and organogel-based emulsion either in the fast-state or fed -state lipolysis. It indicated that the lipid in the emulsion samples was almost completely hydrolyzed by the enzymes after 2-hour digestion. The results of the bioaccessibility of 5-DMN in these delivery systems are shown in **Figs. 38A and 38B**. In both fast- and fed-state lipolysis, the organogel-based emulsion was more effective to enhance the bioaccessibility of 5-DMN than the conventional emulsion, when oil suspension was used as the comparison/baseline. The bioaccessibility of 5-DMN was the highest in the organogel-based emulsion digested in the fed-state buffer. The amplification times by organogel-based emulsion was 10.4 times as compared to oil suspension in the fast-state lipolysis, which was significantly higher than the amplification times (about 2.3) in the fed-state lipolysis.

(A)

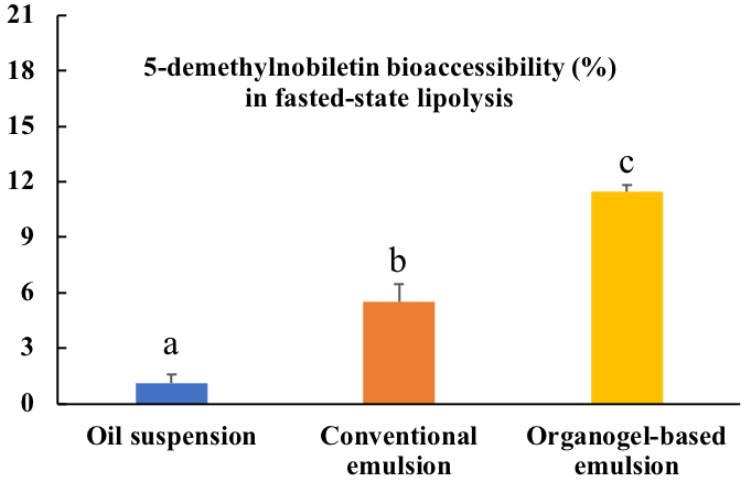

(B)

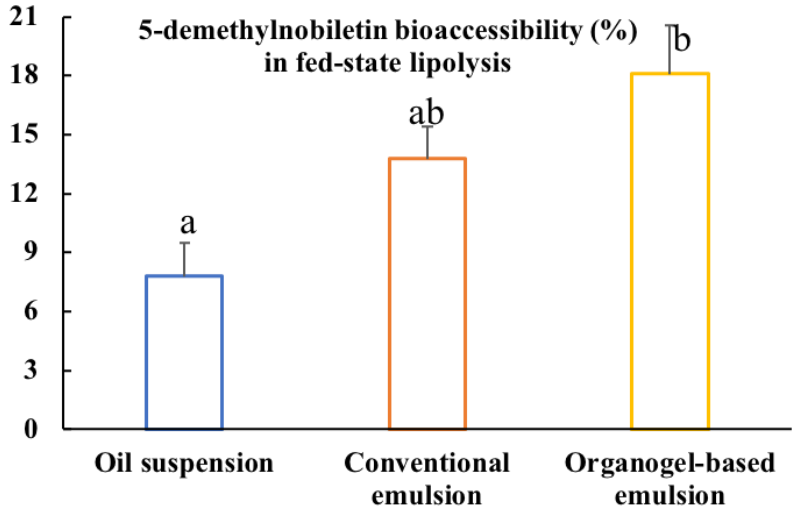

Figure 38: The bioaccessibility of 5-demethynobiletin delivered by oil suspension, conventional emulsion and organogel-based emulsion after 2-hour (A) fast-state and (B) fed-state lipolysis.

5-DMN had a relatively low bioaccessibility among PMFs evaluated by *in vitro* pH-static lipolysis, especially in the fast-state lipolysis (about 1.1% in MCT suspension). As the comparison, the bioaccessibility of tangeretin was about 9.7% (*59*) and nobiletin was about 17.9% (our unpublished data) in MCT suspension using the same fast-state lipolysis method. The bioaccessibility of lipophilic compounds was related to their solubilization in the mixed micelle after digestion, which depended on the interaction of lipophilic compounds and surfactant colloidal structure (*237, 259*). The low bioaccessibility of 5-DMN might be due to the neighboring participation effect between the 5-hydroxyl and carbonyl groups (*10*). The stable-six membraned ring between the A-ring and C-ring of flavones might made it difficult for 5-DMN to be entrapped in the mixed micelle formed by free fatty acids in the digested lipolysis juice. Moreover, Ting, Jiang (*59*) found that

the conventional emulsion, as compared to oil suspension, could increase the bioaccessibility/bioavailability of tangeretin to about 3 times higher using the *in vitro* fast-state lipolysis and 2.3 times higher using the *in vivo* mice study, respectively. The *in vitro* and *in vivo* data was quite consistent to access the oral bioavailability of PMFs from her study. Our results suggested that the organogel-based emulsion was a promising way to further enhance the bioaccessibility of PMFs due to the reduction of crystals, as compared to the conventional emulsion.

6.4 Conclusion

In this study, the organogel was developed to improve the solubility of 5-DMN in medium-chain triglycerides to 3.5 times higher level without crystal formation during 5-day storage. Increasing the concentration of the gelator (sugar ester) led to the increase of viscosity and gel-network structure of the organogel. The ternary phase diagram of organogel-based emulsion with different ratios of Tween 80 (0-27%) and organogel (0-70%) was explored. The emulsion containing 40% organogel was selected for further investigation because of the desired higher loading of 5-DMN. Increasing the concentration of the aqueous surfactant (Tween 80) from 0% to 6% decreased the droplet size and viscoelasticity of the emulsion. Furthermore, the organogel-based emulsion showed better enhancement for the 5-DMN bioaccessibility than conventional emulsion in both fast- and fed-state *in vitro* lipolysis models, as compared to oil suspension. Our results suggested that the organogel-based emulsion was a potential and effective way as the delivery system

to enhance the solubility and bioaccessibility of lipophilic compounds with high crystallinity.

SUMMARY AND FUTURE WORK

Given the increasing obesity prevalence among adults, the metabolic syndrome (MetS) is becoming a common health concern in our modern life. The identification and exploration of dietary compounds against MetS is an attractive strategy for functional food development. Polymethoxyflavones (PMFs), abundantly existing in the citrus peels, possess a broad spectrum of bioactivities, including neuroprotection, anti-inflammation, anti-obesity, anti-arteriolosclerosis, etc. Importantly, PMFs have shown very good bioefficacy to maintain the metabolic homeostasis *in vivo*. PMFs have local effect on gastrointestinal tract by interacting with gut microbiota and intestinal membrane; and also have systemic effect after entering or releasing signal molecules into the circulation system.

Many previous studies have found PMFs have anti-obesity effect. Notably, gut microbiota receives increasing attentions for their critical role on energy homeostasis. However, few studies have clearly demonstrated the interplay of PMFs and gut microbiota and its implication for obesity control. This study finds that PMFs can attenuate obesity by modulating gut microbiota using the DIO mice treated with PMFs extracted from *chenpi* or pure nobiletin. PMFs promote the fecal short chain fatty acids production and enriched functional bacteria in the colon digesta, such as *Akkermansia*, *Allobaculum*, *Lactobacillus* and *Bifidobacterium.* In addition, gut microbiota can extensively metabolize on PMFs and yield demethylated PMFs with higher bioactivity than their precursors.

In order to study the systemic effect of PMFs, this study investigates the bioavailability and biotransformation of nobiletin in the lean- and obese rats. The bioavailability of nobiletin is about 20% for either lean rats or obese rats. However, higher extent of demethylated metabolites was found in the feces and plasma in the obese rats than the lean rats. The different structure of the microbiome and the altered intestinal membrane are considered as the two leading factors for this phenomenon. Give the demethylated metabolites have higher bioactivity than their precursors, it suggests that PMFs may have better treatment effect for the obese individuals.

Apart from the physiological status of animals, the bioavailability and biotransformation of PMFs is influenced by delivery systems. From the pharmacokinetic study using rats, the conventional emulsion increases the bioavailability and biotransformation of nobiletin in the blood by around two times, as compared to the oil suspension. In order to rapidly screen various delivery system, this study develops a combined *in vitro* model containing the lipolysis and Franz diffusion cell, which shows good correlation with the *in vivo* data in terms of the relative bioavailability. Moreover, the formulation of conventional emulsion can be improved to effectively prevent the PMFs crystallization by forming organogel. The organogel-based emulsion shows larger enhancement for the bioaccessibility of PMFs, indicated by the *in vitro* models.

The regulation of metabolic homeostasis is an important area and has realistic significance in our modern life. However, the mechanisms of PMFs on maintining

metabolic homeostasis still remain unclear. Further investigations are called for attentions in the following aspects. 1) Better understanding the absorption, distribution, metabolism and excretion (ADME) of PMFs is needed. The ADME may be influenced by several factors, such as chemical structure of PMFs, food matrix/delivery systems, administrative dosage and the physiological state of the host. 2) The bioavailability-bioactivity relations need to be addressed. Many recent studies are trying to improve the bioavailability of PMFs by developing delivery systems. However, the association between the increased bioavailability and improved metabolic syndromes seems unclear and controversial, since gut microbiota is an important factor for metabolic homeostasis but often omitted in studies aiming to enhance bioavailability. 3) The interplay between PMFs and gut microbiota needs further exploration. The colonic biotransformation is suggested to contribute to the overall bioactivities of flavonoids, but the colonic degradation dynamics of PMFs and the responsible microbes remain unclear. Besides, as gut microbiota played an important role on the pathogenies of obesity and CVD, it is interesting for ongoing studies to focus on PMFs-mediated changes for microbial composition and obesity/CVD related metabolites. 4) The beneficial role of PMFs on circadian clock is a new and important research interest, but the investigation is still in its infancy stage. 5) Given metabolic homeostasis is regulated by CNS and multiple peripheral organs, it is interesting to explore the PMF-mediated communications among organ systems. In particular, the gut-brain axis is important for appetite control and circadian function. In-depth investigations are needed to unveil PMFs'

function/influence on the gut-brain axis as well as the gut-liver axis.

REFERENCES

1. WHO. Obesity and overweight https://www.who.int/en/news-room/fact-sheets/detail/obesity-and-overweight2020 [
2. CDC. Adult Obesity Facts https://www.cdc.gov/obesity/data/adult.html2020 [
3. Hotamisligil GS. Inflammation and metabolic disorders. Nature. 2006;444(7121):860-7.
4. Cani PD, Delzenne NM. Gut microflora as a target for energy and metabolic homeostasis. Current Opinion in Clinical Nutrition & Metabolic Care. 2007;10(6):729-34.
5. Hotamisligil GS. Inflammation, metaflammation and immunometabolic disorders. Nature. 2017;542(7640):177-85.
6. Falcone Ferreyra ML, Rius S, Casati P. Flavonoids: biosynthesis, biological functions, and biotechnological applications. Frontiers in Plant Science. 2012;3:222.
7. Kawser Hossain M, Abdal Dayem A, Han J, Yin Y, Kim K, Kumar Saha S, et al. Molecular mechanisms of the anti-obesity and anti-diabetic properties of flavonoids. International Journal of Molecular Sciences. 2016;17(4):569.
8. Farzaei MH, Singh AK, Kumar R, Croley CR, Pandey AK, Coy-Barrera E, et al. Targeting Inflammation by Flavonoids: Novel Therapeutic Strategy for Metabolic Disorders. International Journal of Molecular Sciences. 2019;20(19):4957.
9. Gao Z, Gao W, Zeng S-L, Li P, Liu E-H. Chemical structures, bioactivities and molecular mechanisms of citrus polymethoxyflavones. Journal of Functional Foods. 2018;40:498-509.
10. Li S, Pan M-H, Lo C-Y, Tan D, Wang Y, Shahidi F, et al. Chemistry and health effects of polymethoxyflavones and hydroxylated polymethoxyflavones. Journal of Functional Foods. 2009;1(1):2-12.
11. Li S, Wang H, Guo L, Zhao H, Ho C-T. Chemistry and bioactivity of nobiletin and its metabolites. Journal of Functional Foods. 2014;6:2-10.
12. Kurowska EM, Manthey JA. Hypolipidemic effects and absorption of citrus polymethoxylated flavones in hamsters with diet-induced hypercholesterolemia. Journal of Agricultural and Food Chemistry. 2004;52(10):2879-86.
13. Lin Y, Vermeer MA, Bos W, van Buren L, Schuurbiers E, Miret-Catalan S, et al. Molecular structures of citrus flavonoids determine their effects on lipid metabolism in HepG2 cells by primarily suppressing apoB secretion. Journal of Agricultural and Food Chemistry. 2011;59(9):4496-503.
14. Burke AC, Sutherland BG, Telford DE, Morrow MR, Sawyez CG, Edwards JY, et al. Intervention with citrus flavonoids reverses obesity and improves metabolic syndrome and atherosclerosis in obese Ldlr−/− mice. Journal of Lipid Research. 2018;59(9):1714-28.
15. Lai CS, Wu JC, Ho CT, Pan MH. Disease chemopreventive effects and molecular mechanisms of hydroxylated polymethoxyflavones. Biofactors. 2015;41(5):301-13.
16. Wang X, Li S, Wei C-C, Huang J, Pan M-H, Shahidi F, et al. Anti-inflammatory effects of polymethoxyflavones from citrus peels: A review. Journal of Food Bioactives. 2018;3:76-86.

17. Dunn TN, Adams SH. Relations between metabolic homeostasis, diet, and peripheral afferent neuron biology. Advances in Nutrition. 2014;5(4):386-93.
18. Lam TK. Neuronal regulation of homeostasis by nutrient sensing. Nature Medicine. 2010;16(4):392-5.
19. Begg DP, Woods SC. The central insulin system and energy balance. Appetite Control: Springer; 2012. p. 111-29.
20. Woods SC, Lutz TA, Geary N, Langhans W. Pancreatic signals controlling food intake; insulin, glucagon and amylin. Philosophical Transactions of the Royal Society B: Biological Sciences. 2006;361(1471):1219-35.
21. Simpson K, Parker J, Plumer J, Bloom S. CCK, PYY and PP: the control of energy balance. Appetite Control: Springer; 2012. p. 209-30.
22. Smith JK. Exercise, obesity and CNS control of metabolic homeostasis: a review. Frontiers in Physiology. 2018;9:574.
23. Stern JH, Rutkowski JM, Scherer PE. Adiponectin, leptin, and fatty acids in the maintenance of metabolic homeostasis through adipose tissue crosstalk. Cell Metabolism. 2016;23(5):770-84.
24. Miyata Y, Tanaka H, Shimada A, Sato T, Ito A, Yamanouchi T, et al. Regulation of adipocytokine secretion and adipocyte hypertrophy by polymethoxyflavonoids, nobiletin and tangeretin. Life Sciences. 2011;88(13-14):613-8.
25. Briggs DI, Andrews ZB. Metabolic status regulates ghrelin function on energy homeostasis. Neuroendocrinology. 2011;93(1):48-57.
26. Gallwitz B. Anorexigenic effects of GLP-1 and its analogues. Appetite Control: Springer; 2012. p. 185-207.
27. Everard A, Cani PD. Gut microbiota and GLP-1. Reviews in Endocrine and Metabolic Disorders. 2014;15(3):189-96.
28. Torres-Fuentes C, Schellekens H, Dinan TG, Cryan JF. The microbiota–gut–brain axis in obesity. The Lancet Gastroenterology & Hepatology. 2017;2(10):747-56.
29. van de Wouw M, Schellekens H, Dinan TG, Cryan JF. Microbiota-gut-brain axis: modulator of host metabolism and appetite. The Journal of Nutrition. 2017;147(5):727-45.
30. Frost G, Sleeth ML, Sahuri-Arisoylu M, Lizarbe B, Cerdan S, Brody L, et al. The short-chain fatty acid acetate reduces appetite via a central homeostatic mechanism. Nature Communications. 2014;5(1):1-11.
31. Samodien E, Johnson R, Pheiffer C, Mabasa L, Erasmus M, Louw J, et al. Diet-induced hypothalamic dysfunction and metabolic disease, and the therapeutic potential of polyphenols. Molecular Metabolism. 2019;27:1.
32. Williams LM. Hypothalamic dysfunction in obesity. Proceedings of the Nutrition Society. 2012;71(4):521-33.
33. Chambers AP, Woods SC. The role of neuropeptide Y in energy homeostasis. Appetite Control: Springer; 2012. p. 23-45.
34. Sun L, Ma L, Ma Y, Zhang F, Zhao C, Nie Y. Insights into the role of gut microbiota in obesity:

pathogenesis, mechanisms, and therapeutic perspectives. Protein & Cell. 2018;9(5):397-403.

35. Walle T, Ta N, Kawamori T, Wen X, Tsuji PA, Walle UK. Cancer chemopreventive properties of orally bioavailable flavonoids—methylated versus unmethylated flavones. Biochemical Pharmacology. 2007;73(9):1288-96.

36. Li S, Lo C-Y, Ho C-T. Hydroxylated polymethoxyflavones and methylated flavonoids in sweet orange (Citrus sinensis) peel. Journal of Agricultural and Food Chemistry. 2006;54(12):4176-85.

37. Li S, Wang Z, Sang S, Huang MT, Ho CT. Identification of nobiletin metabolites in mouse urine. Molecular Nutrition & Food Research. 2006;50(3):291-9.

38. Li S, Sang S, Pan M-H, Lai C-S, Lo C-Y, Yang CS, et al. Anti-inflammatory property of the urinary metabolites of nobiletin in mouse. Bioorganic & Medicinal Chemistry Letters. 2007;17(18):5177-81.

39. Cheng Z, Surichan S, Ruparelia K, Arroo R, Boarder M. Tangeretin and its metabolite 4′-hydroxytetramethoxyflavone attenuate EGF-stimulated cell cycle progression in hepatocytes; role of inhibition at the level of mTOR/p70S6K. British Journal of Pharmacology. 2011;162(8):1781-91.

40. Li Y, Xiao H, McClements DJ. Encapsulation and delivery of crystalline hydrophobic nutraceuticals using nanoemulsions: Factors affecting polymethoxyflavone solubility. Food Biophysics. 2012;7(4):341-53.

41. Sun G, Lei L, Chen H, Li B, Cao Y, Li Y. Tailoring of structured hydroxypropyl methylcellulose-stabilized emulsions for encapsulation of nobiletin: modification of the oil and aqueous phases. Food & Function. 2018;9(7):3657-64.

42. Wan J, Li D, Song R, Shah BR, Li B, Li Y. Enhancement of physical stability and bioaccessibility of tangeretin by soy protein isolate addition. Food Chemistry. 2017;221:760-70.

43. Xiao J, Zhao Y, Wang H, Yuan Y, Yang F, Zhang C, et al. Non-covalent interaction of dietary polyphenols with total plasma proteins of type II diabetes: molecular structure/property–affinity relationships. Integrative Biology. 2011;3(11):1087-94.

44. Shimada T, Tanaka K, Takenaka S, Murayama N, Martin MV, Foroozesh MK, et al. Structure−function relationships of inhibition of human cytochromes P450 1A1, 1A2, 1B1, 2C9, and 3A4 by 33 flavonoid derivatives. Chemical Research in Toxicology. 2010;23(12):1921-35.

45. Tsuji PA, Stephenson KK, Wade KL, Liu H, Fahey JW. Structure-activity analysis of flavonoids: direct and indirect antioxidant, and antiinflammatory potencies and toxicities. Nutrition and Cancer. 2013;65(7):1014-25.

46. Verhoeckx K, Cotter P, López-Expósito I, Kleiveland C, Lea T, Mackie A, et al. The Impact of Food Bioactives on Health: in vitro and ex vivo models: Springer; 2015.

47. Ting Y, Zhao Q, Xia C, Huang Q. Using in vitro and in vivo models to evaluate the oral bioavailability of nutraceuticals. Journal of Agricultural and Food Chemistry. 2015;63(5):1332-8.

48. Martens EC, Neumann M, Desai MS. Interactions of commensal and pathogenic microorganisms with the intestinal mucosal barrier. Nature Reviews Microbiology. 2018;16(8):457-70.

49. Oteiza P, Fraga CG, Mills D, Taft D. Flavonoids and the gastrointestinal tract: Local and systemic effects. Molecular Aspects of Medicine. 2018;61:41-9.

50. Ting Y, Jiang Y, Ho C-T, Huang Q. Common delivery systems for enhancing in vivo bioavailability

and biological efficacy of nutraceuticals. Journal of Functional Foods. 2014;7:112-28.

51. McClements DJ, Li F, Xiao H. The nutraceutical bioavailability classification scheme: classifying nutraceuticals according to factors limiting their oral bioavailability. Annual Review of Food Science and Technology. 2015;6:299-327.

52. Hung WL, Chang WS, Lu WC, Wei GJ, Wang Y, Ho CT, et al. Pharmacokinetics, bioavailability, tissue distribution and excretion of tangeretin in rat. Journal of Food & Drug Analysis. 2018;26(2):849-57.

53. Teng H, Chen L. Polyphenols and bioavailability: an update. Critical Reviews in Food Science and Nutrition. 2019;59(13):2040-51.

54. Lambert JD, Hong J, Kim DH, Mishin VM, Yang CS. Piperine enhances the bioavailability of the tea polyphenol (−)-epigallocatechin-3-gallate in mice. The Journal of Nutrition. 2004;134(8):1948-52.

55. Manthey JA, Cesar TB, Jackson E, Mertens-Talcott S. Pharmacokinetic study of nobiletin and tangeretin in rat serum by high-performance liquid chromatography− electrospray ionization− mass spectrometry. Journal of Agricultural and Food Chemistry. 2011;59(1):145-51.

56. Chen J, Zheng J, Decker EA, McClements DJ, Xiao H. Improving nutraceutical bioavailability using mixed colloidal delivery systems: lipid nanoparticles increase tangeretin bioaccessibility and absorption from tangeretin-loaded zein nanoparticles. Rsc Advances. 2015;5(90):73892-900.

57. Chen J, Zheng J, McClements DJ, Xiao H. Tangeretin-loaded protein nanoparticles fabricated from zein/β-lactoglobulin: Preparation, characterization, and functional performance. Food Chemistry. 2014;158:466-72.

58. Yang Y, Zhao C, Chen J, Tian G, McClements DJ, Xiao H, et al. Encapsulation of polymethoxyflavones in citrus oil emulsion-based delivery systems. Journal of Agricultural and Food Chemistry. 2017;65(8):1732-9.

59. Ting Y, Jiang Y, Lan Y, Xia C, Lin Z, Rogers MA, et al. Viscoelastic emulsion improved the bioaccessibility and oral bioavailability of crystalline compound: A mechanistic study using in vitro and in vivo models. Molecular Pharmaceutics. 2015;12(7):2229-36.

60. Ting Y, Xia Q, Li S, Ho C-T, Huang Q. Design of high-loading and high-stability viscoelastic emulsions for polymethoxyflavones. Food Research International. 2013;54(1):633-40.

61. Lu X, Zhang H, Zheng T, Liu Q, Zhu J, Huang Q. Evaluation of Oral Bioaccessibility of Aged Citrus Peel Extracts Encapsulated in Different Lipid-Based Systems: A Comparison Study Using Different in Vitro Digestion Models. Journal of Agricultural and Food Chemistry. 2020;68(1):97-105.

62. Chen H, An Y, Yan X, McClements DJ, Li B, Li Y. Designing self-nanoemulsifying delivery systems to enhance bioaccessibility of hydrophobic bioactives (nobiletin): Influence of hydroxypropyl methylcellulose and thermal processing. Food Hydrocolloids. 2015;51:395-404.

63. Chou Y-C, Li S, Ho C-T, Pan M-H. Preparation and evaluation of self-microemulsifying delivery system containing 5-demethyltangeretin on inhibiting xenograft tumor growth in mice. International Journal of Pharmaceutics. 2020;579:119134.

64. Onoue S, Nakamura T, Uchida A, Ogawa K, Yuminoki K, Hashimoto N, et al. Physicochemical and biopharmaceutical characterization of amorphous solid dispersion of nobiletin, a citrus

polymethoxylated flavone, with improved hepatoprotective effects. European Journal of Pharmaceutical Sciences. 2013;49(4):453-60.

65. Onoue S, Uchida A, Takahashi H, Seto Y, Kawabata Y, Ogawa K, et al. Development of high-energy amorphous solid dispersion of nanosized nobiletin, a citrus polymethoxylated flavone, with improved oral bioavailability. Journal of Pharmaceutical Sciences. 2011;100(9):3793-801.

66. Ting Y, Chiou Y-S, Pan M-H, Ho C-T, Huang Q. In vitro and in vivo anti-cancer activity of tangeretin against colorectal cancer was enhanced by emulsion-based delivery system. Journal of Functional Foods. 2015;15:264-73.

67. Zhao L. The gut microbiota and obesity: from correlation to causality. Nature Reviews Microbiology. 2013;11(9):639.

68. Van Duynhoven J, Vaughan EE, Jacobs DM, Kemperman RA, Van Velzen EJ, Gross G, et al. Metabolic fate of polyphenols in the human superorganism. Proceedings of the National Academy of Sciences. 2011;108(Supplement 1):4531-8.

69. Liu J, He Z, Ma N, Chen Z-Y. Beneficial effects of dietary polyphenols on high-fat diet-induced obesity linking with modulation of gut microbiota. Journal of Agricultural and Food Chemistry. 2019;68(1):33-47.

70. Yao X, Zhu X, Pan S, Fang Y, Jiang F, Phillips GO, et al. Antimicrobial activity of nobiletin and tangeretin against Pseudomonas. Food Chemistry. 2012;132(4):1883-90.

71. Barreca D, Bisignano C, Ginestra G, Bisignano G, Bellocco E, Leuzzi U, et al. Polymethoxylated, C- and O-glycosyl flavonoids in tangelo (Citrus reticulata× Citrus paradisi) juice and their influence on antioxidant properties. Food Chemistry. 2013;141(2):1481-8.

72. Tung Y-C, Chang W-T, Li S, Wu J-C, Badmeav V, Ho C-T, et al. Citrus peel extracts attenuated obesity and modulated gut microbiota in mice with high-fat diet-induced obesity. Food & Function. 2018.

73. Zhang M, Zhu J, Zhang X, Zhao D, Ma Y, Li D, et al. Aged citrus peel (chenpi) extract causes dynamic alteration of colonic microbiota in high-fat diet induced obese mice. Food & Function. 2020;11(3):2667-78.

74. Zeng S-L, Li S-Z, Xiao P-T, Cai Y-Y, Chu C, Chen B-Z, et al. Citrus polymethoxyflavones attenuate metabolic syndrome by regulating gut microbiome and amino acid metabolism. Science Advances. 2020;6(1):eaax6208.

75. Selma MV, Espin JC, Tomas-Barberan FA. Interaction between phenolics and gut microbiota: role in human health. Journal of Agricultural and Food Chemistry. 2009;57(15):6485-501.

76. Burapan S, Kim M, Han J. Demethylation of polymethoxyflavones by human gut bacterium, Blautia sp. MRG-PMF1. Journal of Agricultural and Food Chemistry. 2017;65(8):1620-9.

77. Chiou Y-S, Wu J-C, Huang Q, Shahidi F, Wang Y-J, Ho C-T, et al. Metabolic and colonic microbiota transformation may enhance the bioactivities of dietary polyphenols. Journal of Functional Foods. 2014;7:3-25.

78. Zheng J, Bi J, Johnson D, Sun Y, Song M, Qiu P, et al. Analysis of 10 metabolites of polymethoxyflavones with high sensitivity by electrochemical detection in high-performance liquid

chromatography. Journal of Agricultural and Food Chemistry. 2015;63(2):509-16.

79. Chiou Y-S, Zheng Y-N, Tsai M-L, Lai C-S, Ho C-T, Pan M-H. 5-Demethylnobiletin more potently inhibits colon cancer cell growth than nobiletin in vitro and in vivo. Journal of Food Bioactives. 2018;2:91–7-–7.

80. Kim M, Kim N, Han J. Metabolism of Kaempferia parviflora polymethoxyflavones by human intestinal bacterium Bautia sp. MRG-PMF1. Journal of Agricultural and Food Chemistry. 2014;62(51):12377-83.

81. Wu X, Song M, Wang M, Zheng J, Gao Z, Xu F, et al. Chemopreventive effects of nobiletin and its colonic metabolites on colon carcinogenesis. Molecular Nutrition & Food Research. 2015;59(12):2383-94.

82. Song M, Lan Y, Wu X, Han Y, Wang M, Zheng J, et al. Chemopreventive effect of 5-demethylnobiletin, a unique citrus flavonoid on colitis-driven colorectal carcinogenesis in mice is associated with its colonic metabolites. Food & Function. 2020.

83. Guo S, Wu X, Zheng J, Charoensinphon N, Dong P, Qiu P, et al. Anti-inflammatory effect of xanthomicrol, a major colonic metabolite of 5-demethyltangeretin. Food & Function. 2018;9(6):3104-13.

84. Salaritabar A, Darvishi B, Hadjiakhoondi F, Manayi A, Sureda A, Nabavi SF, et al. Therapeutic potential of flavonoids in inflammatory bowel disease: A comprehensive review. World Journal of Gastroenterology. 2017;23(28):5097.

85. Xiong Y, Chen D, Yu C, Lv B, Peng J, Wang J, et al. Citrus nobiletin ameliorates experimental colitis by reducing inflammation and restoring impaired intestinal barrier function. Molecular Nutrition & Food Research. 2015;59(5):829-42.

86. Wen X, Zhao H, Wang L, Wang L, DU G, Guan W, et al. Nobiletin Attenuates DSS-Induced Intestinal Barrier Damage through HNF4α-claudin-7 Signaling Pathway. Journal of Agricultural and Food Chemistry. 2020.

87. Eun S-H, Woo J-T, Kim D-H. Tangeretin inhibits IL-12 expression and NF-κB activation in dendritic cells and attenuates colitis in mice. Planta Medica. 2017;234(06):527-33.

88. Xiong Y-j, Deng Z-b, Liu J-n, Qiu J-j, Guo L, Feng P-p, et al. Enhancement of epithelial cell autophagy induced by sinensetin alleviates epithelial barrier dysfunction in colitis. Pharmacological Research. 2019;148:104461.

89. Hagenlocher Y, Feilhauer K, Schäffer M, Bischoff SC, Lorentz A. Citrus peel polymethoxyflavones nobiletin and tangeretin suppress LPS-and IgE-mediated activation of human intestinal mast cells. European Journal of Nutrition. 2017;56(4):1609-20.

90. Hagenlocher Y, Gommeringer S, Held A, Feilhauer K, Köninger J, Bischoff SC, et al. Nobiletin acts anti-inflammatory on murine IL-10−/− colitis and human intestinal fibroblasts. European Journal of Nutrition. 2019;58(4):1391-401.

91. Cani PD, Amar J, Iglesias MA, Poggi M, Knauf C, Bastelica D, et al. Metabolic endotoxemia initiates obesity and insulin resistance. Diabetes. 2007;56(7):1761-72.

92. Louis P, Hold GL, Flint HJ. The gut microbiota, bacterial metabolites and colorectal cancer. Nature

Reviews Microbiology. 2014;12(10):661.
93. Nohara K, Nemkov T, D'Alessandro A, Yoo S-H, Chen Z. Coordinate regulation of cholesterol and bile acid metabolism by the clock modifier nobiletin in metabolically challenged old mice. International Journal of Molecular Sciences. 2019;20(17):4281.
94. Wu JC, Tsai ML, Lai CS, Lo CY, Ho CT, Wang YJ, et al. Polymethoxyflavones prevent benzo [a] pyrene/dextran sodium sulfate-induced colorectal carcinogenesis through modulating xenobiotic metabolism and ameliorate autophagic defect in ICR mice. International Journal of Cancer. 2018;142(8):1689-701.
95. König J, Wells J, Cani PD, García-Ródenas CL, MacDonald T, Mercenier A, et al. Human intestinal barrier function in health and disease. Clinical and Translational Gastroenterology. 2016;7(10):e196.
96. He W, Liu M, Li Y, Yu H, Wang D, Chen Q, et al. Flavonoids from Citrus aurantium ameliorate TNBS-induced ulcerative colitis through protecting colonic mucus layer integrity. European Journal of Pharmacology. 2019;857:172456.
97. Zhang L, Zhao H, Zhang X, Chen L, Zhao X, Bai X, et al. Nobiletin protects against cerebral ischemia via activating the p-Akt, p-CREB, BDNF and Bcl-2 pathway and ameliorating BBB permeability in rat. Brain Research Bulletin. 2013;96:45-53.
98. Cani PD, Possemiers S, Van de Wiele T, Guiot Y, Everard A, Rottier O, et al. Changes in gut microbiota control inflammation in obese mice through a mechanism involving GLP-2-driven improvement of gut permeability. Gut. 2009;58(8):1091-103.
99. Everard A, Belzer C, Geurts L, Ouwerkerk JP, Druart C, Bindels LB, et al. Cross-talk between Akkermansia muciniphila and intestinal epithelium controls diet-induced obesity. Proceedings of the National Academy of Sciences. 2013;110(22):9066-71.
100. Wang Z, Zhao Y. Gut microbiota derived metabolites in cardiovascular health and disease. Protein & Cell. 2018:1-16.
101. Gonçalves P, Araújo JR, Di Santo JP. A cross-talk between microbiota-derived short-chain fatty acids and the host mucosal immune system regulates intestinal homeostasis and inflammatory bowel disease. Inflammatory Bowel Diseases. 2018;24(3):558-72.
102. Gloston GF, Yoo S-H, Chen ZJ. Clock-enhancing small molecules and potential applications in chronic diseases and aging. Frontiers in Neurology. 2017;8:100.
103. Takahashi JS, Hong H-K, Ko CH, McDearmon EL. The genetics of mammalian circadian order and disorder: implications for physiology and disease. Nature Reviews Genetics. 2008;9(10):764-75.
104. Asher G, Sassone-Corsi P. Time for food: the intimate interplay between nutrition, metabolism, and the circadian clock. Cell. 2015;161(1):84-92.
105. Paschos GK. Circadian clocks, feeding time, and metabolic homeostasis. Frontiers in Pharmacology. 2015;6:112.
106. He B, Nohara K, Park N, Park Y-S, Guillory B, Zhao Z, et al. The small molecule nobiletin targets the molecular oscillator to enhance circadian rhythms and protect against metabolic syndrome. Cell Metabolism. 2016;23(4):610-21.
107. Qi G, Guo R, Tian H, Li L, Liu H, Mi Y, et al. Nobiletin protects against insulin resistance and

disorders of lipid metabolism by reprogramming of circadian clock in hepatocytes. Biochimica et Biophysica Acta (BBA)-Molecular and Cell Biology of Lipids. 2018;1863(6):549-62.
108. Bass J, Takahashi JS. Circadian integration of metabolism and energetics. Science. 2010;330(6009):1349-54.
109. Panda S, Antoch MP, Miller BH, Su AI, Schook AB, Straume M, et al. Coordinated transcription of key pathways in the mouse by the circadian clock. Cell. 2002;109(3):307-20.
110. Bass J. Circadian topology of metabolism. Nature. 2012;491(7424):348-56.
111. Guarente L, editor Sirtuins, aging, and metabolism. Cold Spring Harbor symposia on quantitative biology; 2011: Cold Spring Harbor Laboratory Press.
112. Masri S, Rigor P, Cervantes M, Ceglia N, Sebastian C, Xiao C, et al. Partitioning circadian transcription by SIRT6 leads to segregated control of cellular metabolism. Cell. 2014;158(3):659-72.
113. Liu C, Li S, Liu T, Borjigin J, Lin JD. Transcriptional coactivator PGC-1α integrates the mammalian clock and energy metabolism. Nature. 2007;447(7143):477-81.
114. Lamia KA, Sachdeva UM, DiTacchio L, Williams EC, Alvarez JG, Egan DF, et al. AMPK regulates the circadian clock by cryptochrome phosphorylation and degradation. Science. 2009;326(5951):437-40.
115. Hussain MM. Regulation of intestinal lipid absorption by clock genes. Annual Review of Nutrition. 2014;34:357-75.
116. Leone V, Gibbons SM, Martinez K, Hutchison AL, Huang EY, Cham CM, et al. Effects of diurnal variation of gut microbes and high-fat feeding on host circadian clock function and metabolism. Cell Host & Microbe. 2015;17(5):681-9.
117. Thaiss CA, Zeevi D, Levy M, Zilberman-Schapira G, Suez J, Tengeler AC, et al. Transkingdom control of microbiota diurnal oscillations promotes metabolic homeostasis. Cell. 2014;159(3):514-29.
118. Shinozaki A, Misawa K, Ikeda Y, Haraguchi A, Kamagata M, Tahara Y, et al. Potent effects of flavonoid nobiletin on amplitude, period, and phase of the circadian clock rhythm in PER2:: LUCIFERASE mouse embryonic fibroblasts. PloS One. 2017;12(2):e0170904.
119. Petrenko V, Gandasi NR, Sage D, Tengholm A, Barg S, Dibner C. In pancreatic islets from type 2 diabetes patients, the dampened circadian oscillators lead to reduced insulin and glucagon exocytosis. Proceedings of the National Academy of Sciences. 2020;117(5):2484-95.
120. Petrenko V, Saini C, Giovannoni L, Gobet C, Sage D, Unser M, et al. Pancreatic α-and β-cellular clocks have distinct molecular properties and impact on islet hormone secretion and gene expression. Genes & Development. 2017;31(4):383-98.
121. Yoshida I, Kumagai M, Ide M, Horigome S, Takahashi Y, Mishima T, et al. Polymethoxyflavones in black ginger (Kaempferia parviflora) regulate the expression of circadian clock genes. Journal of Functional Foods. 2020;68:103900.
122. Nohara K, Mallampalli V, Nemkov T, Wirianto M, Yang J, Ye Y, et al. Nobiletin fortifies mitochondrial respiration in skeletal muscle to promote healthy aging against metabolic challenge. Nature Communications. 2019;10(1):1-15.
123. Le Martelot G, Claudel T, Gatfield D, Schaad O, Kornmann B, Sasso GL, et al. REV-ERBα participates in circadian SREBP signaling and bile acid homeostasis. PLoS Biol. 2009;7(9):e1000181.

124. Takeda Y, Kang HS, Lih FB, Jiang H, Blaner WS, Jetten AM. Retinoid acid-related orphan receptor γ, RORγ, participates in diurnal transcriptional regulation of lipid metabolic genes. Nucleic Acids Research. 2014;42(16):10448-59.
125. Solt LA, Kojetin DJ, Burris TP. The REV-ERBs and RORs: molecular links between circadian rhythms and lipid homeostasis. Future Medicinal Chemistry. 2011;3(5):623-38.
126. Mulvihill EE, Huff MW. Protection from metabolic dysregulation, obesity, and atherosclerosis by citrus flavonoids: activation of hepatic PGC1α-mediated fatty acid oxidation. PPAR Research. 2012;2012.
127. Li RW, Theriault AG, Au K, Douglas TD, Casaschi A, Kurowska EM, et al. Citrus polymethoxylated flavones improve lipid and glucose homeostasis and modulate adipocytokines in fructose-induced insulin resistant hamsters. Life Sciences. 2006;79(4):365-73.
128. Mulvihill EE, Assini JM, Lee JK, Allister EM, Sutherland BG, Koppes JB, et al. Nobiletin attenuates VLDL overproduction, dyslipidemia, and atherosclerosis in mice with diet-induced insulin resistance. Diabetes. 2011;60(5):1446-57.
129. Kim YJ, Choi MS, Woo JT, Jeong MJ, Kim SR, Jung UJ. Long-term dietary supplementation with low-dose nobiletin ameliorates hepatic steatosis, insulin resistance, and inflammation without altering fat mass in diet-induced obesity. Molecular Nutrition & Food Research. 2017;61(8):1600889.
130. Feng K, Lan Y, Zhu X, Li J, Chen T, Huang Q, et al. Hepatic Lipidomics Analysis Reveals the Anti-obesity and Cholesterol-lowering Effects of Tangeretin in High-Fat Diet-Fed Rats. Journal of Agricultural and Food Chemistry. 2020.
131. Feng K, Zhu X, Chen T, Peng B, Lu M, Zheng H, et al. Prevention of obesity and hyperlipidemia by heptamethoxyflavone in high-fat diet-induced rats. Journal of Agricultural and Food Chemistry. 2019;67(9):2476-89.
132. Tsutsumi R, Yoshida T, Nii Y, Okahisa N, Iwata S, Tsukayama M, et al. Sudachitin, a polymethoxylated flavone, improves glucose and lipid metabolism by increasing mitochondrial biogenesis in skeletal muscle. Nutrition & Metabolism. 2014;11(1):32.
133. Choi Y, Kim Y, Ham H, Park Y, Jeong H-S, Lee J. Nobiletin suppresses adipogenesis by regulating the expression of adipogenic transcription factors and the activation of AMP-activated protein kinase (AMPK). Journal of Agricultural and Food Chemistry. 2011;59(24):12843-9.
134. Tung Y-C, Hsieh P-H, Pan M-H, Ho C-T. Cellular models for the evaluation of the antiobesity effect of selected phytochemicals from food and herbs. Journal of Food and Drug Analysis. 2017;25(1):100-10.
135. Sawamoto A, Nakanishi M, Okuyama S, Furukawa Y, Nakajima M. Heptamethoxyflavone inhibits adipogenesis via enhancing PKA signaling. European Journal of Pharmacology. 2019;865:172758.
136. Guo J, Cao Y, Ho C-T, Jin S, Huang Q. Aged citrus peel (chenpi) extract reduces lipogenesis in differentiating 3T3-L1 adipocytes. Journal of Functional Foods. 2017;34:297-303.
137. Lai C-S, Ho M-H, Tsai M-L, Li S, Badmaev V, Ho C-T, et al. Suppression of adipogenesis and obesity in high-fat induced mouse model by hydroxylated polymethoxyflavones. Journal of Agricultural and Food Chemistry. 2013;61(43):10320-8.

138. Lone J, Parray HA, Yun JW. Nobiletin induces brown adipocyte-like phenotype and ameliorates stress in 3T3-L1 adipocytes. Biochimie. 2018;146:97-104.
139. Yasunaga S, Domen M, Nishi K, Kadota A, Sugahara T. Nobiletin suppresses monocyte chemoattractant protein-1 (MCP-1) expression by regulating MAPK signaling in 3T3-L1 cells. Journal of Functional Foods. 2016;27:406-15.
140. Nagarajan SR, Paul-Heng M, Krycer JR, Fazakerley DJ, Sharland AF, Hoy AJ. Lipid and glucose metabolism in hepatocyte cell lines and primary mouse hepatocytes: a comprehensive resource for in vitro studies of hepatic metabolism. American Journal of Physiology-Endocrinology and Metabolism. 2019;316(4):E578-E89.
141. Kurowska EM, Manthey JA, Casaschi A, Theriault AG. Modulation of HepG2 cell net apolipoprotein B secretion by the citrus polymethoxyflavone, tangeretin. Lipids. 2004;39(2):143-51.
142. Nichols LA, Jackson DE, Manthey JA, Shukla SD, Holland LJ. Citrus flavonoids repress the mRNA for stearoyl-CoA desaturase, a key enzyme in lipid synthesis and obesity control, in rat primary hepatocytes. Lipids in Health and Disease. 2011;10(1):36.
143. Morin B, Nichols LA, Zalasky KM, Davis JW, Manthey JA, Holland LJ. The citrus flavonoids hesperetin and nobiletin differentially regulate low density lipoprotein receptor gene transcription in HepG2 liver cells. The Journal of Nutrition. 2008;138(7):1274-81.
144. Mahmoud AM, Hernandez Bautista RJ, Sandhu MA, Hussein OE. Beneficial effects of citrus flavonoids on cardiovascular and metabolic health. Oxidative Medicine and Cellular Longevity. 2019;2019.
145. Bornfeldt KE, Tabas I. Insulin resistance, hyperglycemia, and atherosclerosis. Cell Metabolism. 2011;14(5):575-85.
146. Lee Y-S, Cha B-Y, Saito K, Yamakawa H, Choi S-S, Yamaguchi K, et al. Nobiletin improves hyperglycemia and insulin resistance in obese diabetic ob/ob mice. Biochemical Pharmacology. 2010;79(11):1674-83.
147. Govers R. Cellular regulation of glucose uptake by glucose transporter GLUT4. Advances in Clinical chemistry. 2014;66:173-240.
148. Kim MS, Hur HJ, Kwon DY, Hwang J-T. Tangeretin stimulates glucose uptake via regulation of AMPK signaling pathways in C2C12 myotubes and improves glucose tolerance in high-fat diet-induced obese mice. Molecular and Cellular Endocrinology. 2012;358(1):127-34.
149. Ruiz-Vargas JA, Morales-Ferra DL, Ramírez-Ávila G, Zamilpa A, Negrete-León E, Acevedo-Fernández JJ, et al. α-Glucosidase inhibitory activity and in vivo antihyperglycemic effect of secondary metabolites from the leaf infusion of Ocimum campechianum mill. Journal of Ethnopharmacology. 2019;243:112081.
150. Guo J, Tao H, Cao Y, Ho C-T, Jin S, Huang Q. Prevention of obesity and type 2 diabetes with aged citrus peel (Chenpi) extract. Journal of Agricultural and Food Chemistry. 2016;64(10):2053-61.
151. Lee Y-S, Cha B-Y, Choi S-S, Choi B-K, Yonezawa T, Teruya T, et al. Nobiletin improves obesity and insulin resistance in high-fat diet-induced obese mice. The Journal of Nutritional Biochemistry. 2013;24(1):156-62.

152. Sundaram R, Shanthi P, Sachdanandam P. Tangeretin, a polymethoxylated flavone, modulates lipid homeostasis and decreases oxidative stress by inhibiting NF-κB activation and proinflammatory cytokines in cardiac tissue of streptozotocin-induced diabetic rats. Journal of Functional Foods. 2015;16:315-33.
153. Sundaram R, Shanthi P, Sachdanandam P. Effect of tangeretin, a polymethoxylated flavone on glucose metabolism in streptozotocin-induced diabetic rats. Phytomedicine. 2014;21(6):793-9.
154. Judy W, Stogsdill W, Judy D, Judy J, Sharma P, Evans M, et al. Efficacy of Diabetinol™ on glycemic control in insulin resistant hamsters and subjects with impaired fasting glucose–a pilot study. Journal of Functional Foods. 2010;2(3):171-8.
155. Evans M, Sharma P, Guthrie N. Bioavailability of citrus polymethoxylated flavones and their biological role in metabolic syndrome and hyperlipidemia. Readings in Advanced Pharmacokinetics-Theory, Methods and Applications: IntechOpen; 2012.
156. Kang S-I, Shin H-S, Kim H-M, Hong Y-S, Yoon S-A, Kang S-W, et al. Immature Citrus sunki peel extract exhibits antiobesity effects by β-oxidation and lipolysis in high-fat diet-induced obese mice. Biological and Pharmaceutical Bulletin. 2012;35(2):223-30.
157. Kou G, Hu Y, Jiang Z, Li Z, Li P, Song H, et al. Citrus aurantium L. polymethoxyflavones promote thermogenesis of brown and white adipose tissue in high-fat diet induced C57BL/6J mice. Journal of Functional Foods. 2020;67:103860.
158. Morrow NM, Burke AC, Samsoondar JP, Seigel KE, Wang A, Telford DE, et al. The citrus flavonoid nobiletin confers protection from metabolic dysregulation in high-fat-fed mice independent of AMPK. Journal of Lipid Research. 2020;61(3):387-402.
159. Tung Y-C, Li S, Huang Q, Hung W-L, Ho C-T, Wei G-J, et al. 5-Demethylnobiletin and 5-Acetoxy-6, 7, 8, 3′, 4′-pentamethoxyflavone Suppress Lipid Accumulation by Activating the LKB1-AMPK Pathway in 3T3-L1 Preadipocytes and High Fat Diet-Fed C57BL/6 Mice. Journal of Agricultural and Food Chemistry. 2016;64(16):3196-205.
160. Sonnenburg JL, Bäckhed F. Diet–microbiota interactions as moderators of human metabolism. Nature. 2016;535(7610):56.
161. Brown JM, Hazen SL. Microbial modulation of cardiovascular disease. Nature Reviews Microbiology. 2018;16(3):171-81.
162. Mulvihill EE, Burke AC, Huff MW. Citrus flavonoids as regulators of lipoprotein metabolism and atherosclerosis. Annual Review of Nutrition. 2016;36:275-99.
163. Jayachandran M, Chung SSM, Xu B. A critical review on diet-induced microbiota changes and cardiovascular diseases. Critical Reviews in Food Science and Nutrition. 2019:1-12.
164. Whitman SC, Kurowska EM, Manthey JA, Daugherty A. Nobiletin, a citrus flavonoid isolated from tangerines, selectively inhibits class A scavenger receptor-mediated metabolism of acetylated LDL by mouse macrophages. Atherosclerosis. 2005;178(1):25-32.
165. Yen JH, Weng CY, Li S, Lo YH, Pan MH, Fu SH, et al. Citrus flavonoid 5-demethylnobiletin suppresses scavenger receptor expression in THP-1 cells and alters lipid homeostasis in HepG2 liver cells. Molecular Nutrition & Food Research. 2011;55(5):733-48.

166. Eguchi A, Murakami A, Li S, Ho CT, Ohigashi H. Suppressive effects of demethylated metabolites of nobiletin on phorbol ester-induced expression of scavenger receptor genes in THP-1 human monocytic cells. Biofactors. 2007;31(2):107-16.
167. Kou M-C, Fu S-H, Yen J-H, Weng C-Y, Li S, Ho C-T, et al. Effects of citrus flavonoids, 5-hydroxy-3, 6, 7, 8, 3′, 4′-hexamethoxyflavone and 3, 5, 6, 7, 8, 3′, 4′-heptamethoxyflavone, on the activities of macrophage scavenger receptors and the hepatic LDL receptor. Food & Function. 2013;4(4):602-9.
168. Seo J, Lee HS, Ryoo S, Seo JH, Min B-S, Lee J-H. Tangeretin, a citrus flavonoid, inhibits PGDF-BB-induced proliferation and migration of aortic smooth muscle cells by blocking AKT activation. European Journal of Pharmacology. 2011;673(1-3):56-64.
169. Chiangsaen P, Maneesai P, Kukongviriyapan U, Tong-un T, Ishida W, Prachaney P, et al. Tangeretin ameliorates erectile and testicular dysfunction in a rat model of hypertension. Reproductive Toxicology. 2020.
170. Vaiyapuri S, Ali MS, Moraes LA, Sage T, Lewis KR, Jones CI, et al. Tangeretin regulates platelet function through inhibition of phosphoinositide 3-kinase and cyclic nucleotide signaling. Arteriosclerosis, Thrombosis, and Vascular Biology. 2013;33(12):2740-9.
171. Vaiyapuri S, Roweth H, Ali MS, Unsworth AJ, Stainer AR, Flora GD, et al. Pharmacological actions of nobiletin in the modulation of platelet function. British Journal of Pharmacology. 2015;172(16):4133-45.
172. Mayerhofer CC, Ueland T, Broch K, Vincent RP, Cross GF, Dahl CP, et al. Increased secondary/primary bile acid ratio in chronic heart failure. Journal of Cardiac Failure. 2017;23(9):666-71.
173. Chen P-Y, Li S, Koh Y-C, Wu J-C, Yang M-J, Ho C-T, et al. Oolong tea extract and citrus peel polymethoxyflavones reduce transformation of L-Carnitine to trimethylamine-N-oxide and decrease vascular inflammation in L-Carnitine feeding mice. Journal of Agricultural and Food Chemistry. 2019;67(28):7869-79.
174. Yang G, Lin C-C, Yuan L, Wang P, Yang Y, Wen X, et al. Nobiletin prevents TMAO-induced vascular oxidative stress in rats. Journal of Food Bioactives. 2019;5:131–5-–5.
175. Tang WW, Wang Z, Levison BS, Koeth RA, Britt EB, Fu X, et al. Intestinal microbial metabolism of phosphatidylcholine and cardiovascular risk. New England Journal of Medicine. 2013;368(17):1575-84.
176. Brown JM, Hazen SL. The gut microbial endocrine organ: bacterially derived signals driving cardiometabolic diseases. Annual Review of Medicine. 2015;66:343-59.
177. Lai C-S, Wu J-C, Pan M-H. Molecular mechanism on functional food bioactives for anti-obesity. Current Opinion in Food Science. 2015;2:9-13.
178. González-Castejón M, Rodriguez-Casado A. Dietary phytochemicals and their potential effects on obesity: a review. Pharmacological Research. 2011;64(5):438-55.
179. Mohamed S. Functional foods against metabolic syndrome (obesity, diabetes, hypertension and dyslipidemia) and cardiovasular disease. Trends in Food Science & Technology. 2014;35(2):114-28.
180. Pan MH, Yang G, Li S, Li MY, Tsai ML, Wu JC, et al. Combination of citrus polymethoxyflavones, green tea polyphenols, and Lychee extracts suppresses obesity and hepatic steatosis in high-fat diet

induced obese mice. Molecular Nutrition & Food Research. 2017;61(11):1601104.
181. Ho S-C, Lin C-C. Investigation of heat treating conditions for enhancing the anti-inflammatory activity of citrus fruit (Citrus reticulata) peels. Journal of Agricultural and Food Chemistry. 2008;56(17):7976-82.
182. Qiu P, Dong P, Guan H, Li S, Ho CT, Pan MH, et al. Inhibitory effects of 5-hydroxy polymethoxyflavones on colon cancer cells. Molecular Nutrition & Food Research. 2010;54(S2):S244-S52.
183. Flint HJ, Scott KP, Louis P, Duncan SH. The role of the gut microbiota in nutrition and health. Nature reviews Gastroenterology & Hepatology. 2012;9(10):577.
184. Tremaroli V, Bäckhed F. Functional interactions between the gut microbiota and host metabolism. Nature. 2012;489(7415):242.
185. Turnbaugh PJ, Ley RE, Mahowald MA, Magrini V, Mardis ER, Gordon JI. An obesity-associated gut microbiome with increased capacity for energy harvest. Nature. 2006;444(7122):1027.
186. Ley RE, Turnbaugh PJ, Klein S, Gordon JI. Microbial ecology: human gut microbes associated with obesity. Nature. 2006;444(7122):1022.
187. Ravussin Y, Koren O, Spor A, LeDuc C, Gutman R, Stombaugh J, et al. Responses of gut microbiota to diet composition and weight loss in lean and obese mice. Obesity. 2012;20(4):738-47.
188. Zhang X, Zhao Y, Zhang M, Pang X, Xu J, Kang C, et al. Structural changes of gut microbiota during berberine-mediated prevention of obesity and insulin resistance in high-fat diet-fed rats. PloS One. 2012;7(8):e42529.
189. Zhang X, Zhao Y, Xu J, Xue Z, Zhang M, Pang X, et al. Modulation of gut microbiota by berberine and metformin during the treatment of high-fat diet-induced obesity in rats. Scientific Reports. 2015;5:14405.
190. Roopchand DE, Carmody RN, Kuhn P, Moskal K, Rojas-Silva P, Turnbaugh PJ, et al. Dietary polyphenols promote growth of the gut bacterium Akkermansia muciniphila and attenuate high fat diet-induced metabolic syndrome. Diabetes. 2015:db141916.
191. Collins B, Hoffman J, Martinez K, Grace M, Lila MA, Cockrell C, et al. A polyphenol-rich fraction obtained from table grapes decreases adiposity, insulin resistance and markers of inflammation and impacts gut microbiota in high-fat-fed mice. The Journal of Nutritional Biochemistry. 2016;31:150-65.
192. Chen X-M, Tait AR, Kitts DD. Flavonoid composition of orange peel and its association with antioxidant and anti-inflammatory activities. Food Chemistry. 2017;218:15-21.
193. Kawahata I, Yoshida M, Sun W, Nakajima A, Lai Y, Osaka N, et al. Potent activity of nobiletin-rich Citrus reticulata peel extract to facilitate cAMP/PKA/ERK/CREB signaling associated with learning and memory in cultured hippocampal neurons: identification of the substances responsible for the pharmacological action. Journal of Neural Transmission. 2013;120(10):1397-409.
194. Jin MJ, Kim U, Kim IS, Kim Y, Kim D-H, Han SB, et al. Effects of gut microflora on pharmacokinetics of hesperidin: a study on non-antibiotic and pseudo-germ-free rats. Journal of Toxicology and Environmental Health, Part A. 2010;73(21-22):1441-50.
195. Liu H, Wu B, Pan G, He L, Li Z, Fan M, et al. Metabolism and pharmacokinetics of mangiferin in

conventional rats, pseudo-germ-free rats, and streptozotocin-induced diabetic rats. Drug Metabolism and Disposition. 2012:dmd. 112.045849.
196. Pang X, Hua X, Yang Q, Ding D, Che C, Cui L, et al. Inter-species transplantation of gut microbiota from human to pigs. The ISME journal. 2007;1(2):156.
197. Zhang X, Chen Y, Zhu J, Zhang M, Ho CT, Huang Q, et al. Metagenomics Analysis of Gut Microbiota in a High Fat Diet-Induced Obesity Mouse Model Fed with (-)-Epigallocatechin 3-O-(3-O-Methyl) Gallate (EGCG3''Me). Molecular Nutrition & Food Research. 2018:1800274.
198. Segata N, Izard J, Waldron L, Gevers D, Miropolsky L, Garrett WS, et al. Metagenomic biomarker discovery and explanation. Genome Biology. 2011;12(6):R60.
199. Hsu CL, Yen GC. Phenolic compounds: evidence for inhibitory effects against obesity and their underlying molecular signaling mechanisms. Molecular Nutrition & Food Research. 2008;52(1):53-61.
200. den Besten G, Bleeker A, Gerding A, van Eunen K, Havinga R, van Dijk TH, et al. Short-chain fatty acids protect against high-fat diet-induced obesity via a PPARγ-dependent switch from lipogenesis to fat oxidation. Diabetes. 2015:db141213.
201. Shin N-R, Whon TW, Bae J-W. Proteobacteria: microbial signature of dysbiosis in gut microbiota. Trends in Biotechnology. 2015;33(9):496-503.
202. David LA, Maurice CF, Carmody RN, Gootenberg DB, Button JE, Wolfe BE, et al. Diet rapidly and reproducibly alters the human gut microbiome. Nature. 2014;505(7484):559.
203. Kübeck R, Bonet-Ripoll C, Hoffmann C, Walker A, Müller VM, Schüppel VL, et al. Dietary fat and gut microbiota interactions determine diet-induced obesity in mice. Molecular Metabolism. 2016;5(12):1162-74.
204. Chevre R, Silvestre-Roig C, Soehnlein O. Nutritional Modulation of Innate Immunity: The Fat–Bile–Gut Connection. Trends in Endocrinology & Metabolism. 2018.
205. Devkota S, Chang EB. Interactions between diet, bile acid metabolism, gut microbiota, and inflammatory bowel diseases. Digestive Diseases. 2015;33(3):351-6.
206. Huang F, Zheng X, Ma X, Jiang R, Zhou W, Zhou S, et al. Theabrownin from Pu-erh tea attenuates hypercholesterolemia via modulation of gut microbiota and bile acid metabolism. Nature Communications. 2019;10(1):1-17.
207. Million M, Lagier J-C, Yahav D, Paul M. Gut bacterial microbiota and obesity. Clinical Microbiology and Infection. 2013;19(4):305-13.
208. Schell MA, Karmirantzou M, Snel B, Vilanova D, Berger B, Pessi G, et al. The genome sequence of Bifidobacterium longum reflects its adaptation to the human gastrointestinal tract. Proceedings of the National Academy of Sciences. 2002;99(22):14422-7.
209. Van Hul M, Geurts L, Plovier H, Druart C, Everard A, Ståhlman M, et al. Reduced obesity, diabetes, and steatosis upon cinnamon and grape pomace are associated with changes in gut microbiota and markers of gut barrier. American Journal of Physiology-Endocrinology and Metabolism. 2017;314(4):E334-E52.
210. Anhê FF, Roy D, Pilon G, Dudonné S, Matamoros S, Varin TV, et al. A polyphenol-rich cranberry extract protects from diet-induced obesity, insulin resistance and intestinal inflammation in association

with increased Akkermansia spp. population in the gut microbiota of mice. Gut. 2015;64(6):872-83.
211. Nakajima A, Aoyama Y, Shin E-J, Nam Y, Kim H-C, Nagai T, et al. Nobiletin, a citrus flavonoid, improves cognitive impairment and reduces soluble Aβ levels in a triple transgenic mouse model of Alzheimer's disease (3XTg-AD). Behavioural Brain Research. 2015;289:69-77.
212. Chen G, Xie M, Dai Z, Wan P, Ye H, Zeng X, et al. Kudingcha and Fuzhuan Brick Tea Prevent Obesity and Modulate Gut Microbiota in High-Fat Diet Fed Mice. Molecular Nutrition & Food Research. 2018;62(6):1700485.
213. Koga N, Matsuo M, Ohta C, Haraguchi K, Matsuoka M, Kato Y, et al. Comparative study on nobiletin metabolism with liver microsomes from rats, guinea pigs and hamsters and rat cytochrome P450. Biological and Pharmaceutical Bulletin. 2007;30(12):2317-23.
214. Li S, Pan M-H, Lai C-S, Lo C-Y, Dushenkov S, Ho C-T. Isolation and syntheses of polymethoxyflavones and hydroxylated polymethoxyflavones as inhibitors of HL-60 cell lines. Bioorganic & Medicinal Chemistry. 2007;15(10):3381-9.
215. Saigusa D, Shibuya M, Jinno D, Yamakoshi H, Iwabuchi Y, Yokosuka A, et al. High-performance liquid chromatography with photodiode array detection for determination of nobiletin content in the brain and serum of mice administrated the natural compound. Analytical and Bioanalytical Chemistry. 2011;400(10):3635-41.
216. Singh SP, Tewari D, Patel K, Jain GK. Permeability determination and pharmacokinetic study of nobiletin in rat plasma and brain by validated high-performance liquid chromatography method. Fitoterapia. 2011;82(8):1206-14.
217. Wu GD, Compher C, Chen EZ, Smith SA, Shah RD, Bittinger K, et al. Comparative metabolomics in vegans and omnivores reveal constraints on diet-dependent gut microbiota metabolite production. Gut. 2016;65(1):63-72.
218. Hehemann J-H, Correc G, Barbeyron T, Helbert W, Czjzek M, Michel G. Transfer of carbohydrate-active enzymes from marine bacteria to Japanese gut microbiota. Nature. 2010;464(7290):908.
219. Herrmann E, Young W, Rosendale D, Reichert-Grimm V, Riedel CU, Conrad R, et al. RNA-based stable isotope probing suggests Allobaculum spp. as particularly active glucose assimilators in a complex murine microbiota cultured in vitro. BioMed Research International. 2017;2017.
220. Tamanai-Shacoori Z, Smida I, Bousarghin L, Loreal O, Meuric V, Fong SB, et al. Roseburia spp.: a marker of health? Future Microbiology. 2017;12(2):157-70.
221. Patterson AM, Mulder IE, Travis AJ, Lan A, Cerf-Bensussan N, Gaboriau-Routhiau V, et al. Human gut symbiont Roseburia hominis promotes and regulates innate immunity. Frontiers in Immunology. 2017;8:1166.
222. Kasahara K, Krautkramer KA, Org E, Romano KA, Kerby RL, Vivas EI, et al. Interactions between Roseburia intestinalis and diet modulate atherogenesis in a murine model. Nature Microbiology. 2018;3(12):1461.
223. Karn A, Zhao C, Yang F, Cui J, Gao Z, Wang M, et al. In-vivo biotransformation of citrus functional components and their effects on health. Critical Reviews in Food Science and Nutrition. 2020:1-21.
224. Ho C, Pan M, Lai C, Li S. Polymethoxyflavones as food factors for the management of

inflammatory diseases. Neuropathology. 2012;20:337-41.
225. Goodrich R, Braddock R. Major by-products of the Florida citrus processing industry. Document FSHN05-22, Series of the Food Science and Human Nutrition Department, Florida Cooperative Extension Service, Institute of Food and Agricultural Sciences, University of Florida. 2006.
226. Chen B, Zhou J, Meng Q, Zhang Y, Zhang S, Zhang L. Comparative analysis of fecal phenolic content between normal and obese rats after oral administration of tea polyphenols. Food & Function. 2018;9(9):4858-64.
227. Tomás-Barberán FA, Selma MV, Espín JC. Interactions of gut microbiota with dietary polyphenols and consequences to human health. Current Opinion in Clinical Nutrition and Metabolic Care. 2016;19(6):471-6.
228. Koppel N, Rekdal VM, Balskus EP. Chemical transformation of xenobiotics by the human gut microbiota. Science. 2017;356(6344):eaag2770.
229. Fang J. Bioavailability of anthocyanins. Drug Metabolism Reviews. 2014;46(4):508-20.
230. Zhu M, Chen Y, Li RC. Oral absorption and bioavailability of tea catechins. Planta Medica. 2000;66(05):444-7.
231. Xu JZ, Yeung SYV, Chang Q, Huang Y, Chen Z-Y. Comparison of antioxidant activity and bioavailability of tea epicatechins with their epimers. British Journal of Nutrition. 2004;91(6):873-81.
232. Estrela JM, Mena S, Obrador E, Benlloch M, Castellano G, Salvador R, et al. Polyphenolic phytochemicals in cancer prevention and therapy: bioavailability versus bioefficacy. Journal of Medicinal Chemistry. 2017;60(23):9413-36.
233. Holst B, Williamson G. Nutrients and phytochemicals: from bioavailability to bioefficacy beyond antioxidants. Current Opinion in Biotechnology. 2008;19(2):73-82.
234. Varma MV, Obach RS, Rotter C, Miller HR, Chang G, Steyn SJ, et al. Physicochemical space for optimum oral bioavailability: contribution of human intestinal absorption and first-pass elimination. Journal of Medicinal Chemistry. 2010;53(3):1098-108.
235. Bergström CA, Strafford M, Lazorova L, Avdeef A, Luthman K, Artursson P. Absorption classification of oral drugs based on molecular surface properties. Journal of Medicinal Chemistry. 2003;46(4):558-70.
236. Lei L, Zhang Y, He L, Wu S, Li B, Li Y. Fabrication of nanoemulsion-filled alginate hydrogel to control the digestion behavior of hydrophobic nobiletin. LWT-Food Science and Technology. 2017;82:260-7.
237. McClements DJ, Li Y. Review of in vitro digestion models for rapid screening of emulsion-based systems. Food & Function. 2010;1(1):32-59.
238. Van De Waterbeemd H, Smith DA, Beaumont K, Walker DK. Property-based design: optimization of drug absorption and pharmacokinetics. Journal of Medicinal Chemistry. 2001;44(9):1313-33.
239. Yu H, Huang Q. Improving the oral bioavailability of curcumin using novel organogel-based nanoemulsions. Journal of Agricultural and Food Chemistry. 2012a;60(21):5373-9.
240. Dezani AB, Pereira TM, Caffaro AM, Reis JM, dos Reis Serra CH. Determination of lamivudine and zidovudine permeability using a different ex vivo method in Franz cells. Journal of Pharmacological

and Toxicological Methods. 2013;67(3):194-202.
241. Reis J, Dezani AB, Pereira T, Avdeef A, Serra CHdR. Lamivudine permeability study: A comparison between PAMPA, ex vivo and in situ Single-Pass Intestinal Perfusion (SPIP) in rat jejunum. European Journal of Pharmaceutical Sciences. 2013;48(4-5):781-9.
242. Lundquist P, Artursson P. Oral absorption of peptides and nanoparticles across the human intestine: Opportunities, limitations and studies in human tissues. Advanced Drug Delivery Reviews. 2016;106:256-76.
243. Yu H, Shi K, Liu D, Huang Q. Development of a food-grade organogel with high bioaccessibility and loading of curcuminoids. Food Chemistry. 2012b;131(1):48-54.
244. Liebenberg W, Engelbrecht E, Wessels A, Devarakonda B, Yang W, De Villiers MM. A comparative study of the release of active ingredients from semisolid cosmeceuticals measured with Franz, enhancer or flow-through cell diffusion apparatus. Journal of Food and Drug Analysis. 2004;12(1):19-28.
245. van de Waterbeemd H. The fundamental variables of the biopharmaceutics classification system (BCS): a commentary. European journal of pharmaceutical sciences: official journal of the European Federation for Pharmaceutical Sciences. 1998;7(1):1.
246. Yao M, Chen J, Zheng J, Song M, McClements DJ, Xiao H. Enhanced lymphatic transport of bioactive lipids: cell culture study of polymethoxyflavone incorporation into chylomicrons. Food & Function. 2013;4(11):1662-7.
247. Li S, Pan MH, Lo CY, Tan D, Wang Y, Shahidi F, et al. Chemistry and health effects of polymethoxyflavones and hydroxylated polymethoxyflavones. Journal of Functional Foods. 2009;1(1):2-12.
248. Martins AJ, Vicente AA, Cunha RL, Cerqueira MA. Edible oleogels: an opportunity for fat replacement in foods. Food & Function. 2018;9(2):758-73.
249. Davidovich-Pinhas M, Barbut S, Marangoni A. Development, characterization, and utilization of food-grade polymer oleogels. Annual Review of Food Science and Technology. 2016;7:65-91.
250. O'Sullivan CM, Barbut S, Marangoni AG. Edible oleogels for the oral delivery of lipid soluble molecules: Composition and structural design considerations. Trends in Food Science & Technology. 2016;57:59-73.
251. Lu M, Cao Y, Ho C-T, Huang Q. Development of organogel-derived capsaicin nanoemulsion with improved bioaccessibility and reduced gastric mucosa irritation. Journal of Agricultural and Food Chemistry. 2016;64(23):4735-41.
252. Wei Z, Huang Q. Developing organogel-based Pickering emulsions with improved freeze-thaw stability and hesperidin bioaccessibility. Food Hydrocolloids. 2019;93:68-77.
253. Dinarvand R, Moghadam S, Sheikhi A, Atyabi F. Effect of surfactant HLB and different formulation variables on the properties of poly-D, L-lactide microspheres of naltrexone prepared by double emulsion technique. Journal of Microencapsulation. 2005;22(2):139-51.
254. Chemical M. RYOTO™ SUGAR ESTER https://www.m-chemical.co.jp/en/products/departments/group/mfc/product/1201443_7739.html: The website of

MItsubishi Chemical.
255. Patel AR, Babaahmadi M, Lesaffer A, Dewettinck K. Rheological profiling of organogels prepared at critical gelling concentrations of natural waxes in a triacylglycerol solvent. Journal of Agricultural and Food Chemistry. 2015;63(19):4862-9.
256. Jadhav SR, Hwang H, Huang Q, John G. Medium-chain sugar amphiphiles: a new family of healthy vegetable oil structuring agents. Journal of Agricultural and Food Chemistry. 2013;61(49):12005-11.
257. Posocco P, Perazzo A, Preziosi V, Laurini E, Pricl S, Guido S. Interfacial tension of oil/water emulsions with mixed non-ionic surfactants: comparison between experiments and molecular simulations. RSC Advances. 2016;6(6):4723-9.
258. Sanatkaran N, Masalova I, Malkin AY. Effect of surfactant on interfacial film and stability of highly concentrated emulsions stabilized by various binary surfactant mixtures. Colloids and Surfaces A: Physicochemical and Engineering Aspects. 2014;461:85-91.
259. McClements DJ, Decker EA, Park Y, Weiss J. Structural design principles for delivery of bioactive components in nutraceuticals and functional foods. Critical Reviews in Food Science and Nutrition. 2009;49(6):577-606.